Available online at www.sciencedirect.com

ScienceDirect

Nuclear Physics B 884 (2014) 206–256

NUCLEAR PHYSICS B

www.elsevier.com/locate/nuclphysb

Event shapes in $\mathcal{N} = 4$ super-Yang–Mills theory

A.V. Belitsky [a,b], S. Hohenegger [c], G.P. Korchemsky [b], E. Sokatchev [c,d,e], A. Zhiboedov [f]

[a] *Department of Physics, Arizona State University, Tempe, AZ 85287-1504, USA*

[b] *Institut de Physique Théorique [1], CEA Saclay, 91191 Gif-sur-Yvette Cedex, France*

[c] *Physics Department, Theory Unit, CERN, CH-1211 Geneva 23, Switzerland*

[d] *Institut Universitaire de France, 103, bd Saint-Michel, F-75005 Paris, France*

[e] *LAPTH [2], Université de Savoie, CNRS, B.P. 110, F-74941 Annecy-le-Vieux, France*

[f] *Department of Physics, Princeton University, Princeton, NJ 08544, USA*

Received 27 February 2014; received in revised form 24 April 2014; accepted 24 April 2014

Available online 30 April 2014

Editor: Stephan Stieberger

Abstract

We study event shapes in $\mathcal{N} = 4$ SYM describing the angular distribution of energy and R-charge in the final states created by the simplest half-BPS scalar operator. Applying the approach developed in the companion paper arXiv:1309.0769, we compute these observables using the correlation functions of certain components of the $\mathcal{N} = 4$ stress-tensor supermultiplet: the half-BPS operator itself, the R-symmetry current and the stress tensor. We present master formulas for the all-order event shapes as convolutions of the Mellin amplitude defining the correlation function of the half-BPS operators, with a coupling-independent kernel determined by the choice of the observable. We find remarkably simple relations between various event shapes following from $\mathcal{N} = 4$ superconformal symmetry. We perform thorough checks at leading order in the weak coupling expansion and show perfect agreement with the conventional calculations based on amplitude techniques. We extend our results to strong coupling using the correlation function of half-BPS operators obtained from the AdS/CFT correspondence.

[1] Unité de Recherche Associée au CNRS URA 2306.

[2] UMR 5108 du CNRS, associée à l'Université de Savoie.

http://dx.doi.org/10.1016/j.nuclphysb.2014.04.019

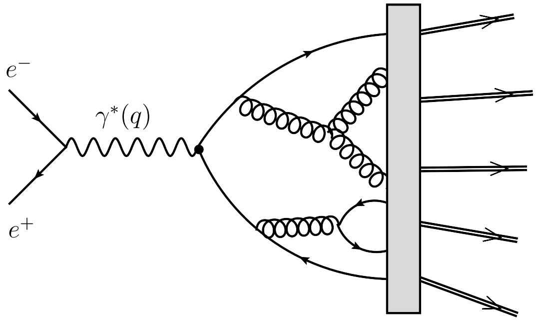

Fig. 1. Final states in e^+e^- annihilation in QCD. The electron and positron annihilate to produce a virtual photon $\gamma^*(q)$ that decays into an arbitrary number of quarks and gluons which go through a hadronization process (shaded rectangle) to become hadrons (double lines). The dot denotes the electromagnetic QCD current.

1. Introduction

Recently, significant progress has been made in understanding properties of correlation functions and scattering amplitudes in maximally supersymmetric Yang–Mills theory ($\mathcal{N} = 4$ SYM). There is growing evidence that the theory possesses a hidden integrability symmetry which is powerful enough to determine both quantities for an arbitrary value of the coupling constant, at least in the planar limit. Correlation functions and scattering amplitudes have different properties and carry complementary information about the dynamics of $\mathcal{N} = 4$ SYM. Unlike the correlation functions, the on-shell scattering amplitudes are not well defined in four dimensions due to infrared (IR) singularities and, hence, they require regularization. This introduces a dependence on unphysical parameters (such as the dimensional regularization scale playing the role of the IR regulator) which break (super)conformal symmetry. At the same time, the correlation functions of protected (half-BPS) operators are well-defined functions of the coordinates of the operators in four-dimensional $\mathcal{N} = 4$ SYM. As a consequence, they do not require regularization and enjoy the full unbroken $\mathcal{N} = 4$ superconformal symmetry.

The main goal of this paper is to study a different class of gauge invariant quantities in $\mathcal{N} = 4$ SYM which admit two equivalent representations: They are given by integrated correlation functions and, at the same time, they can be expressed as (infinite) sums over absolute squares of scattering amplitudes. These quantities are closely related to various observables which have been thoroughly studied in the context of QCD for the final states produced in e^+e^- annihilation [1–3]. In the latter case, the electron and positron annihilate to produce a virtual photon, which in turn creates an energetic quark–antiquark pair from the vacuum. The outgoing particles move away from each other and emit a lot of radiation before fragmenting into hadrons (see Fig. 1). The distribution of particles in the final state of e^+e^- annihilation can be characterized by a set of observables, the so-called event shapes (see, e.g., [2]). One of them, the energy–energy correlation [4], plays a distinct role in our analysis.

Needless to say, QCD is quite different from $\mathcal{N} = 4$ SYM. Due to the presence of a mass gap in the hadron spectrum, QCD scattering amplitudes are free from IR singularities but their calculation is still impossible due to our inability to control the confining (hadronization) regime in the theory. A remarkable property of the event shapes is that, for asymptotically large values of the center-of-mass energy q^2, the hadronization corrections become negligible (for a review see, e.g., [5]). As a consequence, the event shapes can be approximated at high energy by a perturbative QCD expansion. It is in this context that $\mathcal{N} = 4$ SYM arises as a simpler model of gauge dynamics in four space–time dimensions. It shares many features with perturbative QCD, on the one hand, and can be studied analytically using its symmetries, on the other. In particular, the AdS/CFT correspondence opens up a possibility to explore the previously unreachable regime of strong coupling.

To generalize the QCD process shown in Fig. 1 to $\mathcal{N}=4$ SYM, we have to find an appropriate analog of the QCD electromagnetic current. For this purpose we can choose any local protected operator in $\mathcal{N}=4$ SYM, e.g., the half-BPS operator $O_{\mathbf{20'}}(x)$ built from two scalar fields. At weak coupling one can think about the state created by this operator as follows. The operator $O_{\mathbf{20'}}(x)$ produces out of the vacuum a pair of scalars that propagate into the final state and radiate on-shell particles of $\mathcal{N}=4$ SYM – scalars, gluinos and gluons. The fact that these particles are massless leads to a degeneracy of the final states. For instance, a single-particle state is undistinguishable from the state containing an additional gluon with vanishing momentum and from the state containing a pair of particles with aligned momenta and the same total charge. According to the Kinoshita–Lee–Nauenberg mechanism [6,7], the degeneracy of on-shell states leads to (soft and collinear) divergences in the perturbative expansion of the corresponding scattering amplitudes.

This phenomenon is quite general when massless particles are present in the spectrum. An important issue in the early days of QCD was whether one could define quantities that are free from infrared divergences at all orders of perturbation theory. The answer was found with the introduction of the so-called inclusive infrared safe observables. The latter are given by a sum over an infinite number of scattering amplitudes involving an arbitrary number of degenerate states [1,4]. Each amplitude has infrared divergences but they cancel in the sum, so that infrared safe observables are well defined in four dimensions order-by-order in the coupling. The question arises whether there is another way to compute the same observables that bypasses the introduction of any regularization and, therefore, makes all symmetries of the theory manifest at each step of the calculation.

As a simple example, consider the total probability of the transition $O_{\mathbf{20'}} \to$ everything. This is an infrared safe quantity, but it is given by (an infinite) sum over all final states, with each individual term being infrared divergent. The optical theorem allows us to express the same quantity as the imaginary part of the two-point (time-ordered) correlation function of the half-BPS operators $O_{\mathbf{20'}}(x)$ (see Eq. (2.8) below). This two-point function is well defined in four dimensions and its form is uniquely fixed by $\mathcal{N}=4$ superconformal symmetry. In this way, we obtain a definite prediction for the total transition amplitude $O_{\mathbf{20'}} \to$ everything that agrees with the result of an explicit calculation [8] based on amplitudes.

In this paper, we deal with a special class of event shape distributions related to the flow of various quantum numbers (energy, charge) in the final state. A typical event contributing to such an observable is shown in Fig. 4 below. There, the particles propagate into the final state where the detectors measure the flow of their quantum numbers per solid angle in the directions indicated by the unit vectors $\vec{n}, \vec{n}', \ldots$. As was shown in Refs. [9–12] in the context of QCD, the optical theorem can be generalized to such differential distributions. For instance, the energy flow distributions can be expressed in terms of the correlation functions $\langle O_{\mathbf{20'}}(x)\mathcal{E}(\vec{n})\mathcal{E}(\vec{n}')\ldots O_{\mathbf{20'}}(0)\rangle$ containing additional energy flow operators $\mathcal{E}(\vec{n}), \mathcal{E}(\vec{n}'), \ldots$ (one for each detector). Quantities of this type have been studied in the framework of conformal field theories in [13], particularly in connection with the AdS/CFT correspondence. An unusual feature of these correlation functions is that the operators are not time-ordered. In other words, we are dealing with correlation functions of the Wightman type defined on a space–time with Lorentzian signature. Notice, however, that significant advances have been made in the calculation of their Euclidean counterparts. The natural question arises whether we can make use of the latter to compute the weighted cross sections. The answer was presented in the companion paper [14], where we explained in detail how to obtain the charge flow correlators in a generic CFT, starting from the Euclidean correlation functions and making a nontrivial analytic continuation. We briefly review it below to make the exposition self-contained. In this paper, we apply the approach of [14] to the particular case of $\mathcal{N}=4$ SYM.

The paper is organized as follows. In Section 2, we consider the process $O_{\mathbf{20'}} \to$ everything in $\mathcal{N}=4$ SYM and introduce a set of infrared safe observables, determined by weighted cross sections, describing the flow of various quantum numbers into the final state in this process. We also work out a representation for these observables in terms of Wightman correlation functions involving insertions of flow operators. In Section 3, we consider weighted cross sections with one or two flow operators and evaluate them to the lowest order in the coupling using the conventional amplitude techniques. In Sections 4 and 5, we elaborate on the main result of this work and explain how the same observables can be obtained from the known results for Euclidean correlation functions of half-BPS and other operators, such as the R-current and the energy–momentum tensor, in the same $\mathcal{N}=4$ supermultiplet. In particular, we derive a master formula which yields an all-loop result for the weighted cross sections as a convolution of the Mellin amplitude defined by the Euclidean correlation function with a coupling-independent 'detector kernel' corresponding to the choice of the flow operators. In Section 6, we demonstrate the efficiency of the formalism making use of the same examples as covered in Section 3, first at weak and then at strong coupling. Section 7 contains concluding remarks. Several technical details are deferred to Appendices A–E.

2. Correlations in $\mathcal{N}=4$ SYM

In the context of $\mathcal{N}=4$ SYM, we can introduce an analog of the quark electromagnetic current, the lowest-dimension half-BPS Hermitian operator $O^{IJ}_{\mathbf{20'}}(x)$ built from the six real scalars $\Phi^I(x)$ (with $SO(6)$ vector indices $I, J = 1, \dots, 6$),

$$O^{IJ}_{\mathbf{20'}}(x) = \mathrm{tr}\left[\Phi^I\Phi^J - \frac{1}{6}\delta^{IJ}\Phi^K\Phi^K\right]. \tag{2.1}$$

Here $\Phi^I \equiv \Phi^{Ia}T^a$ and the generators T^a of the gauge group $SU(N_c)$ are normalized as $\mathrm{tr}[T^aT^b] = \frac{1}{2}\delta^{ab}$ (with $a, b = 1, \dots, N_c^2 - 1$). The operator (2.1) possesses a protected scaling dimension, $\Delta = 2$, very much like the QCD electromagnetic current. Moreover, it is the lowest-weight state of the $\mathcal{N}=4$ stress-tensor supermultiplet and is related by supersymmetry to the R-symmetry current, which can be viewed as a 'cousin' of the electromagnetic current.

The operator (2.1) belongs to the real irrep $\mathbf{20'}$ of the R-symmetry group $SO(6) \sim SU(4)$. To keep track of the isotopic structure, it is convenient to consider the projected operator

$$O(x, Y) = Y^IY^JO^{IJ}_{\mathbf{20'}}(x) = Y^IY^J\,\mathrm{tr}\big[\Phi^I(x)\Phi^J(x)\big], \tag{2.2}$$

where Y^I is an auxiliary six-dimensional (complex) null vector, $Y^2 = \sum_{I=1}^6 Y^IY^I = 0$, defining the orientation of the operator in the isotopic space.[3]

Next, we can ask the question about the properties of the final states created by the operator (2.2) from the vacuum. To lowest order in the coupling, the final state consists of a pair of scalars.

[3] We can always reveal the index structure of the $SO(6)$ tensor $O^{IJ}_{\mathbf{20'}}(x)$ by differentiating the final expressions involving $O(x, Y)$ with respect to the Y's, bearing in mind the restriction $Y^2 = 0$.

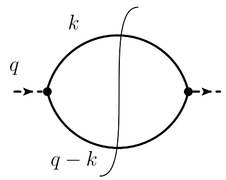

Fig. 2. The Feynman diagram contributing to $\sigma_{\text{tot}}(q)$. The thin line stands for the unitarity cut.

For arbitrary coupling, the state $\int d^4x\, e^{iqx} O(x,Y)|0\rangle$ can be decomposed into an infinite tower of asymptotic on-shell states, $|\text{ss}\rangle$, $|\text{ssg}\rangle$, $|\text{s}\lambda\lambda\rangle$, ... involving an arbitrary number of scalars (s), gluinos (λ) and gauge fields (g). Each on-shell state carries the same quantum numbers – the total momentum q^μ, zero (color) $SU(N_c)$ charge and R-charges of the irrep $\mathbf{20}'$. We can then define the amplitude for creation of a particular final state $|X\rangle$ out of the vacuum,

$$\langle X| \int d^4x\, e^{iqx} O(x,Y)|0\rangle = (2\pi)^4 \delta^{(4)}(q-k_X)\mathcal{M}_{O_{\mathbf{20}'}\to X}, \tag{2.3}$$

where k_X is the total momentum of the state $|X\rangle$. Defined in this fashion, the amplitude $\mathcal{M}_{O\to X}$ has the meaning of a form-factor,

$$\mathcal{M}_{O_{\mathbf{20}'}\to X} = \langle X|O(0,Y)|0\rangle. \tag{2.4}$$

For a given on-shell state $|X\rangle$, it suffers from IR divergences that require a regularization procedure. In addition, this quantity depends on the number of colors N_c and on the coupling constant g_{YM}. For our purposes it proves convenient to introduce the 't Hooft coupling $g^2 = g_{\text{YM}}^2 N_c$ and the analog of the fine structure constant, $a = g_{\text{YM}}^2 N_c/(4\pi^2)$, familiar from QCD.

2.1. Total transition probability

In close analogy with the QCD process $e^+e^- \to$ everything, we can examine the transition $O_{\mathbf{20}'} \to$ everything. The total probability of this process is given by the sum over all final states

$$\sigma_{\text{tot}}(q) = \sum_X (2\pi)^4 \delta^{(4)}(q-k_X)|\mathcal{M}_{O_{\mathbf{20}'}\to X}|^2, \tag{2.5}$$

where the summation runs over the quantum numbers of the produced particles including their helicity, color, $SU(4)$ indices, etc. To lowest order in the coupling, it describes the production of a pair of scalars as shown in Fig. 2,[4]

$$\sigma_{\text{tot}}(q) = \frac{1}{2}\big(N_c^2-1\big)(Y\bar{Y})^2 \int \frac{d^4k}{(2\pi)^4}(2\pi)^2\delta_+\big(k^2\big)\delta_+\big((q-k)^2\big) + \ldots, \tag{2.6}$$

where the ellipsis stand for omitted higher order corrections and the integration in the first term goes over the phase space of the two massless particles carrying the total momentum q^μ. The prefactor accompanying the integral is the $SO(6)$ invariant contraction of the auxiliary internal variables $(Y\bar{Y}) = \sum_I Y^I \bar{Y}^I$.

Using the completeness condition on the asymptotic states, $\sum_X |X\rangle\langle X| = 1$, we can rewrite (2.5) as

[4] We use Minkowski signature $(+,-,-,-)$ and the shorthand notation $\delta_+(k^2) = \delta(k^2)\theta(k^0)$.

$$\sigma_{\rm tot}(q) = \int d^4x\, e^{iqx} \sum_X \langle 0|O(0,\bar{Y})|X\rangle e^{-ixk_X} \langle X|O(0,Y)|0\rangle$$
$$= \int d^4x\, e^{iqx} \langle 0|O(x,\bar{Y})O(0,Y)|0\rangle, \tag{2.7}$$

where $O(x,\bar{Y}) = O^{IJ}_{\mathbf{20'}}\bar{Y}^I\bar{Y}^J = (O(x,Y))^\dagger$ (we recall that the operator $O^{IJ}_{\mathbf{20'}}$ is Hermitian). Notice that the operators in (2.7) are not time-ordered.

The optical theorem allows us to rewrite (2.7) as the imaginary part of the time-ordered correlation function

$$\sigma_{\rm tot}(q) = \operatorname{Im}\left[2i \int d^4x\, e^{iqx} \langle 0|T\,O(x,\bar{Y})O(0,Y)|0\rangle\right]. \tag{2.8}$$

The correlation function on the right-hand side is well defined in four dimensions and the same is true for $\sigma_{\rm tot}(q)$. This is not the case however for each term on the right-hand side of (2.5) since $\mathcal{M}_{O_{\mathbf{20'}}\to X}$ suffers from IR divergences. In agreement with the Lee–Nauenberg–Kinoshita theorem [6,7], the infrared finiteness of $\sigma_{\rm tot}(q)$ is restored in the infinite sum over the final states $|X\rangle$ in (2.5).

Another advantage of the representation (2.8) is that it allows us to compute $\sigma_{\rm tot}(q)$ exactly, to all orders in the coupling. Indeed, in $\mathcal{N}=4$ SYM the two-point correlation function of the half-BPS operators $O(x,Y)$ is protected from loop corrections[5] and is given by the Born level expression

$$\langle 0|T\,O(x,\bar{Y})O(0,Y)|0\rangle = \frac{1}{2}\left(N_c^2-1\right)(Y\bar{Y})^2\left[D_F(x)\right]^2, \tag{2.9}$$

where $D_F(x) = 1/(4\pi^2(-x^2+i0))$ is the Feynman propagator of the scalar field. Its substitution into (2.8) yields the leading tree-level term in (2.6). Performing the integration in (2.6) we arrive at

$$\sigma_{\rm tot}(q) = \frac{1}{16\pi}\left(N_c^2-1\right)(Y\bar{Y})^2\theta\left(q^0\right)\theta\left(q^2\right). \tag{2.10}$$

The fact that $\sigma_{\rm tot}(q)$ does not depend on the coupling constant implies that the perturbative corrections cancel order by order in $\mathcal{N}=4$ SYM. To two loop accuracy, this property has been verified in Ref. [19] by an explicit calculation. The product of the two step functions on the right-hand side of (2.10) ensures that the cross section is different from zero for the total momentum $q^0>0$ and $q^2>0$. In what follows we tacitly assume that this condition is satisfied and we do not display the step functions in any formulas that follow.

2.2. *Weighted cross section*

The quantity (2.5) is completely inclusive with respect to the final states. We can define a less inclusive quantity by assigning a weight factor $w(X)$ to the contribution of each state $|X\rangle$

$$\sigma_W(q) = \sigma_{\rm tot}^{-1} \sum_X (2\pi)^4 \delta^{(4)}(q-k_X) w(X) |\mathcal{M}_{O_{\mathbf{20'}}\to X}|^2$$
$$= \sigma_{\rm tot}^{-1} \int d^4x\, e^{iqx} \sum_X \langle 0|O(x,\bar{Y})|X\rangle w(X) \langle X|O(0,Y)|0\rangle, \tag{2.11}$$

[5] See, e.g., [15–17] for non-renormalization theorems and Refs. [18] and [19] for explicit one- and two-loop perturbative tests, respectively.

where the additional factor of $1/\sigma_{\text{tot}}$ is inserted to obtain the normalization condition $\sigma_W(q) = 1$ for $w(X) = 1$. Appropriately choosing the weight factors $w(X)$ and evaluating the corresponding weighted cross section $\sigma_W(q)$, we can get a more detailed description of the flow of various quantum numbers of particles (energy, charge, etc.) in the final state $|X\rangle$.

For a generic final state $|X\rangle$, the scattering amplitude $\mathcal{M}_{O_{\mathbf{20'}}\to X}$ contains soft and collinear divergences as we reviewed in the introduction. They arise from the integration over the loop momenta of virtual particles and appear as poles in ϵ in dimensional regularization with $D = 4 - 2\epsilon$. Taken by itself, each term in the sum in the first relation in (2.11) vanishes as $|\mathcal{M}_{O_{\mathbf{20'}}\to X}|^2 \sim \mathrm{e}^{-f(g^2)/\epsilon^2} \to 0$ for $\epsilon \to 0$ (with a positive-definite function $f(g^2)$ related to the cusp anomalous dimension), due to the exponentiation of infrared singularities (see, e.g., Ref. [20]). However, these are not the only divergences that we encounter in the calculation of the cross section. Namely, additional poles in $1/\epsilon$ come from the integration over the phase space of soft and collinear massless particles in the final state $|X\rangle$. For the cross section to be IR finite, the two effects, i.e., virtual and real singularities should cancel each other, thus producing a finite net result. In the case of the total transition probability σ_{tot}, the cancellation of IR divergences follows from the Kinoshita–Lee–Nauenberg theorem. For weighted cross sections, the condition of infrared finiteness imposes a severe restriction on the weights $w(X)$ [21]. Namely, the weight should be insensitive to adding one particle to the final state $|X\rangle$, with the momentum either soft, or collinear to the momenta of the parent particles in the state $|X\rangle$.

2.2.1. Energy flow

One of the well-known examples of a weight factor, which was introduced in the context of e^+e^-– annihilation and which is very useful for our purposes, corresponds to the energy flow. For a given final on-shell state $|X\rangle = |k_1, \ldots, k_\ell\rangle$, consisting of ℓ massless particles, $k_i^2 = 0$, with the total momentum $\sum_i k_i^\mu = q^\mu$, it is defined in the rest frame $q^\mu = (q^0, \vec{0})$ as

$$w_{\mathcal{E}}(k_1, \ldots, k_\ell) = \sum_{i=1}^{\ell} k_i^0 \delta^{(2)}(\Omega_{\vec{k}_i} - \Omega_{\vec{n}}), \tag{2.12}$$

where $k_i^\mu = (k_i^0, \vec{k}_i)$ and $\Omega_{\vec{k}_i} = \vec{k}_i/|\vec{k}_i|$ is the solid angle in the direction of $\vec{k}_i$. The corresponding weighted cross section has a simple physical meaning – it measures the distribution of energy in the final state that flows in the direction of the vector $\vec{n}$. Most importantly, the weight (2.12) can be identified with the eigenvalue of the energy flow operator,

$$\mathcal{E}(\vec{n})|X\rangle = w_{\mathcal{E}}(X)|X\rangle. \tag{2.13}$$

As we show below, this relation allows us to simplify (2.11) along the same lines as in (2.7) and to express the cross section $\sigma_{\mathcal{E}}$ in terms of the correlation function $\langle 0|O(x, \bar{Y})\mathcal{E}(\vec{n})O(0, Y)|0\rangle$ with an insertion of the energy flow operator.

The explicit expression for the operator $\mathcal{E}(\vec{n})$ is given in terms of the energy–momentum tensor of $\mathcal{N} = 4$ SYM [9–12] (see also [13])

$$\mathcal{E}(\vec{n}) = \int_0^\infty dt \lim_{r\to\infty} r^2 n^i T_{0i}(t, r\vec{n}), \tag{2.14}$$

where the unit vector $\vec{n} = (n^1, n^2, n^3)$ (with $\vec{n}^2 = 1$) indicates the spatial direction of the energy flow. To get a better understanding of the action of the operator $\mathcal{E}(\vec{n})$ on the asymptotic states, we replace the energy–momentum tensor $T_{\mu\nu}(x)$ in (2.14) by its expression in terms of free fields and obtain the following representation for $\mathcal{E}(\vec{n})$ in terms of creation and annihilation operators:

$$\mathcal{E}(\vec{n}) = \int \frac{d^4k}{(2\pi)^4} 2\pi\delta_+\big(k^2\big)k_0\delta^{(2)}(\Omega_{\vec{n}} - \Omega_{\vec{k}}) \sum_{p=\mathrm{s},\lambda,\mathrm{g}} a_p^{b\dagger}(k)a_p^b(k), \tag{2.15}$$

where the sum goes over all on-shell states (scalars, helicity $(\pm 1/2)$ gluinos and helicity (± 1) gluons) carrying an $SU(N_c)$ index $b = 1, \ldots, N_c^2 - 1$. To simplify the formulas, in what follows we do not display the $SU(N_c)$ indices of the creation/annihilation operators. Making use of the (anti)commutation relations between $a_i^\dagger(k)$ and $a_i(k)$ (see, e.g., Eq. (A.3)), it is straightforward to verify the relations (2.13) and (2.12), as well as the commutativity condition

$$\big[\mathcal{E}(\vec{n}), \mathcal{E}\big(\vec{n}'\big)\big] = 0, \quad \text{for } \vec{n} \neq \vec{n}'. \tag{2.16}$$

The latter equality states that the energy flows in two different directions $\vec{n}$ and $\vec{n}'$ are independent from each other and can be measured separately.

Making use of (2.16), we can define a weight which measures the energy flows in various directions $\vec{n}_1, \ldots, \vec{n}_\ell$ simultaneously:

$$\mathcal{E}(\vec{n}_1)\ldots\mathcal{E}(\vec{n}_\ell)|X\rangle = w_{\mathcal{E}(\vec{n}_1)}(X)\ldots w_{\mathcal{E}(\vec{n}_\ell)}(X)|X\rangle \equiv w(X)|X\rangle. \tag{2.17}$$

Substituting this relation into (2.11) we can apply the completeness relation $\sum_X |X\rangle\langle X| = 1$ and obtain the following representation of the corresponding weighted cross section[6]

$$\begin{aligned}\big\langle\mathcal{E}(\vec{n}_1)\ldots\mathcal{E}(\vec{n}_\ell)\big\rangle &\equiv \sigma_{\mathcal{E}}(q;\vec{n}_1,\ldots,\vec{n}_\ell)\\ &= \sigma_{\mathrm{tot}}^{-1}\int d^4x\, \mathrm{e}^{iqx}\langle 0|O(x,\bar{Y})\mathcal{E}(\vec{n}_1)\ldots\mathcal{E}(\vec{n}_\ell)O(0,Y)|0\rangle,\end{aligned} \tag{2.18}$$

which has the meaning of an energy flow correlation. Notice that the product of operators on the right-hand side of (2.18) is not time-ordered and, therefore, their correlation function is of the Wightman type.

2.2.2. Charge flow

In close analogy with (2.12) we can define a weight that measures the flow of the R-charges through the detector. We recall that in $\mathcal{N} = 4$ SYM only the scalars and gluinos are charged with respect to the R-symmetry group $SU(4)$. The flow of the R-charge is defined by the operator

$$\mathcal{Q}_A^B(\vec{n}) = \int_0^\infty dt\, \lim_{r\to\infty} r^2 (J_0)_A^B(t, r\vec{n}), \tag{2.19}$$

involving the time component of the R-current $(J_\mu)_A^B(x)$. An important difference as compared with (2.14) is that the operator transforms under $SU(4)$. We shall come back to this point in a moment.

Replacing the R-current in (2.19) by its expression in terms of the free fields, we obtain

$$\begin{aligned}\mathcal{Q}_A^B(\vec{n}) = \int \frac{d^4k}{(2\pi)^4} &2\pi\delta_+\big(k^2\big)\delta^{(2)}(\Omega_{\vec{n}} - \Omega_{\vec{k}})\\ &\times \big[a_{AC}^\dagger(k)a^{CB}(k) + a_{A,1/2}^\dagger(k)a_{-1/2}^B(k) - a_{-1/2}^{B,\dagger}(k)a_{A,1/2}(k)\big] - (\text{trace}),\end{aligned} \tag{2.20}$$

[6] Below we show that dividing by σ_{tot}, Eq. (2.10), the Y-dependence drops out from (2.18).

where (trace) denotes terms proportional to δ_A^B that are needed to ensure the tracelessness condition $\delta_B^A \mathcal{Q}_A^B(\vec{n}) = 0$. Here $a^\dagger_{A,1/2}$ and $a^{B\dagger}_{-1/2}$ are the creation operators of gluinos with helicity $\pm 1/2$, respectively, and $a^\dagger_{AC}(k)$ are the creation operators of the scalars in $SU(4)$ notation (see Appendix B). Using (2.20) we can work out the action of the operator $\mathcal{Q}_A^B(\vec{n})$ on the asymptotic states. For instance, for a single-particle gluino state $|k\rangle_E \equiv a^\dagger_{E,1/2}(k)|0\rangle$ we get

$$\mathcal{Q}_A^B(\vec{n})|k\rangle_E = \delta^{(2)}(\Omega_{\vec{k}} - \Omega_{\vec{n}})\left[\delta_E^B|k\rangle_A - \frac{1}{4}\delta_A^B|k\rangle_E\right], \tag{2.21}$$

from where we conclude that the operator $\mathcal{Q}_A^B(\vec{n})$ does not change the momentum of the particle but it rotates its $SU(4)$ index. The same is true for the scalar states whereas the gluon state has zero R-charge and, therefore, is not affected by $\mathcal{Q}_A^B(\vec{n})$.

Relation (2.21) seems to contradict our definition of the flow operator (2.13), according to which the on-shell states should diagonalize the operator $\mathcal{Q}_A^B(\vec{n})$. To restore the diagonal action of the operator $\mathcal{Q}_A^B(\vec{n})$ on the asymptotic states we introduce an auxiliary traceless matrix Q_B^A and consider the following linear combination of the operators (2.20)

$$\mathcal{Q}(\vec{n}; Q) = Q_B^A \mathcal{Q}_A^B(\vec{n}). \tag{2.22}$$

To preserve the reality condition on the eigenvalues of the flow operator (2.22), the matrix Q_B^A should be Hermitian. This allows us to decompose it over its eigenvectors,

$$Q_B^A = \sum_{\alpha=1}^{4} Q_\alpha \bar{u}_\alpha^A u_B^\alpha, \qquad \sum_{A=1}^{4} \bar{u}_\alpha^A u_A^\beta = \delta_\beta^\alpha, \qquad \sum_{\alpha=1}^{4} \bar{u}_\alpha^A u_B^\alpha = \delta_B^A. \tag{2.23}$$

Its real eigenvalues satisfy the tracelessness condition $\sum_{\alpha=1}^4 Q_\alpha = 0$.[7]

Using the eigenvectors of Q_B^A, we can define the projected on-shell states $|k\rangle_\alpha = \bar{u}_\alpha^A |k\rangle_A$. Such states allow us to rewrite the action of the $SU(4)$ flow operator (2.22) on, e.g., a single-particle gluino state $|k\rangle_A$, in a form analogous to the diagonal action of the energy flow operator in (2.13). Indeed, the charge flow operator (2.22) acts diagonally on the projected states $|k\rangle_\alpha$,

$$\mathcal{Q}(\vec{n}; Q)|k\rangle_\alpha = Q_\alpha \delta^{(2)}(\Omega_{\vec{k}} - \Omega_{\vec{n}})|k\rangle_\alpha. \tag{2.24}$$

The contribution of the gluino state to (2.11) can be written in two equivalent forms, $\sum_A |k\rangle_A \langle k|^A = \sum_\alpha |k\rangle_A \bar{u}_\alpha^A u_B^\alpha \langle k|^B = \sum_\alpha |k\rangle_\alpha \langle k|^\alpha$. Then, the action of the charge flow operator $\mathcal{Q}(\vec{n}; Q)$ takes a diagonal form in the new basis:

$$\begin{aligned}\mathcal{Q}(\vec{n}; Q)\sum_{A=1}^{4} |k\rangle_A \langle k|^A &= \big(\delta^{(2)}(\Omega_{\vec{k}} - \Omega_{\vec{n}}) Q_A^B |k\rangle_B\big)\langle k|^A = \mathcal{Q}(\vec{n}; Q)\sum_\alpha |k\rangle_\alpha \langle k|^\alpha \\ &= \sum_{\alpha=1}^{4} |k\rangle_\alpha \big(Q_\alpha \delta^{(2)}(\Omega_{\vec{k}} - \Omega_{\vec{n}})\big)\langle k|^\alpha.\end{aligned} \tag{2.25}$$

[7] The eigenvectors define a unitary matrix, $\bar{u}_\alpha^A = (u_A^\alpha)^*$ and $uu^\dagger = \mathbb{I}$, which diagonalizes the Hermitian projection matrix Q_B^A. They can be interpreted as harmonic variables on the coset $SU(4)/[U(1)]^3$ [22,23].

According to (2.25), the charge detector, described by the flow operator $\mathcal{Q}(\vec{n}; Q)$, decomposes the on-shell state of each particle, propagating in the direction of the vector $\vec{n}$, over the four basis vectors u_A^α in the $SU(4)$ space and assigns a charge Q_α to each component.[8]

Like in (2.16), the charge flow operators depending on two distinct vectors $\vec{n} \neq \vec{n}'$ commute with each other and with the energy flow operators,

$$\big[\mathcal{Q}(\vec{n}; Q), \mathcal{Q}\big(\vec{n}'; Q'\big)\big] = \big[\mathcal{Q}(\vec{n}; Q), \mathcal{E}\big(\vec{n}'\big)\big] = 0. \tag{2.26}$$

Along the same lines as before, we can define the charge flow along various directions $\vec{n}_1, \dots, \vec{n}_\ell$ and express the corresponding weighted cross section as

$$\begin{aligned}\big\langle \mathcal{Q}(\vec{n}_1) \dots \mathcal{Q}(\vec{n}_\ell)\big\rangle &\equiv \sigma_{\mathcal{Q}}(q; \vec{n}_1, \dots, \vec{n}_\ell; Q_1, \dots, Q_\ell; Y) \\ &= \sigma_{\rm tot}^{-1} \int d^4x\, \mathrm{e}^{iqx} \langle 0| O(x, \bar{Y}) \mathcal{Q}(\vec{n}_1, Q_1) \dots \mathcal{Q}(\vec{n}_\ell, Q_\ell) O(0, Y)|0\rangle.\end{aligned} \tag{2.27}$$

Here each detector is specified by the unit vector $\vec{n}_i$ and by the Hermitian matrix $(Q_i)_{A_i}^{B_i}$, where $i = 1, \dots, \ell$. Unlike the case of the energy correlations in (2.18), this weighted cross section has a non-trivial dependence on the isotopic variables Q and Y (see Eq. (3.9) below).

2.2.3. Scalar flow

The definition of the energy and charge flow, Eqs. (2.14) and (2.19), respectively, involves two of the conserved currents of the $\mathcal{N} = 4$ SYM theory, the energy–momentum tensor $T_{\mu\nu}(x)$ and the R-current $(J_\mu)_A^B$. As was already mentioned, they belong to the same $\mathcal{N} = 4$ stress-tensor supermultiplet whose lowest-weight state is the half-BPS scalar operator $O_{\mathbf{20'}}^{IJ}(x)$, Eq. (2.1). This suggests to introduce, in addition to the energy and charge flow, a 'scalar flow' operator corresponding to $O_{\mathbf{20'}}^{IJ}(x)$,

$$\mathcal{O}^{IJ}(\vec{n}) = \int_0^\infty dt \lim_{r\to\infty} r^2 O_{\mathbf{20'}}^{IJ}(t, r\vec{n}). \tag{2.28}$$

These three flow operators have scaling dimensions

$$\Delta_{\mathcal{O}} = -1, \qquad \Delta_{\mathcal{Q}} = 0, \qquad \Delta_{\mathcal{E}} = 1, \tag{2.29}$$

respectively, as follows from the dimensions $\Delta_O = 2$, $\Delta_J = 3$, $\Delta_T = 4$ of the defining operators $O^{IJ}(x)$, $(J_\mu)_A^B(x)$ and $T^{\mu\nu}(x)$. The fact that the scaling dimension of $\mathcal{O}$ is negative has important consequences, as we demonstrate below. Yet another basic difference of $O_{\mathbf{20'}}^{IJ}$ compared to $(J_\mu)_A^B$ and $T^{\mu\nu}$ is that it is a Lorentz scalar and is not a conserved current. Since the operators O^{IJ}, $(J_\mu)_A^B$ and $T^{\mu\nu}$ belong to the same supermultiplet, we anticipate that the correlations of the corresponding flow operators $\mathcal{O}$, $\mathcal{Q}$ and $\mathcal{E}$ should be related to each other by supersymmetry. In Section 6, we provide a lot of evidence for such relations, but the precise mechanism will be worked out in our future work.

[8] This decomposition corresponds to introducing the Cartan basis for the Lie algebra $su(4)$. The charges Q_α can be interpreted as linear combinations of the three Cartan charges.

The expression for the scalar flow operator (2.28) in terms of the free scalar fields looks as[9]

$$\mathcal{O}^{IJ}(\vec{n}) = \frac{1}{2}\int \frac{d^4k}{(2\pi)^4} 2\pi\delta_+\big(k^2\big)k_0^{-1}\delta^{(2)}(\Omega_{\vec{n}} - \Omega_{\vec{k}})a^{\dagger\{I}(k)a^{J\}}(k), \tag{2.30}$$

where $a^{I\dagger}(k)$ and $a^J(k)$ are the creation and annihilation operators of scalars in $SO(6)$ notations (see Appendix B) and $\{IJ\}$ denotes traceless symmetrization of the pair of $SO(6)$ indices I and J. The operator $\mathcal{O}^{IJ}(\vec{n})$ acts non-trivially only on the scalar on-shell states, $|k\rangle^I \equiv a^{\dagger I}(k)|0\rangle$, by rotating them in the isotopic $SO(6)$ space. What is the most unusual about (2.30) is the inverse power of the energy (in the rest frame of the source $q^\mu = (q^0, \vec{0})$). Its presence is a consequence of the negative dimension (-1) of the operator $\mathcal{O}(\vec{n})$ (see (2.29)).

To define the corresponding scalar flow operator we introduce, in close analogy with (2.22), the following projection of the operators (2.30),

$$\mathcal{O}(\vec{n}; S) = S_{IJ}\mathcal{O}^{IJ}(\vec{n}). \tag{2.31}$$

Since $\mathcal{O}^{IJ}(\vec{n})$ is symmetric and traceless, the projection matrix S_{IJ} has to have the same properties. In addition, the reality condition on the detector measurement leads to the reality condition $S_{IJ} = S^*_{IJ}$. This allows us to decompose S_{IJ} over its real eigenvectors,

$$S_{IJ} = \sum_{i=1}^{6} S_i\phi_I^i\phi_J^i, \qquad \sum_{I=1}^{6}\phi_I^i\phi_I^j = \delta^{ij}, \qquad \sum_{i=1}^{6}\phi_I^i\phi_J^i = \delta_{IJ}, \tag{2.32}$$

with real eigenvalues S_i. The condition for S_{IJ} to be traceless leads to $\sum_{i=1}^{6} S_i = 0$.[10]

Then, the scalar flow operator (2.30) takes the following form

$$\mathcal{O}(\vec{n}; S) = \frac{1}{2}\sum_{i=1}^{6} S_i \int \frac{d^4k}{(2\pi)^4} 2\pi\delta_+\big(k^2\big)k_0^{-1}\delta^{(2)}(\Omega_{\vec{n}} - \Omega_{\vec{k}})\big(\phi^i a^\dagger(k)\big)\big(\phi^i a(k)\big), \tag{2.33}$$

and it is diagonalized by the projected on-shell scalar states $|k\rangle^i = \phi_I^i|k\rangle^I$:

$$\begin{aligned}\mathcal{O}(\vec{n}; S)\sum_{I=1}^{6}|k\rangle^I\langle k|^I &= (2k_0)^{-1}\delta^{(2)}(\Omega_{\vec{k}} - \Omega_{\vec{n}})\sum_{I,J=1}^{6} S_{IJ}|k\rangle^J\langle k|^I \\ &= \mathcal{O}(\vec{n}; S)\sum_{i=1}^{6}|k\rangle^i\langle k|^i = \sum_{i=1}^{6}|k\rangle^i\left(\frac{S_i}{2k_0}\delta^{(2)}(\Omega_{\vec{k}} - \Omega_{\vec{n}})\right)\langle k|^i.\end{aligned} \tag{2.34}$$

The interpretation of (2.34) is similar to that of (2.25) for the charge flow. The scalar flow operator decomposes the on-shell scalar state moving in the direction of the vector $\vec{n}$ over the basis of eigenvectors (or $SO(6)$ harmonics) ϕ_I^i and assigns to each component an eigenvalue S_i divided by (twice) the energy of the particle.

[9] The additional factor of 1/2 on the right-hand side is due to our normalization of the gauge group generators $\mathrm{tr}[T^aT^b] = \delta_{ab}/2$.

[10] The eigenvectors define an $SO(6)$ matrix, $\phi\phi^T = \mathbb{I}$, which diagonalizes the projection matrix S_{IJ}. They play the role of harmonic variables on the coset $SO(6)/[SO(2)]^3$.

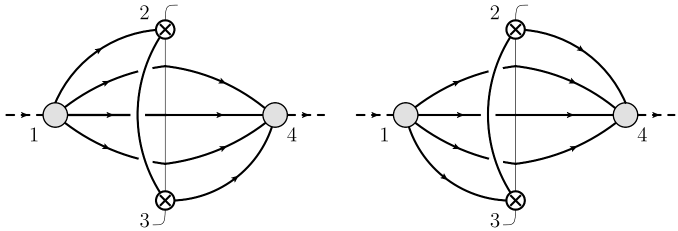

Fig. 3. Cross-talk between the two detectors. The thin line stands for the unitarity cut. The shaded blobs (vertices 1 and 4) stand for the source and sink. The crosses denote the two detectors (vertices 2 and 3) oriented along the vectors $\vec{n}$ and $\vec{n}'$. The detectors interact with each other by exchanging a particle with zero momentum.

Notice the appearance of the inverse energy factor in the last relation in (2.34). It leads to some unusual properties of the scalar flow operator (2.33) as compared to its energy and charge counterparts. To show this, we examine the commutator $[\mathcal{O}(\vec{n};S),\mathcal{O}(\vec{n}';S')]$. Since each operator receives contributions from particles propagating along two different directions $\vec{n}$ and $\vec{n}'$, we may expect that

$$\mathcal{O}(\vec{n};S)\mathcal{O}\big(\vec{n}';S'\big)|k\rangle \sim \delta^{(2)}(\Omega_{\vec{k}}-\Omega_{\vec{n}})\delta^{(2)}(\Omega_{\vec{k}}-\Omega_{\vec{n}'})|k\rangle = 0. \tag{2.35}$$

Hence, the commutator should vanish since the same particle cannot go through the two detectors simultaneously. This is correct unless the momentum of the particle vanishes. Indeed, for $\vec{n}\neq\vec{n}'$, the conditions imposed by the two delta functions, $\vec{k}=k^0\vec{n}=k^0\vec{n}'$, are verified only if $k^0=\vec{k}=0$. Thus, the commutator $[\mathcal{O}(\vec{n};S),\mathcal{O}(\vec{n}';S')]$ can receive contributions only from particles with zero momentum. The corresponding Feynman diagrams are shown in Fig. 3. Carefully examining their contributions (see Appendix A), we find that, precisely due to the factor of $1/k_0$ in (2.33), the commutator is different from zero,

$$\big[\mathcal{O}(\vec{n};S),\mathcal{O}\big(\vec{n}';S'\big)\big] \sim \frac{a^{\dagger I}(0)(SS'-S'S)_{IJ}a^J(0)}{1-(\vec{n}\vec{n}')}. \tag{2.36}$$

At the same time, the scalar flow operator commutes with those of the energy and charge flow,

$$\big[\mathcal{O}(\vec{n};S),\mathcal{E}\big(\vec{n}'\big)\big] = \big[\mathcal{O}(\vec{n};S),\mathcal{Q}\big(\vec{n}';Q\big)\big] = 0. \tag{2.37}$$

The non-vanishing commutator (2.36) leads to a divergence in certain weighted cross sections, as explained later in the paper.

We observe that the expression on the right-hand side of (2.36) involves the commutator of the matrices defining the two scalar detectors. Therefore, we can restore the commutativity of the operators $\mathcal{O}(\vec{n};S)$ and $\mathcal{O}(\vec{n}';S')$ by requiring

$$\big[S,S'\big]=0. \tag{2.38}$$

In physical terms, this condition prohibits the cross-talk between the two detectors mediated by the exchange of particles with zero momentum. Notice that while this is a necessary condition on the detector matrices, which eliminates potentially divergent contributions due to particle exchanges with zero energy, it is not sufficient when we try to match the weighted cross sections with the integrated correlation functions. The latter require further constraints on the projection matrices S, see Appendix D for details.

Having defined the scalar flow operator (2.33), we can introduce the corresponding multiple-detector weighted cross section

$$\langle\mathcal{O}(\vec{n}_1)\dots\mathcal{O}(\vec{n}_\ell)\rangle \equiv \sigma_{\mathcal{S}}(q;\vec{n}_1,\dots,\vec{n}_\ell;S_1,\dots,S_\ell;Y)$$
$$= \sigma_{\rm tot}^{-1}\int d^4x\, e^{iqx}\langle 0|O(x,\bar{Y})\mathcal{O}(\vec{n}_1,S_1)\dots\mathcal{O}(\vec{n}_\ell,S_\ell)O(0,Y)|0\rangle. \quad (2.39)$$

It depends on a set of vectors $\vec{n}_i$ determining the spatial orientation of the detectors, as well as on the projection matrices S_i, Eq. (2.32). By construction, the scalar flow operators $\mathcal{O}(\vec{n}_i, S_i)$ should commute with each other.

In addition to (2.18), (2.27) and (2.39), we can also define mixed correlations involving all three flow operators, $\mathcal{O}(\vec{n}_i, S_i)$, $\mathcal{Q}(\vec{n}_i, Q_i)$ and $\mathcal{E}(\vec{n}_i)$. As was already mentioned, they are effectively related to each other by supersymmetry. The scalar correlations (2.39) play a special role in our analysis below. Firstly, they can be expressed in terms of the correlation function involving $\ell + 2$ copies of the same half-BPS operator (2.1). Secondly, in the special case $\ell = 2$ the correlation function of the half-BPS operators $O(x)$ uniquely determines, by means of $\mathcal{N} = 4$ supersymmetry transformations, all four-point correlation functions of the other operators from the stress-energy multiplet that generate charge and energy flow correlations. This is not the case for $\ell > 2$ since the solution to the corresponding $\mathcal{N} = 4$ superconformal Ward identities is not unique anymore due to the appearance of nontrivial $\mathcal{N} = 4$ superconformal invariants depending on $2 + \ell \geq 5$ points.

We would like to emphasize that, in virtue of the definition of the flow operators (2.14), (2.19) and (2.28), the weighted cross sections (2.18), (2.27) and (2.39) are related to the integrated Wightman correlation functions defined at spatial infinity. This makes the issue of infrared finiteness of the flow correlations extremely nontrivial. It is believed that the energy flow correlations are IR finite both at weak and strong coupling whereas for the scalar and R-charge flow observables the situation remains unclear. As a counterexample, we can recall that similar problem also arose in QCD, where the flavor observables in jet physics (closely related to charge flow correlations) while perfectly well-defined at leading order of the perturbative expansion, cease to stay finite once higher order corrections are accounted for [24]. The problem requires further studies and will be addressed elsewhere.

3. Weighted cross sections from amplitudes

In this section we employ the conventional approach based on the scattering amplitudes to evaluate the weighted cross sections introduced in the previous section to lowest order in the coupling in $\mathcal{N} = 4$ SYM.

We start by computing the matrix elements (2.4) involving the operator defined in (2.2). At tree level, the final state consists of a pair of scalars denoted by $|\mathrm{s}^I(k_1)\mathrm{s}^J(k_2)\rangle$:

$$\sigma_0 = |\mathcal{M}_{O_{\mathbf{20'}}\to \mathrm{ss}}|^2 = \big|\langle \mathrm{s}(k_1)\mathrm{s}(k_2)\big|O(0,Y)|0\rangle\big|^2 = \frac{1}{2}\big(N_c^2-1\big)(Y\bar{Y})^2. \quad (3.1)$$

To first order in the coupling, the final state also contains three-particle states $|X\rangle = |\mathrm{s},\mathrm{s},\mathrm{g}\rangle$ and $|X\rangle = |\mathrm{s},\lambda,\lambda\rangle$. The corresponding transition amplitudes are

$$|\mathcal{M}_{O_{\mathbf{20'}}\to \mathrm{ssg}}|^2 = \big|\langle \mathrm{s}(k_1)\mathrm{s}(k_2)\mathrm{g}(k_3)\big|O(0,Y)|0\rangle\big|^2 = g^2\sigma_0\frac{4s_{12}}{s_{13}s_{23}},$$
$$|\mathcal{M}_{O_{\mathbf{20'}}\to \mathrm{s}\lambda\lambda}|^2 = \big|\langle \lambda(k_1)\lambda(k_2)\mathrm{s}(k_3)\big|O(0,Y)|0\rangle\big|^2 = g^2\sigma_0\frac{8}{s_{12}}, \quad (3.2)$$

where the notation was introduced for the Mandelstam invariants $s_{ij} = (k_i + k_j)^2$ with $k_i^2 = 0$.

The total transition probability (2.5) is given to order $O(g^2)$ by

$$\sigma_{\rm tot}(q) = \int {\rm dPS}_2\, |\mathcal{M}_{O_{\mathbf{20'}}\to {\rm ss}}|^2 + \int {\rm dPS}_3\, \big(|\mathcal{M}_{O_{\mathbf{20'}}\to {\rm ssg}}|^2 + |\mathcal{M}_{O_{\mathbf{20'}}\to {\rm s}\lambda\lambda}|^2\big) + O\big(g^4\big)$$
$$= \frac{\sigma_0}{8\pi}\big[1 + g^2 F_{\rm virt}\big(q^2\big)\big] + 4g^2\sigma_0 \int {\rm dPS}_3\, \frac{s_{12}^2 + 2s_{13}s_{23}}{s_{12}s_{13}s_{23}} + O\big(g^4\big), \tag{3.3}$$

where $F_{\rm virt}(q^2)$ describes the one-loop (virtual) correction to the transition amplitude (3.1) and the notation was introduced for the Lorentz invariant integration measure on the phase space of ℓ massless particles with total momentum q^μ,

$$\int {\rm dPS}_\ell = \int \left(\prod_{i=1}^{\ell} \frac{d^4 k_i}{(2\pi)^4}\, 2\pi\,\delta_+\big(k_i^2\big)\right)(2\pi)^4 \delta^{(4)}\left(q - \sum_{i=1}^{\ell} k_i\right). \tag{3.4}$$

The symmetry of this integration measure under the exchange of any pair of particles allows us to rewrite (3.3) as

$$\sigma_{\rm tot}(q) = \frac{\sigma_0}{8\pi} + g^2\frac{\sigma_0}{8\pi}\left[F_{\rm virt}\big(q^2\big) + \int {\rm dPS}_3\, \frac{32\pi(q^2)^2}{3s_{12}s_{13}s_{23}}\right] + O\big(g^4\big), \tag{3.5}$$

where we symmetrized the one-loop integrand with respect to the particle momenta and used the identity $q^2 = s_{12} + s_{23} + s_{13}$.

As was already mentioned, the total transition amplitude $\sigma_{\rm tot}(q)$ is protected from perturbative corrections and, therefore, the terms proportional to g^2 on the right-hand side of (3.5) should vanish. This allows us to fix the virtual correction $F_{\rm virt}(q^2)$.[11] Taking into account (3.1) we verify that the resulting expression for $\sigma_{\rm tot}(q)$ coincides with (2.10).

3.1. Single detector

Let us now examine the weighted cross sections involving a single detector. We start with the energy flow. According to the definition (2.11), the corresponding cross section can be obtained from the first relation in (3.3) by inserting the energy weight factor (2.12) into the phase space integrals. The weight factor $w_{\mathcal{E}(\vec{n})}(k_1, k_2)$ for the transition $\mathcal{M}_{O_{\mathbf{20'}}\to {\rm ss}}$ depends on the energy of the two scalars (in the rest frame of the source), whereas for $\mathcal{M}_{O_{\mathbf{20'}}\to {\rm ssg}}$ and $\mathcal{M}_{O_{\mathbf{20'}}\to {\rm s}\lambda\lambda}$ it is given by $w_{\mathcal{E}(\vec{n})}(k_1, k_2, k_3)$ that receives additive contributions from all produced particles, as seen from Eq. (2.12). In this way, we obtain

$$\sigma_{\mathcal{E}}(q;\vec{n}) = \sigma_{\rm tot}^{-1} \int {\rm dPS}_2\, w_{\mathcal{E}}(k_1, k_2)|\mathcal{M}_{O_{\mathbf{20'}}\to {\rm ss}}|^2$$
$$+ \sigma_{\rm tot}^{-1} \int {\rm dPS}_3\, w_{\mathcal{E}}(k_1, k_2, k_3)\big(|\mathcal{M}_{O_{\mathbf{20'}}\to {\rm ssg}}|^2 + |\mathcal{M}_{O_{\mathbf{20'}}\to {\rm s}\lambda\lambda}|^2\big)$$
$$+ O\big(g^4\big). \tag{3.6}$$

Replacing the matrix elements on the right-hand side by their explicit expressions (3.1) and (3.2), we symmetrize the integrands with respect to the particle momenta and find, after a simple calculation,

[11] Strictly speaking, both terms in the square brackets in (3.5) are IR divergent and require regularization. Their sum vanishes in the dimensional regularization scheme.

$$\big\langle\mathcal{E}(\vec{n})\big\rangle \equiv \sigma_{\mathcal{E}}(q;\vec{n}) = \frac{1}{8\pi}\int \mathrm{dPS}_2 \sum_{i=1,2} k_i^0 \delta^{(2)}(\Omega_{\vec{k}_i} - \Omega_{\vec{n}}) = \frac{1}{4\pi} q^0. \tag{3.7}$$

Notice that this expression does not depend on the coupling constant. In Section 4 we show that $\langle\mathcal{E}(\vec{n})\rangle$ is indeed protected from loop corrections.[12] We verify that the integral of (3.7) over $\vec{n}$ correctly reproduces the total energy, $\int d^2\Omega_{\vec{n}} \langle\mathcal{E}(\vec{n})\rangle = q_0$, in agreement with the results in [13].

For the charge flow the analysis goes along the same lines, with the only difference that the non-trivial weight factor $w_{\mathcal{Q}}$ is different from zero only for scalars and gluinos carrying non-zero R-charges. As explained in Section 2.2.2, the charge flow operator introduces the projection (or 'polarization') matrix Q_A^B for the $SU(4)$ states of these particles. More precisely, at tree level, the contribution of the transition $\mathcal{M}_{O_{\mathbf{20'}}\to\mathrm{ss}}$ to the total transition probability involves the R-symmetry factor (in $SU(4)$ notation, see Appendix B) $|\mathcal{M}_{O_{\mathbf{20'}}\to\mathrm{ss}}|^2 \sim y_{A_1B_1} y_{A_2B_2} \bar{y}^{A_1B_1} \bar{y}^{A_2B_2} = \mathrm{tr}(y\bar{y})^2$. Here the sum over the $SU(4)$ indices corresponds to the summation over the quantum numbers of the particles propagating in the final state. The contribution to the weighted cross section reads

$$\begin{aligned} & y_{A_1B_1}\big[2Q^{A_1}_{A_1'}\delta^{(2)}(\Omega_{\vec{k}_1} - \Omega_{\vec{n}})\big]\bar{y}^{A_1'B_1} y_{A_2B_2}\bar{y}^{A_2B_2} \\ &\quad + y_{A_1B_1}\bar{y}^{A_1B_1} y_{A_2B_2}\big[2Q^{A_2}_{A_2'}\delta^{(2)}(\Omega_{\vec{k}_2} - \Omega_{\vec{n}})\big]\bar{y}^{A_2'B_2} \\ & = 2\,\mathrm{tr}(y\bar{y})\,\mathrm{tr}(yQ\bar{y})\big[\delta^{(2)}(\Omega_{\vec{k}_1} - \Omega_{\vec{n}}) + \delta^{(2)}(\Omega_{\vec{k}_2} - \Omega_{\vec{n}})\big], \end{aligned} \tag{3.8}$$

where the last expression is the corresponding weight factor.[13] Inserting this result in the phase space integral $\int \mathrm{dPS}_2\, |\mathcal{M}_{O_{\mathbf{20'}}\to ss}|^2$ and taking into account (3.1) and (B.5), we obtain

$$\big\langle\mathcal{Q}(\vec{n})\big\rangle \equiv \sigma_{\mathcal{Q}}\big(q;(\vec{n},Q);y\big) = \frac{\langle Q\rangle}{4\pi}\int \mathrm{dPS}_2 \sum_{i=1,2} \delta^{(2)}(\Omega_{\vec{k}_i} - \Omega_{\vec{n}}) = \frac{1}{\pi}\langle Q\rangle, \tag{3.9}$$

where $\langle Q\rangle$ is an isotopic factor keeping track of the R-charges,

$$\langle Q\rangle = \frac{\mathrm{tr}(yQ\bar{y})}{\mathrm{tr}(y\bar{y})}. \tag{3.10}$$

To first order in the coupling constant, the correction to (3.9) has the same form as (3.6) with the only difference that the corresponding charge weight factor is given by an expression analogous to (3.8). Calculating the $O(g^2)$ correction to (3.9) we find that it vanishes (see footnote 12).

Finally, for the scalar flow, the weight factor $w_{\mathcal{O}}$ is different from zero only for scalar particles. According to (2.34), for a scalar with momentum k_i in the final state, the insertion of the weight factor modifies the $SO(6)$ tensor structure as follows:

$$Y^I\delta^{IJ}\bar{Y}^J \to Y^I\bigg(\big(k_i^0\big)^{-1}\delta^{(2)}(\Omega_{\vec{k}_i} - \Omega_{\vec{n}})\frac{1}{2}S^{IJ}\bigg)\bar{Y}^J, \tag{3.11}$$

where S^{IJ} is the projection matrix of the scalar detector. Repeating the calculation at Born level we obtain

$$\big\langle\mathcal{O}(\vec{n})\big\rangle \equiv \sigma_{\mathcal{O}}\big(q;(\vec{n},S);Y\big) = \frac{\langle S\rangle}{16\pi}\int \mathrm{dPS}_2 \sum_{i=1,2} \big(k_i^0\big)^{-1}\delta^{(2)}(\Omega_{\vec{k}_i} - \Omega_{\vec{n}}) = \frac{1}{2\pi}\frac{\langle S\rangle}{q^0}, \tag{3.12}$$

[12] This property is related to the well-known fact that the three-point functions of half-BPS multiplets are protected [15,16,18,17,19], see Section 4.

[13] The factor of 2 takes into account that the charge flow operator rotates both indices of y_{AB} (we recall that $y_{AB} = -y_{BA}$).

where $\langle S\rangle$ is an isotopic factor keeping track of the tensor structure,

$$\langle S\rangle = \frac{(YS\bar{Y})}{(Y\bar{Y})}, \tag{3.13}$$

with $(YS\bar{Y}) \equiv Y^I S_{IJ} \bar{Y}^J$. The calculation of the $O(g^2)$ correction to this expression shows that it vanishes in the same manner as for $\langle\mathcal{E}(\vec{n})\rangle$ and $\langle\mathcal{Q}(\vec{n})\rangle$ (see footnote 12).

We recall that the expressions for the one-point correlations (3.7), (3.9) and (3.12) were obtained in the rest frame of the source, $q^\mu = (q^0, \vec{0})$. We present the same expressions in Lorentz covariant form in Section 4.3.

3.2. Double correlations

In the previous subsection we have shown that the single-detector weighted cross sections (3.7), (3.9) and (3.12) do not depend on the spatial orientation of the detector $\vec{n}$. For weighted cross sections involving two detectors oriented along the vectors $\vec{n}$ and $\vec{n}'$, the rotation symmetry implies that they can only depend on the relative angle $0 \le \theta \le \pi$ between the vectors, $(\vec{n}\cdot\vec{n}') = \cos\theta$. We call such observables 'double correlations'. For $\theta = 0$ the orientations of the two detectors coincide so that the same particle can go through them sequentially. For $\theta = \pi$ the detectors capture particles moving back-to-back in the rest frame of the source.

The calculation of the double correlations at one loop goes along the same lines as in the previous subsection. For the double energy correlation $\langle\mathcal{E}(\vec{n})\mathcal{E}(\vec{n}')\rangle$, the only difference as compared with (3.6) is that the weight factor $w_{\mathcal{E}}(\vec{n})$ gets replaced by the product $w_{\mathcal{E}}(\vec{n})w_{\mathcal{E}}(\vec{n}')$, which fixes the spatial orientation of the momenta of the two particles in the final state.

At Born level, the final state consists of two scalar particles moving collinearly in the rest frame $q^\mu = (q^0, \vec{0})$, each carrying energy $q^0/2$. As a consequence, their contribution to $\langle\mathcal{E}(\vec{n})\mathcal{E}(\vec{n}')\rangle$ is localized at $\theta = 0$ and $\theta = \pi$,

$$\big\langle\mathcal{E}(\vec{n})\mathcal{E}(\vec{n}')\big\rangle^{(0)} = \frac{q_0^2}{8\pi}\big[\delta(\theta) + \delta(\pi - \theta)\big]. \tag{3.14}$$

Here the first delta-function describes the situation of aligned detectors capturing particles moving into the same direction, while the second delta-function corresponds to two particles moving back-to-back. For $0 < \theta < \pi$, the double-energy correlation receives a non-zero contribution starting from one loop. It comes from the three-particle transitions $\mathcal{M}_{O_{\mathbf{20'}}\to \mathrm{ssg}}$ and $\mathcal{M}_{O_{\mathbf{20'}}\to \mathrm{s}\lambda\lambda}$,

$$\begin{aligned}\big\langle\mathcal{E}(\vec{n})\mathcal{E}(\vec{n}')\big\rangle = \sigma_{\mathrm{tot}}^{-1} \int \mathrm{dPS}_3 \sum_{i,j=1}^{3} k_i^0 k_j^0 \delta^{(2)}(\Omega_{\vec{k}_i} - \Omega_{\vec{n}})\delta^{(2)}(\Omega_{\vec{k}_j} - \Omega_{\vec{n}'}) \\ \times \big(|\mathcal{M}_{O_{\mathbf{20'}}\to \mathrm{s}(k_1)\mathrm{s}(k_2)\mathrm{g}(k_3)}|^2 + |\mathcal{M}_{O_{\mathbf{20'}}\to \mathrm{s}(k_1)\lambda(k_2)\lambda(k_3)}|^2\big).\end{aligned} \tag{3.15}$$

Using the explicit expressions for the matrix elements (3.2) we find (see Appendix C for details)

$$\begin{aligned}\big\langle\mathcal{E}(\vec{n})\mathcal{E}(\vec{n}')\big\rangle &= \frac{g^2}{2(2\pi)^4}\frac{q_0^2}{\sin^2\theta}\int_0^1 \frac{d\tau_1}{1 - \tau_1(1 - \cos\theta)/2} + O(g^4) \\ &= \frac{g^2}{(2\pi)^4} q_0^2 \frac{1 + \cos\theta}{\sin^4\theta} \ln\frac{2}{1 + \cos\theta} + O\big(g^4\big),\end{aligned} \tag{3.16}$$

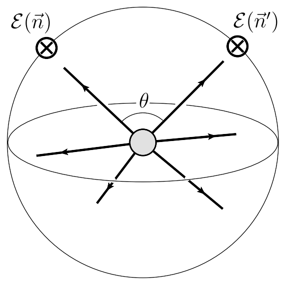

Fig. 4. Graphical representation of the double energy correlation: particles produced out of the vacuum by the source are captured by the two detectors located at spatial infinity in the directions of the unit vectors $\vec{n}$ and $\vec{n}'$.

where the logarithmic correction arises from the integration over the energy fraction of one of the particles, $\tau_1 = 2k_1^0/q^0$. For $\theta \to 0$, the expression on the right-hand side of (3.16) scales as $O(\theta^{-2})$, whereas for $w = \pi - \theta \to 0$ it has the well-known Sudakov behavior $O(w^{-2}\ln(w^{-2}))$. Both asymptotics are modified at higher loops in a controllable way [25].

It is convenient to rewrite (3.16) by introducing the scaling variable

$$z = (1 - \cos\theta)/2, \tag{3.17}$$

where $0 < \theta < \pi$ is the angle between the detector vectors $\vec{n}$ and $\vec{n}'$. Then, the double-energy correlation takes the following form at one loop

$$\big\langle \mathcal{E}(\vec{n})\mathcal{E}(\vec{n}')\big\rangle = \frac{a}{4\pi^2}\frac{q_0^2}{8z^3}\left(-\frac{z\ln(1-z)}{1-z}\right) + O\big(a^2\big), \tag{3.18}$$

with z varying in the range $0 < z < 1$ and $a = g^2/(4\pi^2)$, as defined earlier. It is instructive to compare (3.18) with the analogous expression in QCD. In that case, the final state is created by an electromagnetic current and it consists of quarks and gluons. To lowest order in the coupling, the energy–energy correlation looks as [4]

$$\begin{aligned}\big\langle \mathcal{E}(\vec{n})\mathcal{E}(\vec{n}')\big\rangle_{\text{QCD}} = \frac{a_{\text{QCD}}}{4\pi^2}\frac{q_0^2}{8z^3}\bigg[&\left(-\frac{z}{1-z} + \frac{9}{z^2} - \frac{15}{z} + 3\right)\ln(1-z) \\ &+ \left(\frac{9}{z} - \frac{3}{2(1-z)} - 9\right)\bigg] + O\big(a_{\text{QCD}}^2\big),\end{aligned} \tag{3.19}$$

where $a_{\text{QCD}} = g_{\text{QCD}}^2 C_2/(4\pi^2)$ is the QCD fine structure coupling constant (with $C_2 = (N_c^2 - 1)/(2N_c)$ being the quadratic Casimir in the fundamental representation of the $SU(N_c)$).

We observe that the $\mathcal{N} = 4$ SYM result (3.18) can be obtained from the QCD expression (3.19) by discarding the rational term inside the square brackets in (3.19) and by retaining only the leading singularity for $z \to 1$ in the $\ln(1-z)$ term. In other words, the two expressions have the same leading asymptotic Sudakov behavior as $z \to 1$. According to (3.17), this limit corresponds to the two detectors capturing particles moving back-to-back in the rest frame of the source (see Fig. 4).

For the double-scalar correlation $\langle \mathcal{O}(\vec{n})\mathcal{O}(\vec{n}')\rangle$ the weights corresponding to the particles in the final state of $\mathcal{M}_{O_{\mathbf{20'}} \to X}$ also depend on the detector matrices S and S'. For $0 < \theta < \pi$, to one-loop order, it reduces to the product of isotopic factors $\langle S\rangle\langle S'\rangle$ from the single detector correlation (3.12):

$$\big\langle\mathcal{O}(\vec{n})\mathcal{O}\big(\vec{n}'\big)\big\rangle=\sigma_{\rm tot}^{-1}\int \mathrm{dPS}_3\big(k_1^0k_2^0\big)^{-1}2\delta^{(2)}(\Omega_{\vec{k}_1}-\Omega_{\vec{n}})\delta^{(2)}(\Omega_{\vec{k}_2}-\Omega_{\vec{n}'})$$
$$\times\,(YS\bar{Y})\big(YS'\bar{Y}\big)|\mathcal{M}_{O_{\mathbf{20'}}\to \mathrm{s}(k_1)\mathrm{s}(k_2)\mathrm{g}(k_3)}|^2, \tag{3.20}$$

where the additional factor of 2 comes from the symmetry of the weight factor under exchanging the detectors, $\vec{n}\leftrightarrow\vec{n}'$. Performing the integration over the phase space of the three particles in the final state of $\mathcal{M}_{O_{\mathbf{20'}}\to \mathrm{ssg}}$, we obtain (see Appendix C)

$$\big\langle\mathcal{O}(\vec{n})\mathcal{O}\big(\vec{n}'\big)\big\rangle=\frac{a}{4\pi^2}\frac{\langle S\rangle\langle S'\rangle}{2q_0^2 z}\left(-\frac{z\ln(1-z)}{1-z}\right)+O\big(a^2\big), \tag{3.21}$$

with $0<z<1$.

For the double-charge correlation $\langle\mathcal{Q}(\vec{n})\mathcal{Q}(\vec{n}')\rangle$, with $0<\theta<\pi$, we have to take into account all possible correlations between the charges of scalars and gluinos in the final state

$$\big\langle\mathcal{Q}(\vec{n})\mathcal{Q}\big(\vec{n}'\big)\big\rangle=2\sigma_{\rm tot}^{-1}\int \mathrm{dPS}_3\Big[4\,\mathrm{tr}(yQ\bar{y})\,\mathrm{tr}\big(yQ'\bar{y}\big)\delta^{(2)}(\Omega_{\vec{k}_1}-\Omega_{\vec{n}})\delta^{(2)}(\Omega_{\vec{k}_2}-\Omega_{\vec{n}'})$$
$$\times\big(|\mathcal{M}_{O_{\mathbf{20'}}\to \mathrm{s}(k_1)\mathrm{s}(k_2)\mathrm{g}(k_3)}|^2+|\mathcal{M}_{O_{\mathbf{20'}}\to \mathrm{s}(k_1)\lambda(k_2)\lambda(k_3)}|^2\big)$$
$$+\,\mathrm{tr}[y\bar{y}]\,\mathrm{tr}\big[yQ\bar{y}Q'\big]\delta^{(2)}(\Omega_{\vec{k}_2}-\Omega_{\vec{n}})\delta^{(2)}(\Omega_{\vec{k}_3}-\Omega_{\vec{n}'})$$
$$\times\,|\mathcal{M}_{O_{\mathbf{20'}}\to \mathrm{s}(k_1)\lambda(k_2)\lambda(k_3)}|^2\Big], \tag{3.22}$$

where the three last lines describe the correlations between two gluinos. Note that $\mathrm{tr}[yQ\bar{y}Q']=\mathrm{tr}[yQ'\bar{y}Q]$ due to the antisymmetry of the matrices y, $\bar{y}$. The integration over the final state phase space yields

$$\big\langle\mathcal{Q}(\vec{n})\mathcal{Q}\big(\vec{n}'\big)\big\rangle=-\frac{a}{\pi^2}\frac{\ln(1-z)}{4z^2}\left(\frac{2z}{1-z}\langle Q\rangle\big\langle Q'\big\rangle+\big\langle Q,Q'\big\rangle\right)+O\big(a^2\big), \tag{3.23}$$

where $\langle Q\rangle$ is given by (3.10) and the notation was introduced for the (non-factorizable) correlation between the matrices of the two detectors

$$\big\langle Q,Q'\big\rangle\equiv\frac{\mathrm{tr}[yQ\bar{y}Q'+\tilde{\bar{y}}Q\tilde{y}Q']}{2\,\mathrm{tr}[y\bar{y}]}=\frac{\mathrm{tr}[yQ'\bar{y}Q+\tilde{\bar{y}}Q'\tilde{y}Q]}{2\,\mathrm{tr}[y\bar{y}]}, \tag{3.24}$$

with $\tilde{\bar{y}}_{AB}=\frac{1}{2}\epsilon_{ABCD}\bar{y}^{CD}$ and $\tilde{y}^{AB}=\frac{1}{2}\epsilon^{ABCD}y_{CD}$. In the above calculation we have tacitly assumed that the detectors measure two different particles. In general, we also have to examine the possibility for the same particle to go sequentially through the two detectors. As was already explained, for $\vec{n}\neq\vec{n}'$ (or equivalently $\theta\neq 0$) the momentum of the particle should be necessarily zero in this case and, as a result, its contribution to the charge correlations vanishes. The same is true for the scalar correlations provided that the projection matrices of the detectors satisfy the 'no-cross-talk' condition (2.38).

In a similar manner, we can also define mixed correlations involving various flow operators:

$$\big\langle\mathcal{Q}(\vec{n})\mathcal{E}\big(\vec{n}'\big)\big\rangle=\frac{a}{4\pi^2}\langle Q\rangle q^0\left(-\frac{\ln(1-z)}{z^2(1-z)}\right)+O\big(a^2\big),$$
$$\big\langle\mathcal{O}(\vec{n})\mathcal{E}\big(\vec{n}'\big)\big\rangle=\frac{a}{16\pi^2}\langle S\rangle\left(-\frac{\ln(1-z)}{z^2(1-z)}\right)+O\big(a^2\big),$$
$$\big\langle\mathcal{Q}(\vec{n})\mathcal{O}\big(\vec{n}'\big)\big\rangle=\frac{a}{4\pi^2}\langle Q\rangle\big\langle S'\big\rangle\big(q^0\big)^{-1}\left(-\frac{\ln(1-z)}{z(1-z)}\right)+O\big(a^2\big). \tag{3.25}$$

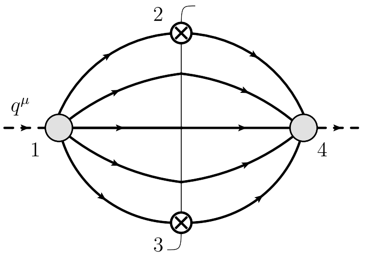

Fig. 5. The relation between the weighted cross section and Wightman correlation function. The operators at points 1 and 4 describe the source and sink, respectively. The operators at points 2 and 3 define the flow operators shown by crosses. ‘$\text{Limit}_{2,3}$’ stands for the detector limit which amounts to sending the operators at point 2 and 3 at null infinity with subsequent integration over their light-cone coordinates (see Eqs. (4.4) and (4.5) below).

Notice that the dependence of these expressions on the total energy q^0 is uniquely fixed by the scaling dimension of the flow operators. The non-trivial dynamical information resides in the z-dependence. Quite remarkably, the obtained one-loop expressions are all proportional to the same function $\ln(1-z)/(1-z)$. Its appearance is not accidental, of course, since it ensures the universal Sudakov behavior of the correlations for $z \to 1$.

The approach described in this section can be extended to higher loops. Namely, to any order in the coupling constant, following (2.11) we can express the correlations as a sum over all possible final states, evaluate the corresponding transition amplitudes (2.4) and, then, perform the integration over the phase space. However, such an approach becomes very cumbersome and inefficient beyond one loop for the following reasons. The number of production channels $O_{\mathbf{20}'} \to X$ grows rapidly at higher loops and, therefore, we have to deal with an increasing number of terms in the sum over the final states. Secondly, with many particles in the final state the integration over their phase space becomes very complicated and cannot be done analytically. Finally, each individual transition amplitude $|\mathcal{M}_{O_{\mathbf{20}'} \to X}|^2$ suffers from infrared divergences and requires regularization. Infrared divergences cancel however in the sum over all final states between contribution involving different number of particles.[14]

In the next section we describe another approach to computing the various double correlations in $\mathcal{N}=4$ SYM. It makes efficient use of the superconformal symmetry of the theory. It also allows us to go to higher loops and even to strong coupling, via the AdS/CFT correspondence.

4. Weighted cross sections from correlation functions

In this section we shall exploit the relation between physical observables and correlation functions involving two half-BPS operators as the source and sink, and various flow operators, Eqs. (2.18), (2.27) and (2.39), as the detectors. Unlike the more familiar Euclidean correlation functions, widely discussed in the $\mathcal{N}=4$ SYM literature, the operators on the right-hand side of (2.18), (2.27) and (2.39) are essentially Minkowskian and are non-time ordered. This means that we will be dealing with Wightman correlation functions. As we have shown in the previous section, they define the charge flow correlations in the detector limit (see Fig. 5).

In this section we explain how the Wightman correlation functions in (2.18), (2.27) and (2.39) can be obtained from their Euclidean counterparts by analytic continuation. The Euclidean corre-

[14] See however the last paragraph in Section 2.

lation functions have singularities at $x_{ij}^2 = 0$, corresponding to short-distance separation between the operators, $x_i \to x_j$. In Minkowski space, additional singularities appear when the operators become light-like separated. In this case the analytic properties of the correlation function crucially depend on the ordering of the operators (time ordering versus Wightman). Therefore, performing the analytic continuation of the correlation functions from Euclid to Minkowski we have to pay special attention to their analytic properties.

4.1. *Lorentz covariant definition of the detectors*

In Section 2.2 we have defined the flow operators (2.14), (2.19) and (2.28) in the rest frame of the source $q^\mu = (q^0, \vec{0})$. To make use of the conformal symmetry of the correlation functions, we have to restore the Lorentz covariance and extend the definitions to any reference frame.

We recall that the time integral in the definition of the flow operators (2.14), (2.19) and (2.28) has the interpretation of the working time of the detector located at the position $r\vec{n}$ relative to the collision point. The space–time coordinate of the detector $x^\mu = (t, r\vec{n})$ can be decomposed in the basis of two light-like vectors,

$$x^\mu = x_+ n^\mu + x_- \bar{n}^\mu, \quad n^\mu = (1, \vec{n}),\ \bar{n}^\mu = (1, -\vec{n}), \tag{4.1}$$

with $x_+ = \frac{1}{2}(t + r) = (x\bar{n})/2$ and $x_- = \frac{1}{2}(t - r) = (xn)/2$. We can restore manifest Lorentz covariance by rescaling each light-like vectors by an *arbitrary* positive scale,

$$n^\mu \to \rho n^\mu, \quad \bar{n}^\mu \to \rho' \bar{n}^\mu, \tag{4.2}$$

with $\rho, \rho' > 0$. This lifts the restriction that the time component of n^μ is equal to 1. Then the covariant definition of the light-cone coordinates in (4.1) looks as

$$x_+ = \frac{(x\bar{n})}{(n\bar{n})}, \qquad x_- = \frac{(xn)}{(n\bar{n})}. \tag{4.3}$$

Notice, however, that covariance can only be maintained if all the expressions we encounter are homogeneous under such *local* rescalings, allowing us to go back to the original form of vectors n and $\bar{n}$ in (4.1). By 'local' we mean that the coordinates of each flow operator should rescale with their own, independent parameter ρ.

The next step is to reformulate the detector limit, $r \to \infty$ and $0 \le t < \infty$, in terms of the light-cone variables $x_\pm$. We illustrate the correct procedure relying on the example of the energy flow. If we just take $r \to \infty$ but keep t fixed, as in the original definition (2.14), we would have $x_\pm \to \pm\infty$ which is clearly too strong. We need to keep one of these variables fixed while taking the other one to infinity. In physical terms, the flow operator admits the following interpretation. We can think of a massless particle captured by the detector as of a wave front propagating in the direction n^μ and spreading along the direction $\bar{n}^\mu$. This suggests to first send the detector to future infinity along, say, the light-cone direction n^μ and then integrate over the position of the massless particles on the wave front along the direction $\bar{n}^\mu$. In terms of the light-cone coordinates this means that we first take the limit $x_+ \to \infty$, whereas x_- remains finite. The time integral in (2.14) then becomes an integral over $-\infty < x_- < \infty$. This brings us to the new definition

$$\mathcal{E}(n) = (n\bar{n}) \int_{-\infty}^{\infty} dx_- \lim_{x_+ \to \infty} x_+^2 T_{++}(x_+ n + x_- \bar{n}), \tag{4.4}$$

in terms of the covariant light-cone component of the stress tensor $T_{++} \equiv \bar{n}^\mu \bar{n}^\nu T_{\mu\nu}(x)/(n\bar{n})^2$. Under the rescaling (4.2) the flow operator transforms homogeneously with the weight (-3), $\mathcal{E} \to \rho^{-3}\mathcal{E}$, as required for maintaining Lorentz covariance.

In a similar manner, we can define the Lorentz covariant generalization of the charge and scalar flow operators, Eqs. (2.19) and (2.28),

$$\mathcal{Q}_A^B(n) = (n\bar{n}) \int_{-\infty}^{\infty} dx_- \lim_{x_+ \to \infty} x_+^2 (J_+)_A^B(x_+ n + x_- \bar{n}),$$
$$\mathcal{O}^{IJ}(n) = (n\bar{n}) \int_{-\infty}^{\infty} dx_- \lim_{x_+ \to \infty} x_+^2 O_{\mathbf{20'}}^{IJ}(x_+ n + x_- \bar{n}), \tag{4.5}$$

where $J_+(x) \equiv \bar{n}^\mu J_\mu(x)/(n\bar{n})$ is the light-cone component of the R-current. They have rescaling weights (-2) and (-1), respectively.

The expressions in the right-hand sides of (4.4) and (4.5) involve the two light-like vectors n and $\bar{n}$, but the dependence on the latter is redundant. To illustrate this point, it is sufficient to rewrite these operators in terms of creation and annihilation operators. For instance, we can start with (4.4) and repeat the calculation of (2.15) to find, with the help of (A.1),

$$\mathcal{E}(n) = \frac{1}{2(2\pi)^3} \int_0^\infty d\tau\, \tau^2 \sum_{i=s,q,g} a_i^\dagger(n\tau) a_i(n\tau), \tag{4.6}$$

so that the dependence on $\bar{n}^\mu$ drops out. Notice that the annihilation/creation operators in (4.6) depend on the momentum $k^\mu = n^\mu \tau$, collinear with the light-like vector defining the space–time orientation of the detector. The charge and scalar flow operators admit similar representations (see Eq. (A.2) for the latter). An important difference is, however, that the corresponding τ-integral measure becomes $\int d\tau\, \tau$ and $\int d\tau$, respectively.

Relation (4.6) (together with the analogous relations for the scalar and charge flow operators) confirms the transformation properties of the flow operators under the rescaling (4.2) derived above. Changing the integration variable $\tau \to \tau/\rho$, we find

$$\mathcal{E}(\rho n) = \rho^{-3}\mathcal{E}(n), \qquad \mathcal{Q}_A^B(\rho n) = \rho^{-2}\mathcal{Q}_A^B(n), \qquad \mathcal{O}^{IJ}(\rho n) = \rho^{-1}\mathcal{O}^{IJ}(n), \tag{4.7}$$

where the factors of ρ are related to the power of τ in the corresponding integral representation. As we show in the next subsection, the requirement of homogeneity under the *independent* rescalings (4.7) of each flow operator imposes a strong constraint on the possible form of the correlations of the flow operators, Eqs. (2.18), (2.27) and (2.39).

4.2. Symmetries

Let us introduce a generic notation $\mathcal{D}_i(n)$ for all flow operators (scalar, charge and energy). We are interested in the symmetry properties of their correlations

$$\langle \mathcal{D}_1(n_1) \dots \mathcal{D}_\ell(n_\ell) \rangle_q = \sigma_{\text{tot}}^{-1} \int d^4x\, e^{iqx} \langle 0| O(x, \bar{Y}) \mathcal{D}_1(n_1) \dots \mathcal{D}_\ell(n_\ell) O(0, Y)|0\rangle. \tag{4.8}$$

Here we introduced the subscript q on the left-hand side to indicate the dependence on the total momentum transferred (see Fig. 5). By construction, the correlation function (4.8) is invariant under permutations of any pair of detectors. In addition, $\langle \mathcal{D}_1(n_1)\dots\mathcal{D}(n_\ell)\rangle_q$ is invariant under Lorentz transformations of the total momentum q^μ and of the light-like vectors n_i^μ defining the detector orientation,

$$\big\langle \mathcal{D}_1(\Lambda n_1)\dots\mathcal{D}_\ell(\Lambda n_\ell)\big\rangle_{\Lambda q} = \big\langle \mathcal{D}_1(n_1)\dots\mathcal{D}_\ell(n_\ell)\big\rangle_q. \tag{4.9}$$

The correlations (4.8) have two additional symmetries related to the independent rescaling of n_i^μ and q^μ. The flow operators are defined in terms of the operators $O_{\mathbf{20'}}$, J^μ and $T^{\mu\nu}$ carrying Lorentz spins 0, 1 and 2, respectively. According to (4.7), the spin controls their transformation properties under the rescaling $n^\mu \to \rho n^\mu$, leading to

$$\big\langle \mathcal{D}_1(\rho_1 n_1)\dots\mathcal{D}_\ell(\rho_\ell n_\ell)\big\rangle_q = \rho_1^{-1-s_1}\dots\rho_\ell^{-1-s_\ell}\big\langle \mathcal{D}_1(n_1)\dots\mathcal{D}_\ell(n_\ell)\big\rangle_q, \tag{4.10}$$

where $s_\mathcal{O} = 0$, $s_\mathcal{Q} = 1$ and $s_\mathcal{E} = 2$.

The other scaling property is related to the rescaling $q^\mu \to \lambda q^\mu$. Since the vectors n_i^μ are dimensionless, this transformation can be compensated by the dilatations $x^\mu \to \lambda^{-1} x^\mu$ of the coordinates,

$$\big\langle \mathcal{D}_1(n_1)\dots\mathcal{D}_\ell(n_\ell)\big\rangle_{\lambda q} = \lambda^{\Delta_1+\dots+\Delta_\ell}\big\langle \mathcal{D}_1(n_1)\dots\mathcal{D}_\ell(n_\ell)\big\rangle_q, \tag{4.11}$$

where Δ_i is the scaling dimension of the flow operator, $\Delta_\mathcal{O} = -1$, $\Delta_\mathcal{Q} = 0$ and $\Delta_\mathcal{E} = 1$. Notice that all three flow operators have the same twist $\Delta - s = -1$.

Relations (4.9)–(4.11) allow us to fix the single-detector correlation of all flow operators up to an overall normalization factor. Denoting by $\mathcal{D}(n; s)$ the flow operator with the spin s and scaling dimension $\Delta = s - 1$, we can write

$$\mathcal{O}(n) = \mathcal{D}(n; 0), \qquad \mathcal{Q}(n) = \mathcal{D}(n; 1), \qquad \mathcal{E}(n) = \mathcal{D}(n; 2). \tag{4.12}$$

By virtue of (4.9), the single-detector correlation $\langle \mathcal{D}(n; s)\rangle$ depends on the two Lorentz invariants (qn) and q^2. The dependence on the former is controlled by the spin s, i.e., by the required degree of homogeneity under the rescalings (4.10). Then the q^2-dependence is fixed by the scaling dimension Δ, resulting in

$$\big\langle \mathcal{D}(n; s)\big\rangle = c_\mathcal{D}\frac{(q^2)^s}{(qn)^{s+1}}. \tag{4.13}$$

For the charge and energy flow correlations, we can fix the normalization constant $c_\mathcal{D}$ by making use of the fact that the flow operator in both cases is determined by a conserved current. As a consequence, integrating over the position of the detector on the sphere $n^\mu = (1, \vec{n})$ with $\vec{n}^2 = 1$ in the rest frame of the source $q^\mu = (q^0, \vec{0})$, we should find the corresponding conserved quantity – the total energy $\int d\Omega_{\vec{n}} \langle \mathcal{E}(\vec{n})\rangle = q^0$ and the total charge $\int d\Omega_{\vec{n}} \langle \mathcal{Q}(\vec{n})\rangle = 4\langle Q\rangle$ of the state.[15] In this way we get

$$c_\mathcal{E} = 1\Big/\int d\Omega_{\vec{n}} = \frac{1}{4\pi}, \qquad c_\mathcal{Q} = \frac{\langle Q\rangle}{\pi}. \tag{4.14}$$

Let us now consider the double-detector correlation $\langle \mathcal{D}(n; s)\mathcal{D}(n'; s')\rangle$. The main difference, compared to the previous case, is that it is not fixed anymore by symmetries. The reason for this is that we can define a ratio invariant under the transformations (4.9)–(4.11),

[15] Equivalently, the three-point functions of two scalars with a current or a stress-energy satisfy a Ward identity which relates their normalization to that of the two-point functions.

$$z = \frac{q^2(nn')}{2(qn)(qn')}. \tag{4.15}$$

Here we introduced the factor of 2 to ensure that $0 \le z \le 1$ for a time-like vector q and light-like vectors n and n'. In particular, in the rest frame of the source $q^\mu = (q^0, \vec{0})$, the variable z is related to the angle between the two detectors, $z = (1 - \cos\theta)/2$. This variable already appeared in the amplitude context, see (3.17).

Thus, all the symmetries mentioned above allow us to determine the double-detector correlation up to an arbitrary function of the invariant variable z,[16]

$$\langle \mathcal{D}(n; s)\mathcal{D}(n'; s')\rangle = \frac{(q^2)^{s'-1}(qn')^{s-s'}}{(nn')^{s+1}} \frac{\mathcal{F}_{ss'}(z)}{4\pi^2}. \tag{4.16}$$

In what follows we shall refer to $\mathcal{F}_{ss'}(z)$ as the *event shape function*. The symmetry of the correlator in the left-hand side of (4.16) under the exchange of the flow operators leads to the crossing symmetry $\mathcal{F}_{ss'}(z) = (2z)^{s'-s}\mathcal{F}_{s's}(z)$. Eq. (4.16) is consistent with the fact that $\langle \mathcal{D}(n; s)\mathcal{D}(n'; s')\rangle$ is related to the four-point correlation function which is fixed by conformal symmetry up to a function depending on two conformally invariant cross-ratios. In the detector limit, i.e., after sending $r \to \infty$ and the subsequent time integration, this function effectively depends on a single variable. It is straightforward to extend (4.16) to the multi-detector correlations (4.8) involving an arbitrary number of flow operators. In that case, $\langle \mathcal{D}_1(n_1)\dots\mathcal{D}_\ell(n_\ell)\rangle$ is given by the product of single-detector correlations (4.13) times an arbitrary function depending on the relative angles between the detectors.

We present below a list of double-detector correlations involving the three types of detectors considered in this paper. Combining together (4.16) and (4.12), we get

$$\begin{aligned}
&\langle \mathcal{E}(n)\mathcal{E}(n')\rangle = \frac{q^2\mathcal{F}_{\mathcal{E}\mathcal{E}}(z)}{4\pi^2(nn')^3}, &&\langle \mathcal{E}(n)\mathcal{Q}(n')\rangle = \frac{(qn')\mathcal{F}_{\mathcal{E}\mathcal{Q}}(z)}{4\pi^2(nn')^3},\\
&\langle \mathcal{Q}(n)\mathcal{Q}(n')\rangle = \frac{\mathcal{F}_{\mathcal{Q}\mathcal{Q}}(z)}{4\pi^2(nn')^2}, &&\langle \mathcal{E}(n)\mathcal{O}(n')\rangle = \frac{(qn')^2\mathcal{F}_{\mathcal{E}\mathcal{O}}(z)}{4\pi^2q^2(nn')^3},\\
&\langle \mathcal{O}(n)\mathcal{O}(n')\rangle = \frac{\mathcal{F}_{\mathcal{O}\mathcal{O}}(z)}{4\pi^2q^2(nn')}, &&\langle \mathcal{Q}(n)\mathcal{O}(n')\rangle = \frac{(qn')\mathcal{F}_{\mathcal{Q}\mathcal{O}}(z)}{4\pi^2q^2(nn')^2},
\end{aligned} \tag{4.17}$$

where $\mathcal{F}(z)$ are arbitrary functions of z. Matching these relations with the amplitude results (3.18), (3.21) and (3.23), we find to the lowest order in the coupling

$$\begin{aligned}
&\mathcal{F}_{\mathcal{E}\mathcal{E}}(z) = -a\frac{z\ln(1-z)}{1-z} + O(a^2),\\
&\mathcal{F}_{\mathcal{Q}\mathcal{Q}}(z) = -4a\left(\frac{2z\ln(1-z)}{1-z}\langle Q\rangle\langle Q'\rangle + \ln(1-z)\langle Q, Q'\rangle\right) + O(a^2),\\
&\mathcal{F}_{\mathcal{O}\mathcal{O}}(z) = -a\frac{z\ln(1-z)}{1-z}\langle S\rangle\langle S'\rangle + O(a^2),
\end{aligned} \tag{4.18}$$

and similarly for the mixed correlations from (3.25),

$$\mathcal{F}_{\mathcal{E}\mathcal{Q}}(z) = -8a\frac{z\ln(1-z)}{1-z}\langle Q'\rangle + O(a^2),$$

[16] For certain detectors $\mathcal{D}$ the function $\mathcal{F}_{ss'}$ will also depend on the auxiliary 'isotopic' variables, see below.

$$\mathcal{F}_{\mathcal{E}\mathcal{O}}(z) = -2a\frac{z\ln(1-z)}{1-z}\langle S'\rangle + O\left(a^2\right),$$
$$\mathcal{F}_{\mathcal{Q}\mathcal{O}}(z) = -4a\frac{z\ln(1-z)}{1-z}\langle Q\rangle\langle S'\rangle + O\left(a^2\right). \tag{4.19}$$

Notice that $\mathcal{F}_{\mathcal{O}\mathcal{O}}(z)$ agrees (up to an overall factor) with the result presented in [26]. We observe that the lowest order corrections to all event shape functions (except $\mathcal{F}_{\mathcal{Q}\mathcal{Q}}(z)$) involve the same function $z\ln(1-z)/(1-z)$. We come back to this issue in Section 6.

4.3. Single-detector correlations

As an illustration of the general considerations above, in this subsection we revisit the calculation of the detector correlations with a single detector insertion, $\langle\mathcal{O}(n)\rangle$, $\langle\mathcal{Q}(n)\rangle$ and $\langle\mathcal{E}(n)\rangle$, by using their relation to the three-point correlation functions of the scalar half-BPS operators $O_{\mathbf{20}'}$, the R-symmetry current and the energy–momentum tensor. The latter was discussed previously in Ref. [13]. Here we illustrate the main steps needed to obtain the cross section from the correlation function: analytic continuation from Euclidean to Wightman functions, taking the detector limit, performing the time integrals and the Fourier transform.

4.3.1. Single scalar detector

According to (2.39), the single scalar detector correlation is given by

$$\left\langle\mathcal{O}(n)\right\rangle = \sigma_{\rm tot}^{-1}\int d^4x_1\, e^{iqx_1}\langle 0|O(x_1,\bar{Y})S^{IJ}\mathcal{O}^{IJ}(n)O(0,Y)|0\rangle, \tag{4.20}$$

with the normalization factor defined in (2.10). At the lowest order in the coupling, $\langle\mathcal{O}(\vec{n})\rangle$ was computed in (3.12) from the amplitudes in the rest frame of the source. Let us obtain the same result from the three-point Wightman function of the half-BPS operators by inserting (4.5) into (4.20):

$$\left\langle\mathcal{O}(n)\right\rangle = \frac{S^{IJ}}{\sigma_{\rm tot}}\int d^4x_1\, e^{iqx_1}\int_{-\infty}^{\infty} dx_{2-}(n\bar{n}) \times \lim_{x_{2+}\to\infty} x_{2+}^2\langle 0|O(x_1,\bar{Y})O_{\mathbf{20}'}^{IJ}(x_{2+}n + x_{2-}\bar{n})O(0,Y)|0\rangle_W. \tag{4.21}$$

We do this in three steps:

(i) start with the expression for the Euclidean three-point correlation function of the half-BPS operators $O_{\mathbf{20}'}^{IJ}(x)$ and project the $SO(6)$ indices according to (4.21);
(ii) perform an analytic continuation to obtain the Wightman function in Minkowski space–time;
(iii) take the detector limit (by sending $x_+\to\infty$ and integrating over $-\infty < x_- < \infty$) and make the Fourier transform with respect to the position of the source to introduce the total momentum q^μ.

The correlation functions of the half-BPS operators $\mathcal{O}_{\mathbf{20}'}^{IJ}$ have a number of remarkable properties in $\mathcal{N}=4$ SYM. First of all, the conformal weight of $\mathcal{O}_{\mathbf{20}'}^{IJ}$ is protected from quantum corrections and, as a consequence, their three-point correlation function in Euclidean space,

$$G_E(1,2,3) = \langle 0|O(x_1,Y_1)O(x_2,Y_2)O(x_3,Y_3)|0\rangle_E, \tag{4.22}$$

is fixed by conformal symmetry up to an overall normalization factor. Furthermore, this factor also does not receive quantum corrections, meaning that the three-point correlation function (4.22) is given by its Born-level expression. Since $\mathcal{O}(x_i, Y_i)$ is bilinear in the scalar fields, the latter expression reduces to the product of three free scalar propagators $D_E(x) \sim 1/x^2$:

$$G_E(1,2,3) = \left(N_c^2 - 1\right)(Y_1Y_2)(Y_2Y_3)(Y_1Y_3)D_E(x_{12})D_E(x_{23})D_E(x_{13}). \tag{4.23}$$

Here $(Y_iY_j) = \sum_{I=1}^{6} Y_i^I Y_j^I$ are the invariant contractions of the auxiliary $SO(6)$ complex null vectors Y_i^I which help us to keep track of the R-symmetry structure. In the context of the correlation function, they play the role of the coordinates in the internal (isotopic) $SU(4)$ space and are treated on equal footing with the space–time coordinates x_i of the operators. As explained above, the definition of the single-detector correlation (4.20) involves the Wightman function $G_W(1,2,3)$ in Minkowski space–time. Knowing the expression in Euclidean space (4.23), we can obtain $G_W(1,2,3)$ by simply replacing the Euclidean scalar propagators by their Wightman counterparts,

$$G_W(1,2,3) = G_E(1,2,3)|_{D_E(x)\to D_W(x)}. \tag{4.24}$$

Here $D_W(x)$ is given by the two-point (non-time ordered!) correlation function of free scalar fields in Minkowski space–time

$$\langle 0|\Phi^I(x_i)\Phi^J(x_j)|0\rangle = \delta^{IJ} D_W(x_{ij}) = -\frac{\delta^{IJ}}{4\pi^2}\frac{1}{x_{ij}^2 - i\epsilon x_{ij}^0}. \tag{4.25}$$

We would like to emphasize that the analytic continuation in (4.24) relied on the simplicity of the three-point correlation function (4.23). Later in the paper we shall consider the four-point correlation function of half-BPS operators $G_E(1,2,3,4)$. It is not protected anymore and the perturbative corrections to $G_E(1,2,3,4)$ are described by a complicated function of the conformal cross-ratios. It then becomes a non-trivial task to find its analytic continuation $G_W(1,2,3,4)$.

The Wightman function (4.24) depends on three auxiliary isotopic null vectors Y_i (with $i = 1,2,3$). In the case of the scalar flow correlation (4.20) the choice of the analogous auxiliary variables was dictated by the requirement for $\langle\mathcal{O}(n)\rangle$ to have real values. This is why we associate the complex null vector Y with the source and its conjugate $\bar{Y}$ with the sink, while the detector matrix S_{IJ} is chosen real. In the case of the correlation function, the variables Y_i are *holomorphic coordinates* of the half-BPS operators in the internal space. However, what really matters is that we can always remove the auxiliary variables Y_i to reveal the R-tensor structure of the correlation function, and then project it with the new set of auxiliary variables $Y, \bar{Y}, S$ appearing in (4.20). In the case of the Wightman function (4.24), this amounts to the substitution rule for the isotopic variables $Y_1^I \to \bar{Y}^I$, $Y_3^I \to Y^I$ and $Y_2^I Y_2^J \to S^{IJ}$, leading to

$$(Y_1Y_2)(Y_2Y_3)(Y_1Y_3) \to (Y\bar{Y})(YS\bar{Y}) \equiv (Y\bar{Y})^2\langle S\rangle. \tag{4.26}$$

For a more detailed discussion of the two sets of auxiliary isotopic variables and their matching see Appendix D.

The next step is to take the detector limit of the Wightman function $G_W(1,2,3)$. To match the correlation function on the right-hand side of (4.21), we put $x_3 = 0$ and identify $x_2^\mu = x_{2+}n^\mu + x_{2-}\bar{n}^\mu$ to be the detector coordinate. Then, for $x_{2+} \to \infty$ we make use of the relations $x_{12}^2 - i0x_{12}^0 \to 2x_{2+}(x_{2-}(n\bar{n}) - (x_1n) + i0)$ and $x_2^2 - i\epsilon x_2^0 \to 2x_{2+}(x_{2-}(n\bar{n}) - i\epsilon)$ to find from (4.24) and (4.23)

$$\lim_{x_{2+}\to\infty} x_{2+}^2 G_W(1,2,3) \sim \frac{(Y\bar{Y})^2\langle S\rangle}{(x_{2-}(n\bar{n}) - (x_1 n) + i\epsilon)(x_{2-}(n\bar{n}) - i\epsilon)(x_1^2 - i\epsilon x_1^0)}. \tag{4.27}$$

According to (4.21), we have to integrate this expression over the detector light-cone coordinate x_{2-}. The expression on the right-hand side of (4.27) has two poles in x_{2-} located on the opposite sides of the real axis. Closing the integration contour in, say, the upper half-plane, we get

$$(n\bar{n}) \int_{-\infty}^{\infty} dx_{2-} \lim_{x_{2+}\to\infty} x_{2+}^2 G_W(1,2,3) \sim \frac{(Y\bar{Y})^2\langle S\rangle}{((x_1 n) - i\epsilon)(x_1^2 - i\epsilon x_1^0)}. \tag{4.28}$$

Notice that, as announced in Section 4.1, the second light-like vector $\bar{n}$ has dropped out of the right-hand side. Finally, we perform the Fourier transform of (4.28) and collect various factors to obtain

$$\langle \mathcal{O}(n)\rangle = \sigma_{\text{tot}}^{-1} \int d^4x\, e^{iqx} \int_{-\infty}^{\infty} dx_{2-}(n\bar{n}) \lim_{x_{2+}\to\infty} x_{2+}^2 G_W(1,2,3) = \frac{1}{2\pi}\frac{\langle S\rangle}{(qn)}. \tag{4.29}$$

In the rest frame of the source $q^\mu = (q^0, \vec{0})$ this relation coincides with (3.12) and agrees with the general form (4.13).

4.3.2. Single charge detector

Let us repeat the above analysis for the single-detector correlation of the charge flow operator (2.27),

$$\langle \mathcal{Q}(n)\rangle = \frac{Q_A^B}{\sigma_{\text{tot}}} \int d^4x\, e^{iqx} \langle 0|O(x,\bar{Y})\mathcal{Q}_B^A(n) O(0,Y)|0\rangle. \tag{4.30}$$

Replacing $\mathcal{Q}_B^A(n)$ with its definition (4.5), we find that it is related to the three-point Wightman correlation function of two half-BPS operators $O_{\mathbf{20}'}$ and the R-symmetry current J,

$$Q_A^B \bar{n}_\mu \langle 0|O(x_1,\bar{Y})\big(J^\mu\big)_B^A(x_2) O(x_3,Y)|0\rangle_W, \tag{4.31}$$

upon appropriate identification of the coordinates.

As before, we start with the Euclidean version of three-point function (4.31). This is another example of a protected correlation function, hence it is given by the Born level result

$$\begin{aligned} G_E{}^\mu &\equiv \langle 0|O^{I_1J_1}(x_1)\big(J^\mu\big)_B^A(x_2) O^{I_3J_3}(x_3)|0\rangle_E \\ &= -i\frac{N_c^2-1}{16\pi^6}\frac{(\Gamma^{\{I_1\{I_3})_B^A\delta^{J_1\}J_3\}}}{x_{12}^2 x_{23}^2 x_{13}^2}\left(\frac{x_{12}^\mu}{x_{12}^2} + \frac{x_{23}^\mu}{x_{23}^2}\right), \end{aligned} \tag{4.32}$$

where Γ^{IJ} is the generator of the fundamental representation of $SU(4)$ defined in (B.4) and $\{IJ\}$ denotes the traceless symmetrization of the pairs of indices I_1J_1 and I_3J_3, as required by the index structure of the operators $O_{\mathbf{20}'}$. It is easy to check that the expression in the right-hand side of (4.32) satisfies the current conservation condition at point 2 and is conformally covariant with the relevant scaling weight at each point.

The expression for $\langle \mathcal{Q}(n)\rangle$ in (4.30) involves a projection of the $SU(4)$ tensor structure in (4.32) with $\bar{Y}^{I_1}\bar{Y}^{J_1} Q_A^B Y^{I_3} Y^{J_3}$, resulting in

$$(Y\bar{Y})\bar{Y}^I\big(\Gamma^{IJ}\big)_B^A Q_A^B Y^J = \frac{1}{4}\operatorname{tr}(y\bar{y})\operatorname{tr}(yQ\bar{y}), \tag{4.33}$$

where $\operatorname{tr}(yQ\bar{y}) = y_{AB} Q_C^B \bar{y}^{CA}$ and the variables y_{AB} and $\bar{y}^{AB}$ are defined in (B.1).

As in the previous case, the Wightman correlation function (4.31) can be obtained from the Euclidean one in (4.32) by replacing the intervals (see footnote 18 below) as $x_{ij}^2 \to -(x_{ij}^2 - i\epsilon x_{ij}^0)$ (for $i < j$) in the right-hand side of (4.32). Further, we specify the coordinates of the operators as $x_3 = 0$ and $x_2^\mu = x_{2+}n^\mu + x_{2-}\bar{n}^\mu$ and obtain in the detector limit $x_{2+} \to \infty$

$$\lim_{x_{2+}\to\infty} x_{2+}^2 G_W{}^\mu \sim \frac{n^\mu (x_1 n)}{((x_1 n) - x_{2-}(n\bar{n}) - i\epsilon)^2 (x_{2-}(n\bar{n}) - i\epsilon)^2 (x_1^2 - i\epsilon x_1^0)}. \tag{4.34}$$

Notice that this expression is proportional to the light-like vector n^μ determining the orientation of the detector. Next, the integral over the detector time produces

$$(n\bar{n}) \int_{-\infty}^{\infty} dx_{2-} \lim_{x_{2+}\to\infty} x_{2+}^2 \bar{n}_\mu G_W{}^\mu \sim \frac{1}{((x_1 n) - i\epsilon)^2 (x_1^2 - i\epsilon x_1^0)}. \tag{4.35}$$

Finally, performing the Fourier integral and reinstating the y/Q-structure from (4.33), we obtain

$$\langle \mathcal{Q}(n)\rangle = \sigma_{\text{tot}}^{-1} \int d^4 x_1\, e^{iqx_1} \int_{-\infty}^{\infty} dx_{2-}(n\bar{n}) \lim_{x_{2+}\to\infty} x_{2+}^2 \bar{n}_\mu G_W{}^\mu = \frac{\langle Q\rangle}{\pi} \frac{q^2}{(qn)^2}, \tag{4.36}$$

where $\langle Q\rangle$ was defined in (3.10). In the rest frame of the source, this relation coincides with (3.9) and agrees with (4.14).

4.3.3. Single energy detector

Here we essentially repeat the calculation from [13]. The single-detector correlation of the energy-flow operator (4.4) takes the form

$$\langle \mathcal{E}(n)\rangle = \sigma_{\text{tot}}^{-1} \int d^4 x\, e^{iqx} \langle 0| O(x, \bar{Y}) \mathcal{E}(n) O(0, Y)|0\rangle. \tag{4.37}$$

As follows from (4.4) and (4.37), the energy correlator $\langle \mathcal{E}(n)\rangle$ is determined by the three-point function of two half-BPS operators and one energy–momentum tensor. In Euclidean space it is given by

$$\begin{aligned}(G_E)^{\mu\nu}(1,2,3) &= \langle 0| O(x_1, \bar{Y}) T^{\mu\nu}(x_2) O(x_3, Y)|0\rangle_E \\ &= -\frac{N_c^2 - 1}{16\pi^6} \frac{(Y\bar{Y})^2}{x_{12}^2 x_{23}^2 x_{13}^2} \left(\frac{x_{12}^\mu}{x_{12}^2} + \frac{x_{23}^\mu}{x_{23}^2}\right)\left(\frac{x_{12}^\nu}{x_{12}^2} + \frac{x_{23}^\nu}{x_{23}^2}\right).\end{aligned} \tag{4.38}$$

Since the energy–momentum tensor is an $SO(6)$ singlet, the R-symmetry tensor structure in (4.38) is much simpler than before. Moreover, the isotopic factor in (4.38) is canceled by that of the total transition probability σ_{tot} in the right-hand side of (4.37). Repeating the steps outlined above, analytic continuation to the Wightman function, detector limit and time integration (see (4.4)), followed by a Fourier transform, we obtain

$$\langle \mathcal{E}(n)\rangle = \frac{1}{4\pi} \frac{(q^2)^2}{(qn)^3}. \tag{4.39}$$

For $q^\mu = (q^0, \vec{0})$, we reproduce the result of the amplitude calculation (3.7), in accord with (4.14).

5. Double-detector correlations from four-point correlation functions

As was explained in the previous section, starting with two (or more) detector insertions we have to deal with Wightman correlation functions involving four (or more) operators – two half-BPS operators serving as the source/sink, and more than one flow operators serving as detectors. Unlike the single-detector case discussed above, such functions are not protected from quantum corrections and we expect them to have a complicated form order-by-order in the coupling constant. As a consequence, the question about the analytic continuation of the Wightman functions from their Euclidean counterparts becomes very non-trivial. In this section we explain the procedure on the example of the double-detector correlations.

5.1. Energy–momentum tensor supermultiplet

We recall that the flow operators (4.4) and (4.5) are built from three protected operators – the half-BPS scalar operator, the R-current and the energy–momentum tensor. It is well known that in $\mathcal{N}=4$ SYM these operators belong to the same supermultiplet $\mathcal{T}(x,Y,\theta,\bar\theta)$,

$$\mathcal{T}(x,Y,\theta,\bar\theta)=O(x,Y)+\cdots+\big(\theta\sigma^{\mu}\bar\theta\big)J_{\mu}(x,Y)+\cdots$$
$$+\big(\theta\sigma^{\mu}\bar\theta\big)\big(\theta\sigma^{\nu}\bar\theta\big)T_{\mu\nu}(x)+\ldots, \tag{5.1}$$

where we do not display the $SU(4)$ indices. Its lowest component is the half-BPS operator (2.2) and the higher components are obtained by successive use of $\mathcal{N}=4$ supersymmetry transformations.

The supermultiplet (5.1) has a number of remarkable properties. First of all, it is annihilated by half of the $\mathcal{N}=4$ supercharges and, as a consequence, its expansion in powers of the Grassmann variables $(\theta,\bar\theta)$ is shorter than one might expect. In particular, one corollary of supersymmetry is the conservation of the R-current J_μ and of the energy–momentum tensor $T_{\mu\nu}$. Secondly, $\mathcal{N}=4$ superconformal symmetry imposes strong constraints on the correlation functions of the superfield (5.1). To compute the double-detector correlations, we need the four-point Euclidean (super)correlation function

$$\mathcal{G}_E(1,2,3,4)=\langle 0|\mathcal{T}(x_1,Y_1,\theta_1,\bar\theta_1)\ldots\mathcal{T}(x_4,Y_4,\theta_4,\bar\theta_4)|0\rangle. \tag{5.2}$$

Setting $\theta_{1,4}=\bar\theta_{1,4}=0$ in (5.2), we select the lowest component O at points 1 and 4, to play the role of the source/sink. The flow operators (4.4) or (4.5) are then given by the relevant components of the superfields at points 2 and 3. Setting all odd variables to zero, we obtain the four-point correlation function of half-BPS operators

$$G_E(1,2,3,4)=\langle 0|O(x_1,Y_1)O(x_2,Y_2)O(x_3,Y_3)O(x_4,Y_4)|0\rangle. \tag{5.3}$$

This is the starting point for the analysis of the scalar–scalar flow correlation. It is known [27,28] that $\mathcal{N}=4$ superconformal symmetry allows one to reconstruct the complete super-correlation function (5.2) in terms of its lowest component (5.3). Each term in the $(\theta,\bar\theta)$ expansion of (5.2) is given by a particular differential operator acting on the coordinates x_i of the scalar operators in (5.3). Most importantly, these differential operators do not depend on the coupling constant. Their explicit form for the cases of interest (the components involving one or two R-currents and/or energy–momentum tensors) will be worked out in a forthcoming paper. Thus, to compute the quantum corrections to the super-correlation function (5.2) it suffices to know the correlation function of the four half-BPS operators (5.3).

5.2. Four-point correlation function of half-BPS operators

The Euclidean four-point function of the half-BPS operators $O_{\mathbf{20}'}$ has been studied extensively in [29–34]. It is convenient to split it into a sum of two terms, $G_E = G_E^{(\text{Born})} + G_E^{(\text{loop})}$, describing the Born approximation and the quantum corrections, respectively.

At Born level, the correlation function (5.3) is given by products of free scalar propagators with the appropriate isotopic factors, $Y_1^I Y_2^J \langle \Phi^I(x_1)\Phi^J(x_2)\rangle \sim y_{12}^2/x_{12}^2$, where we have introduced the shorthand notation $y_{ij}^2 = (Y_i Y_j)$. Thus, we obtain

$$G_E^{(\text{Born})}(1,2,3,4) = \frac{N_c^2-1}{(4\pi^2)^4}\left(\frac{y_{12}^2}{x_{12}^2}\frac{y_{23}^2}{x_{23}^2}\frac{y_{34}^2}{x_{34}^2}\frac{y_{14}^2}{x_{14}^2} + \frac{y_{13}^2}{x_{13}^2}\frac{y_{23}^2}{x_{23}^2}\frac{y_{24}^2}{x_{24}^2}\frac{y_{14}^2}{x_{14}^2} + \frac{y_{12}^2}{x_{12}^2}\frac{y_{24}^2}{x_{24}^2}\frac{y_{34}^2}{x_{34}^2}\frac{y_{13}^2}{x_{13}^2}\right)$$
$$+ \frac{(N_c^2-1)^2}{4(4\pi^2)^4}\left(\frac{y_{12}^4}{x_{12}^4}\frac{y_{34}^4}{x_{34}^4} + \frac{y_{13}^4}{x_{13}^4}\frac{y_{24}^4}{x_{24}^4} + \frac{y_{14}^4}{x_{14}^4}\frac{y_{23}^4}{x_{23}^4}\right). \tag{5.4}$$

It contains six distinct terms corresponding to the six channels in the tensor product of $SU(4)$ irreps $\mathbf{20}' \times \mathbf{20}' = \mathbf{1} + \mathbf{15} + \mathbf{20}' + \mathbf{84} + \mathbf{105} + \mathbf{175}$ (see Appendix D). A remarkable feature of the correlation function (5.3) is that the loop corrections in all six channels are given by a single function of two variables [32],

$$G_E^{(\text{loop})}(1,2,3,4) = \frac{2(N_c^2-1)}{(4\pi^2)^4}\left[\frac{y_{12}^2 y_{23}^2 y_{34}^2 y_{41}^2}{x_{12}^2 x_{23}^2 x_{34}^2 x_{41}^2}(1-u-v) + \frac{y_{12}^2 y_{13}^2 y_{24}^2 y_{34}^2}{x_{12}^2 x_{13}^2 x_{24}^2 x_{34}^2}(v-u-1)\right.$$
$$+ \frac{y_{13}^2 y_{14}^2 y_{23}^2 y_{24}^2}{x_{13}^2 x_{14}^2 x_{23}^2 x_{24}^2}(u-v-1) + \frac{y_{12}^4 y_{34}^4}{x_{12}^4 x_{34}^4}u + \frac{y_{13}^4 y_{24}^4}{x_{13}^4 x_{24}^4}$$
$$\left. + \frac{y_{14}^4 y_{23}^4}{x_{14}^4 x_{23}^4}v\right]\Phi_E(u,v). \tag{5.5}$$

Here $\Phi_E(u,v)$ depends on the two conformal cross-ratios and admits a perturbative expansion,

$$\Phi_E(u,v) = \sum_{\ell=1}^{\infty} a^\ell \Phi_\ell(u,v), \qquad u = \frac{x_{12}^2 x_{34}^2}{x_{13}^2 x_{24}^2}, \quad v = \frac{x_{23}^2 x_{14}^2}{x_{13}^2 x_{24}^2}. \tag{5.6}$$

The functions $\Phi_\ell(u,v)$ are currently known in terms of Euclidean scalar Feynman integrals up to six loops ($\ell = 6$) [35]. The one-loop correction is given by the so-called one-loop box integral

$$\Phi_E(u,v) = a\Phi^{(1)}(u,v) + O\big(a^2\big) = -\frac{a}{4\pi^2}\int \frac{d^4x_0\, x_{13}^2 x_{24}^2}{x_{10}^2 x_{20}^2 x_{30}^2 x_{40}^2} + O\big(a^2\big). \tag{5.7}$$

In Euclidean space, the function $\Phi_E(u,v)$ has logarithmic singularities in the limit $x_{ij}^2 \to 0$, that corresponds to short-distance separations between the operators.

Let us apply (5.4) and (5.5) to obtain the correlation of two scalar flow operators $\langle \mathcal{O}(n)\mathcal{O}(n')\rangle$, Eq. (2.39), from the correlation function $G_E(1,2,3,4)$. At the first step, we associate the operators at points 4 and 1 with the source $O(0,Y)$ (we set $x_4 = 0$) and the conjugate sink $O(x_1,\overline{Y})$, respectively. Further, the operators at points 2 and 3 are associated with the two detectors, i.e., the scalar flow operators $\mathcal{O}(n,S)$ and $\mathcal{O}(n',S')$, involving the real detector matrices S_{IJ} and S'_{IJ}. The description of the correlation function in (5.4) and (5.5) is holomorphic in the auxiliary null vectors Y_i at all four points. So, to match the isotopic structures of the two objects, we have to make the substitutions $\overline{Y} \to Y_1$, $Y \to Y_4$ and $S_{IJ} \to Y_{2I}Y_{2J}$, $S'_{IJ} \to Y_{3I}Y_{3J}$.

Next, we recall that the scalar flow operators $\mathcal{O}(n, S)$ and $\mathcal{O}(n', S')$ do not commute for generic detector matrices S and S' because of a possible cross-talk between the detectors. To avoid this unwanted cross-talk, when defining the scalar detector correlations we had to impose the additional condition (2.38) on the detector matrices. Making the substitution $S_{IJ} \to Y_{2I}Y_{2J}$ and $S'_{IJ} \to Y_{3I}Y_{3J}$ described above, we find that the condition (2.38) on the scalar flow detectors is translated into the orthogonality condition $y_{23}^2 = (Y_2Y_3) = 0$ for the two half-BPS operators at positions 2 and 3 in the internal $SO(6)$ space. This condition eliminates half of the structures in (5.4) and (5.5), leaving us with

$$\widehat{G}_E^{(\text{Born})} = \frac{N_c^2 - 1}{(4\pi^2)^4} \frac{y_{12}^2}{x_{12}^2} \frac{y_{24}^2}{x_{24}^2} \frac{y_{13}^2}{x_{13}^2} \frac{y_{34}^2}{x_{34}^2} + \frac{(N_c^2 - 1)^2}{4(4\pi^2)^4} \left(\frac{y_{12}^4}{x_{12}^4} \frac{y_{34}^4}{x_{34}^4} + \frac{y_{13}^4}{x_{13}^4} \frac{y_{24}^4}{x_{24}^4} \right), \tag{5.8}$$

and

$$\widehat{G}_E^{(\text{loop})} = \frac{2(N_c^2 - 1)}{(4\pi^2)^4} \left[y_{12}^2 y_{13}^2 y_{24}^2 y_{34}^2 (v - u - 1) + y_{12}^4 y_{34}^4 + y_{13}^4 y_{24}^4 u \right] \frac{\Phi_E(u, v)}{x_{12}^2 x_{13}^2 x_{24}^2 x_{34}^2}. \tag{5.9}$$

Here we dressed the symbols in the left-hand side of these equations with hats to indicate that both expressions have been evaluated for $y_{23}^2 = 0$. Comparing these relations with the general expressions (5.4) and (5.5), we observe that the suppression of the cross-talk between the detectors has a simple interpretation in terms of the correlation function. Namely, the condition $y_{23}^2 = 0$ eliminates the most singular terms in (5.4) and (5.5) in the short-distance limit $x_{23}^2 \to 0$.

To conclude the discussion of how to match the isotopic structures of the correlation function of four half-BPS operators in (5.8) and (5.9) and that of the double scalar flow correlation, we give the translation table between the $SO(6)$ invariant y- and Y/S-structures, after imposing the condition $y_{23}^2 = 0$[17]:

$$\begin{aligned} &y_{12}^2 y_{13}^2 y_{24}^2 y_{34}^2 \to (Y S \bar{Y})(Y S' \bar{Y}), \\ &\left(y_{12}^2 y_{34}^2\right)^2 \to (Y S Y)(\bar{Y} S' \bar{Y}), \\ &\left(y_{13}^2 y_{24}^2\right)^2 \to (Y S' Y)(\bar{Y} S \bar{Y}). \end{aligned} \tag{5.10}$$

The next step is to use relations (5.8) and (5.9) to obtain the Wightman correlation function of four half-BPS operators.

5.3. Analytic continuation

Let us first examine the contribution to $\langle \mathcal{O}(n)\mathcal{O}(n') \rangle$ coming from the Born level approximation to the correlation function (5.8).

A distinguishing feature of $\widehat{G}_E^{(\text{Born})}$ is that, like the three-point function (4.23), it is a rational function of the distances x_{ij}^2. This suggests that we can obtain the Wightman function $\widehat{G}_W^{(\text{Born})}(1, 2, 3, 4)$ by replacing $x_{ij}^2 \to (x_{ij}^2 - i\epsilon x_{ij}^0)$ (for $i < j$) on the right-hand side of (5.8). Notice that the Wightman function is not invariant under the exchange of points and the '$-i\epsilon x_{ij}^0$' prescription indicates that the operator at point x_i stands to the left from the operator at point x_j inside $\widehat{G}_W^{(\text{Born})}(1, 2, 3, 4)$. Since we assigned the points 4 and 1 to the source and to its complex conjugated image (sink), respectively, and the points 2 and 3 to the detectors, the above

[17] See Appendix D for more details.

rule should be applied to all factors of $1/x_{ij}^2$ with $i < j$ except $1/x_{23}^2$. Notice that, in virtue of the commutativity of the flow operators, the Wightman function should be insensitive to the ordering of the operators located at points x_2 and x_3. Indeed, it is easy to see from (5.8) that $\widehat{G}_W^{(\text{Born})}$ is regular at $x_{23}^2 = 0$. The same is true for the expression in the square brackets in (5.9).

To compute $\langle \mathcal{O}(n)\mathcal{O}(n')\rangle$, we convert (5.8) into a Wightman function and go to the detector limit by putting $x_4 = 0$ and identifying the coordinates of points 2 and 3 as $x_2 = x_{2+}n + x_{2-}\bar{n}$ and $x_3 = x_{3+}n' + x_{3-}\bar{n}'$. Then, for $x_{2+}, x_{3+} \to \infty$, we notice that the second term on the right-hand side of (5.8) gives rise to an expression containing double poles in x_{2-} and x_{3-}. These poles are located in the same half-plane and, therefore, vanish upon integration over x_{2-} and x_{3-}. In this way, with the help of (5.10) we obtain

$$
\begin{aligned}
\big\langle \mathcal{O}(n)\mathcal{O}\big(n'\big)\big\rangle^{(\text{Born})} &= \sigma_{\text{tot}}^{-1} \int d^4x_1 \mathrm{e}^{iqx_1} \int_{-\infty}^{\infty} dx_{2-}dx_{3-} \lim_{x_{2+},x_{3+}\to\infty} (x_{2+}x_{3+})^2\, \widehat{G}_W^{(\text{Born})} \\
&\sim \int d^4x_1 \mathrm{e}^{iqx_1} \int_{-\infty}^{\infty} \frac{dx_{2-}dx_{3-}\langle S\rangle\langle S'\rangle}{(x_{12-}-i\epsilon)(x_{2-}-i\epsilon)(x_{13-}-i\epsilon)(x_{3-}-i\epsilon)} \\
&\sim \int d^4x_1 \mathrm{e}^{iqx_1} \frac{\langle S\rangle\langle S'\rangle}{((x_1n)-i\epsilon)((x_1n')-i\epsilon)},
\end{aligned}
\tag{5.11}
$$

where in the second relation $x_{12-} = (x_1n) - x_{2-}$, $x_{13-} = (x_1n') - x_{3-}$ and $\langle S\rangle$ was defined in (3.13). The Fourier integral in the last relation reduces to $\int_0^\infty dt dt' \delta^{(4)}(q - nt - n't')$. It is easy to see that, in the rest frame of the source, for $q^\mu = (q^0, \vec{0})$, $n^\mu = (1, \vec{n})$ and $n'^\mu = (1, \vec{n}')$, it vanishes unless $\vec{n} = -\vec{n}'$. The latter case corresponds to detecting particles moving back-to-back and it produces a contribution proportional to $\delta(1 - z)$. This result is in agreement with the calculation of $\langle \mathcal{O}(n)\mathcal{O}(n')\rangle^{(\text{Born})}$ based on the amplitudes, Eq. (3.14). Namely, at Born level, for $q^\mu = (q^0, \vec{0})$, the final state in $\boldsymbol{O_{20'}} \to$ everything consists of two scalar particles moving back-to-back. They can be detected only for $\vec{n} = -\vec{n}'$, corresponding to $z = 1$ in (4.15). Thus, for $z < 1$, the correlation function contributes to the event shape function $\mathcal{F}_O(z)$ defined in (4.17) only starting from order $O(a)$.

Let us now repeat the same analysis for the Euclidean correlation function (5.9). The main difficulty in this case is that it involves a complicated function of the two cross-ratios. How to convert it to the Wightman function $\Phi_W(u, v)$? The answer to this question was proposed in [36] and a particularly elegant formulation was given in Ref. [37]. It relies on the Mellin representation of the correlation function,

$$
\Phi_E(u, v) = \int_{-\delta-i\infty}^{-\delta+i\infty} \frac{dj_1 dj_2}{(2\pi i)^2} M(j_1, j_2) u^{j_1} v^{j_2},
\tag{5.12}
$$

where $u, v > 0$ in Euclidean space and $M(j_1, j_2)$ is a meromorphic function of the Mellin parameters.

At weak coupling, the Mellin amplitude is given by a perturbative expansion in $a = g^2/(4\pi^2)$,

$$
M(j_1, j_2; a) = \sum_{\ell\geq 1} a^\ell M^{(\ell)}(j_1, j_2).
\tag{5.13}
$$

For our purposes here, we will only need the lowest-order term,

$$M^{(1)}(j_1, j_2) = -\frac{1}{4}\big[\Gamma(-j_1)\Gamma(-j_2)\Gamma(j_1+j_2+1)\big]^2, \tag{5.14}$$

which is obtained by rewriting the one-loop box integral in (5.7) in the Mellin form [35]. At strong coupling in planar $\mathcal{N}=4$ SYM, the Mellin amplitude was computed in [38–40] via the AdS/CFT correspondence,

$$M^{(\infty)}(j_1, j_2; a) = -\big[\Gamma(1-j_1)\Gamma(1-j_2)\Gamma(j_1+j_2+1)\big]^2 \frac{1+j_1+j_2}{2j_1 j_2}. \tag{5.15}$$

The invariance of the correlation function $G(1,2,3,4)$ under the exchange of any pair of points $(x_i, Y_i) \leftrightarrow (x_j, Y_j)$ leads to the crossing symmetry relations

$$\Phi_E(u,v) = \Phi_E(v,u) = \frac{1}{v}\Phi_E\left(\frac{u}{v}, \frac{1}{v}\right), \tag{5.16}$$

which translate into relations for the Mellin amplitude,

$$M(j_1, j_2) = M(j_2, j_1) = M(j_1, -1-j_1-j_2). \tag{5.17}$$

It is easy to check that the Mellin amplitudes (5.14) and (5.15) verify these relations.

According to [37], the Mellin amplitude $M(j_1, j_2)$ is a universal function, depending neither on the space–time signature, nor on the ordering of the operators in the four-point correlation function. Extending (5.12) to Minkowski space, we have to specify the analytic continuation of $(x_{ik}^2)^j$ to negative x_{ik}^2 for arbitrary complex j. The choice of the prescription is determined by the ordering of the operators. In the special case of the Wightman function $G_W(1,2,3,4)$, the prescription is $(x_{ik}^2)^j \to (-x_{ik}^2 + i\epsilon x_{ik}^0)^j$ for $i<k$.[18] In this way, we obtain from (5.12)

$$\begin{aligned}\Phi_W(1,2,3,4) = \int_{-\delta-i\infty}^{-\delta+i\infty} \frac{dj_1 dj_2}{(2\pi i)^2} M(j_1, j_2; a)\big(-x_{13}^2 + i\epsilon x_{13}^0\big)^{-j_1-j_2}\big(-x_{24}^2 + i\epsilon x_{24}^0\big)^{-j_1-j_2} \\ \times \big(-x_{12}^2 + i\epsilon x_{12}^0\big)^{j_1}\big(-x_{34}^2 + i\epsilon x_{34}^0\big)^{j_1}\big(-x_{23}^2 + i\epsilon x_{23}^0\big)^{j_2}\big(-x_{14}^2 + i\epsilon x_{14}^0\big)^{j_2}.\end{aligned} \tag{5.18}$$

Notice that Φ_W is locally conformally invariant. It coincides with $\Phi_E(u,v)$ for all $x_{ij}^2 < 0$ and differs otherwise.

For our purposes we will only need the Wightman function (5.18) in the detector limit. As before, we assign points 4 and 1 to the source and sink, respectively, and points 2 and 3 to the detectors. We put $x_4 = 0$, $x_2 = x_{2+}n + x_{2-}\bar{n}$, $x_3 = x_{3+}n' + x_{3-}\bar{n}'$ and take the limit $x_{2+}, x_{3+} \to \infty$ to get[19]

$$\lim_{x_{2+}, x_{3+} \to \infty} \Phi_W(1,2,3,4) = \int_{-\delta-i\infty}^{-\delta+i\infty} \frac{dj_1 dj_2}{(2\pi i)^2} M(j_1, j_2; a) f(j_1, j_2+1), \tag{5.19}$$

where the notation was introduced for the function

[18] For time-ordered operators, the same prescription looks as $(x_{ik}^2)^j \to (-x_{ik}^2 + i\epsilon)^j$ with the additional minus sign due to our choice of signature $(+,-,-,-)$ for Minkowski and $(+,+,+,+)$ for Euclidean space.

[19] Here we have assumed that the detector limit commutes with the Mellin integral.

$$
\begin{aligned}
f(j_1, j_2) = {} & \big((nn')/2\big)^{-j_1-j_2}\big(-x_1^2 + i\epsilon x_1^0\big)^{-j_1-j_2} \\
& \times \big((x_1 n) - x_{2-}(n\bar{n}) - i\epsilon\big)^{j_1}\big(-x_{2-}(n\bar{n}) + i\epsilon\big)^{j_2} \\
& \times \big((x_1 n') - x_{3-}\big(n'\bar{n}'\big) - i\epsilon\big)^{j_2}\big(-x_{3-}\big(n'\bar{n}'\big) + i\epsilon\big)^{j_1}.
\end{aligned} \tag{5.20}
$$

In what follows the dependence of $f(j_1, j_2)$ on the coordinates x_1, x_{2-} and x_{3-} is tacitly assumed. To obtain (5.19), we replaced the integration variable $j_2 \to -1 - j_1 - j_2$ and made use of (5.17). Viewed as a function of the detector times x_{2-} and x_{3-}, the expression in the right-hand side of (5.20) has singularities located on both sides of the real axis. This ensures that the integrals over the detector times x_{2-} and x_{3-} do not vanish.

5.4. Master formulas

We are now ready to perform the detector limit of the four-point Wightman correlation function. Combining together (5.9), (5.10) and (5.19), we find

$$
\begin{aligned}
& \lim_{x_{2+}, x_{3+} \to \infty} (x_{2+} x_{3+})^2 \widehat{G}_W^{(\text{loop})} \\
& = \frac{4\sigma_{\text{tot}}}{(2\pi)^7 (nn')^2}\big(-x_1^2 + i\epsilon x_1^0\big)^{-2} \int\limits_{-\delta - i\infty}^{-\delta + i\infty} \frac{dj_1 dj_2}{(2\pi i)^2} M(j_1, j_2; a) \\
& \quad \times \big[\langle S\rangle\langle S'\rangle f(j_1 - 1, j_2 - 1) + \langle S, S'\rangle f(j_1 - 1, j_2) + \overline{\langle S, S'\rangle} f(j_1, j_2 - 1)\big],
\end{aligned} \tag{5.21}
$$

where σ_{tot} is given by (2.10). Here we see three independent R-symmetry structures,

$$
\begin{aligned}
& \langle S, S'\rangle = \frac{(YSY)(\bar{Y}S'\bar{Y}) - (YS\bar{Y})(YS'\bar{Y})}{(Y\bar{Y})^2}, \\
& \overline{\langle S, S'\rangle} = \langle S, S'\rangle^*, \qquad \langle S\rangle = \frac{(YS\bar{Y})}{(Y\bar{Y})}.
\end{aligned} \tag{5.22}
$$

Each of them is accompanied by the function $f(j_1, j_2)$ with shifted arguments.

Finally, to obtain the correlation $\langle \mathcal{O}(n)\mathcal{O}(n')\rangle$ we have to integrate both sides of (5.21) over the detectors times, x_{2-} and x_{3-}, and perform the Fourier transform with respect to x_1. Assuming that the order of integrations can be exchanged, we find from (5.21)

$$
\begin{aligned}
\big\langle \mathcal{O}(n)\mathcal{O}\big(n'\big)\big\rangle = {} & \frac{1}{4\pi^2 q^2 (nn')} \int\limits_{-\delta - i\infty}^{-\delta + i\infty} \frac{dj_1 dj_2}{(2\pi i)^2} M(j_1, j_2; a)\big[\langle S\rangle\langle S'\rangle K(j_1, j_2; z) \\
& + \langle S, S'\rangle K(j_1, j_2 + 1; z) + \overline{\langle S, S'\rangle} K(j_1 + 1, j_2; z)\big],
\end{aligned} \tag{5.23}
$$

where we introduced a notation for

$$
\begin{aligned}
K(j_1, j_2; z) = {} & \frac{1}{8\pi^5} \frac{q^2}{(nn')} \int \frac{d^4 x_1 \mathrm{e}^{iqx_1}}{(-x_1^2 + i\epsilon x_1^0)^2} \\
& \times \int\limits_{-\infty}^{\infty} dx_{2-}(n\bar{n}) \int\limits_{-\infty}^{\infty} dx_{3-}\big(n'\bar{n}'\big) f(j_1 - 1, j_2 - 1; x_1, x_{2-}, x_{3-}).
\end{aligned} \tag{5.24}
$$

Changing the integration variables, $x_{2-} \to x_{2-}/(n\bar{n})$ and $x_{3-} \to x_{3-}/(n'\bar{n}')$, we verify using (5.20) that $K(j_1, j_2; z)$ is dimensionless and invariant under (independent) rescalings of the light-like vectors n and n'. Therefore, $K(j_1, j_2; z)$ can depend on the four-dimensional vectors only through the scaling variable z defined in (4.15). Going through the calculation of (5.24) we find (see Appendix E for details)

$$K(j_1, j_2; z) = \left(\frac{z}{1-z}\right)^{1-j_1-j_2} \frac{2\pi}{\sin(\pi(j_1+j_2))[\Gamma(j_1+j_2)\Gamma(1-j_1)\Gamma(1-j_2)]^2}, \tag{5.25}$$

where $0 < z < 1$. The function $K(j_1, j_2; z)$ characterizes the scalar detectors. It is a symmetric function of j_1 and j_2 and, most importantly, it is independent of the coupling constant. In what follows we refer to this functions as the *detector kernel*.

Relation (5.23) agrees with the general expression for the scalar detector correlation in (4.17). It leads to the following remarkable *master formula* for the event shape function $\mathcal{F}_{\mathcal{O}\mathcal{O}}(z)$

$$\mathcal{F}_{\mathcal{O}\mathcal{O}}(z) = \langle S\rangle\langle S'\rangle\mathcal{F}^{+}_{\mathcal{O}\mathcal{O}}(z) + \left(\langle S, S'\rangle + \overline{\langle S, S'\rangle}\right)\mathcal{F}^{-}_{\mathcal{O}\mathcal{O}}(z), \tag{5.26}$$

where $\mathcal{F}^{\pm}_{\mathcal{O}\mathcal{O}}(z)$ are given by the Mellin integrals

$$\mathcal{F}^{+}_{\mathcal{O}\mathcal{O}}(z) = \int_{-\delta-i\infty}^{-\delta+i\infty} \frac{dj_1 dj_2}{(2\pi i)^2} M(j_1, j_2; a) K(j_1, j_2; z),$$
$$\mathcal{F}^{-}_{\mathcal{O}\mathcal{O}}(z) = \int_{-\delta-i\infty}^{-\delta+i\infty} \frac{dj_1 dj_2}{(2\pi i)^2} M(j_1, j_2; a) K(j_1, j_2+1; z). \tag{5.27}$$

These relations establish the correspondence between the four-point Euclidean correlation function of half-BPS operators and the double-scalar detector correlation. Given the correlation function $G_E(1,2,3,4)$ in the form (5.5), we start by extracting the Mellin amplitude $M(j_1, j_2; a)$ from (5.12). Then we obtain the event shape function $\mathcal{F}_{\mathcal{O}}(z)$ by integrating the Mellin amplitude in the Mellin space with the kernel $K(j_1, j_2; z)$, which is uniquely fixed by the choice of the detectors. In this representation, the dependence on the coupling constant resides in the Mellin amplitude $M(j_1, j_2; a)$, whereas the z-dependence comes from the detector kernel $K(j_1, j_2; z)$.

5.5. One-loop check

To illustrate the power of the master formula (5.26), let us use the known one-loop expression for the Mellin amplitude (5.14) to compute the event shape functions (5.27) to the lowest order in the coupling. Taking into account (5.25), we find

$$M(j_1, j_2; a)K(j_1, j_2; z) = -\frac{a}{2}\left(\frac{z}{1-z}\right)^{1-j_1-j_2} \frac{\pi(j_1+j_2)^2}{(j_1 j_2)^2 \sin(\pi(j_1+j_2))} + O(a^2),$$
$$M(j_1, j_2; a)K(j_1, j_2+1; z) = \frac{a}{2}\left(\frac{z}{1-z}\right)^{-j_1-j_2} \frac{\pi}{j_1^2 \sin(\pi(j_1+j_2))} + O(a^2). \tag{5.28}$$

To perform the Mellin integration in (5.27) it is useful to shift the integration variable as $j_2 \to j_2 - j_1$. In this way, we obtain

$$\mathcal{F}^{+}_{\mathcal{O}\mathcal{O}}(z) = -\frac{a}{2} \int\limits_{-\delta-i\infty}^{-\delta+i\infty} \frac{dj_1 dj_2}{(2\pi i)^2} \frac{\pi j_2^2}{(j_1(j_2-j_1))^2 \sin(\pi j_2)} \left(\frac{z}{1-z}\right)^{1-j_2} + O\big(a^2\big), \tag{5.29}$$

where the j_2-integration contour goes to the left from the one over j_1. The integral can be easily computed by residue method after closing the j_1-integration contour in the right half-plane and the j_2-integration contour in the left half-plane. Then, the integral is given by the residues at $j_1 = 0$ and $j_2 = -k$ (with $k = 1, 2, \ldots$)

$$\mathcal{F}^{+}_{\mathcal{O}\mathcal{O}}(z) = -a \sum_{k=1}^{\infty} \frac{(-1)^k}{k} \left(\frac{z}{1-z}\right)^{1+k} + O\big(a^2\big) = -a \frac{z}{1-z} \ln(1-z) + O\big(a^2\big). \tag{5.30}$$

Going through the same steps for (5.28) we find

$$\mathcal{F}^{-}_{\mathcal{O}\mathcal{O}}(z) = \frac{a}{2} \int\limits_{-\delta-i\infty}^{-\delta+i\infty} \frac{dj_1 dj_2}{(2\pi i)^2} \frac{\pi}{j_1^2 \sin(\pi j_2)} \left(\frac{z}{1-z}\right)^{-j_2} + O\big(a^2\big), \tag{5.31}$$

where the integration contours are the same as in (5.29). The main difference, however, is that the integrand has only a double pole at $j_1 = 0$ and, therefore, the j_1-integral vanishes,

$$\mathcal{F}^{-}_{\mathcal{O}\mathcal{O}}(z) = O\big(a^2\big). \tag{5.32}$$

Substituting (5.30) and (5.32) into the master formula (5.26) we notice that, firstly, the one-loop correction to the event shape function does not receive a contribution proportional to $\langle S, S' \rangle$ and, secondly, the coefficient of $\langle S \rangle \langle S' \rangle$ coincides with the one-loop result (4.18) based on the amplitude calculation.

6. Generalization of the master formulas

In this section we extend our previous analysis to the general case of double-detector correlations (4.16) and (4.17) involving scalar, charge and energy flow operators. As was explained in Section 4.2, these correlations are uniquely specified by the event shape functions depending on the scaling variable $0 < z < 1$.

To compute the event shape functions (4.16) and (4.17), we can follow the same procedure as before. Namely, we start with the four-point correlation functions involving two half-BPS operators (for the source and sink) and various components of the stress-tensor supermultiplet (5.1) (for the two detectors), analytically continue them to get the corresponding Wightman functions, and finally go to the detector limit to compute the double-detector correlations. We recall that the various four-point functions of this type appear as particular components in the expansion of the super correlation function $\mathcal{G}_E(1, 2, 3, 4)$, Eq. (5.2), in powers of the Grassmann variables.

According to Section 5.1, the super correlation function can be obtained from its lowest component $G_E(1, 2, 3, 4)$ by applying a (complicated) differential operator. This operator does not depend on the coupling constant, so the perturbative corrections to $\mathcal{G}_E(1, 2, 3, 4)$ are described by the unique scalar function $\Phi(u, v)$ from (5.5) and by its derivatives. Therefore, in order to get the Wightman function $\mathcal{G}_W(1, 2, 3, 4)$ it suffices to replace $\Phi(u, v)$ by its Wightman counterpart

$\Phi_W(u, v)$ defined in (5.18). Then, using the Mellin representation (5.19) and going through the same steps as in the previous subsection, we obtain the following general representation for the event shape function (4.17)[20]

$$\mathcal{F}_{\mathcal{AB}}(z) = \sum_R \omega_R \mathcal{F}_{\mathcal{AB};R}(z),$$
$$\mathcal{F}_{\mathcal{AB};R}(z) = \int \frac{dj_1 dj_2}{(2\pi i)^2} M(j_1, j_2; a) K_{\mathcal{AB};R}(j_1, j_2; z). \tag{6.1}$$

Here the subscripts $\mathcal{A}, \mathcal{B} = \mathcal{O}, \mathcal{Q}, \mathcal{E}$ denote the type of detectors (scalar, charge or energy) and $M(j_1, j_2; a)$ is the universal (detector independent) Mellin amplitude defined in (5.12) and (5.13).

For the scalar and charge detectors, the event shape function (6.1) also depends on the detector matrices S_{IJ} and Q_A^B, respectively. This dependence enters into (6.1) through the R-symmetry invariant factors ω_R built from the matrices S, Q and from the auxiliary variables $Y, \bar{Y}$ defining the source and the sink (see Eqs. (3.24) and (5.22)). The set of such factors is in one-to-one correspondence with the set of R-symmetry structures that appear in the four-point correlation function $\langle 0|O(1, \bar{Y})\mathcal{A}(2)\mathcal{B}(3)O(4, Y)|0\rangle$, which we use to compute the event shape function (6.1). Denoting by $\mathbf{A}$ and $\mathbf{B}$ the R-symmetry representations of the two detectors ($\mathbf{20'}$ for scalar, $\mathbf{15}$ for charge and $\mathbf{1}$ for energy flow), we can identify the above mentioned structures with the overlap of irreducible representations in the tensor products $\mathbf{A} \times \mathbf{B}$ and $\mathbf{20'} \times \mathbf{20'}$. They are labeled by the index R on the right-hand side of (6.1). In the detector limit, each irreducible component R of the four-point correlation function gives rise to the detector kernel $K_{\mathcal{AB};R}(j_1, j_2; z)$. As was already explained, this kernel depends on the Mellin variables j_1 and j_2 and the scaling variable z but does not depend on the coupling constant.

Let us first consider the kernels $K_{\mathcal{EE}}$, $K_{\mathcal{EQ}}$ and $K_{\mathcal{EO}}$ involving the energy flow. Since the energy flow is an R-symmetry singlet, the overlap of the two tensor products $\mathbf{1} \times \mathbf{B}$ and $\mathbf{20'} \times \mathbf{20'}$ consists of a single irreducible structure and, therefore, the sum in (6.1) reduces to a single term involving $\omega_{\mathbf{1}}^{\mathcal{EE}}$, $\omega_{\mathbf{15}}^{\mathcal{EQ}}$ and $\omega_{\mathbf{20'}}^{\mathcal{EO}}$ (see (D.13)). Quite remarkably, in these three cases the detector kernels turn out to be equal to the scalar–scalar kernel K defined in (5.25):

$$K_{\mathcal{EE};\mathbf{1}} = K_{\mathcal{EQ};\mathbf{15}} = K_{\mathcal{EO};\mathbf{20'}} = K(j_1, j_2; z). \tag{6.2}$$

As a consequence of these relations, the corresponding event shape functions $\mathcal{F}_{\mathcal{EE}}(z)$, $\mathcal{F}_{\mathcal{EQ}}(z)$ and $\mathcal{F}_{\mathcal{EO}}(z)$ are proportional to each other for any coupling constant. We interpret this as a corollary of $\mathcal{N} = 4$ superconformal symmetry which uniquely fixes the correlation functions $\langle OTTO\rangle$, $\langle OTJO\rangle$ and $\langle OTOO\rangle$, starting from $\langle OOOO\rangle$.

The remaining kernels $K_{\mathcal{OO}}$, $K_{\mathcal{QO}}$ and $K_{\mathcal{QQ}}$ have a more complicated structure. We found however that, similarly to (6.2), they can be expressed in terms of the function K, Eq. (5.25). For $\mathcal{A} = \mathcal{B} = \mathcal{O}$ the range of irreducible representations R in (6.1) corresponds to the tensor product

$$\mathbf{20'} \times \mathbf{20'} = \mathbf{1} + \mathbf{15} + \mathbf{20'} + \mathbf{84} + \mathbf{105} + \mathbf{175}, \tag{6.3}$$

[20] Here we give a short summary of the results, the details will be presented elsewhere. In obtaining them we have used the Mathematica package `xAct` [41], especially the application package `Spinors` [42].

Table 1
Scalar–scalar correlations. The first column lists the various channels R in the tensor product (6.3). The second column gives the polynomial of shift operators which acts on the kernel $K(j_1, j_2; z)$, Eq. (5.25), according to (6.4). The third and fourth columns list the event shape functions $\mathcal{F}_{\mathcal{O}\mathcal{O};R}$ at one loop and at strong coupling, respectively. They were obtained from (6.1) using (5.14) and (5.15).

$\langle\mathcal{O}\mathcal{O}\rangle$	$P_R^{\mathcal{O}\mathcal{O}}(t_1, t_2)$	$\mathcal{F}^{(1)}_{\mathcal{O}\mathcal{O};R}$	$\mathcal{F}^{(\infty)}_{\mathcal{O}\mathcal{O};R}$
1	$t_1^2 + t_2^2 + 4t_1t_2 - \frac{4}{5}(t_1 + t_2) + \frac{1}{10}$	∞	∞
15	$t_1^2 - t_2^2 - \frac{1}{2}(t_1 - t_2)$	0	0
20′	$(t_1 - t_2)^2 - \frac{1}{2}(t_1 + t_2) + \frac{1}{10}$	$-\frac{1}{10}\frac{z\ln(1-z)+10(1-z)\ln z}{1-z}$	∞
84	$3(t_1 + t_2) - 1$	$\frac{z\ln(1-z)}{1-z}$	∞
175	$t_1 - t_2$	0	0
105	1	$-\frac{z\ln(1-z)}{1-z}$	$2z^3$

and the six structures $\omega_R^{\mathcal{O}\mathcal{O}}$ are listed in (D.2). The kernel for each channel can be written as a differential operator acting on K,

$$K_{\mathcal{O}\mathcal{O};R}(j_1, j_2; z) = P_R^{\mathcal{O}\mathcal{O}}(t_1, t_2)K(j_1, j_2; z), \tag{6.4}$$

where $t_i = e^{\partial_{j_i}}$ (for $i = 1, 2$) and $P_R^{\mathcal{O}\mathcal{O}}$ are polynomials in t_1 and t_2 listed in Table 1.[21]

Several comments are in order regarding this table. Each polynomial $P_R^{\mathcal{O}\mathcal{O}}(t_1, t_2)$ corresponds to a particular irreducible representation R of $SU(4)$ appearing in the decomposition (6.3). Comparing these polynomials with those listed in (D.4), we notice that $P_R^{\mathcal{O}\mathcal{O}}(t_1, t_2)$ coincide with the eigenfunctions of the quadratic Casimir of $SU(4)$ in the 'mirror' representation

$$\left(P_{\mathbf{1}}^{\mathcal{O}\mathcal{O}}, P_{\mathbf{15}}^{\mathcal{O}\mathcal{O}}, P_{\mathbf{20'}}^{\mathcal{O}\mathcal{O}}, P_{\mathbf{84}}^{\mathcal{O}\mathcal{O}}, P_{\mathbf{175}}^{\mathcal{O}\mathcal{O}}, P_{\mathbf{105}}^{\mathcal{O}\mathcal{O}}\right) = (\mathcal{Y}_{\mathbf{105}}, \mathcal{Y}_{\mathbf{175}}, \mathcal{Y}_{\mathbf{84}}, \mathcal{Y}_{\mathbf{20'}}, \mathcal{Y}_{\mathbf{15}}, \mathcal{Y}_{\mathbf{1}}). \tag{6.5}$$

In particular, we have $P_{\mathbf{105}}^{\mathcal{O}\mathcal{O}} = \mathcal{Y}_{\mathbf{1}} = 1$, with the corollary

$$K_{\mathcal{O}\mathcal{O};\mathbf{105}} = K(j_1, j_2; z). \tag{6.6}$$

Secondly, from Table 1 we see that the event shape functions $\mathcal{F}_{\mathcal{O}\mathcal{O}}(z)$ in the channels **15** and **175** vanish identically. This is due to the antisymmetry of the kernels $K_{\mathcal{O}\mathcal{O};\mathbf{15}}$ and $K_{\mathcal{O}\mathcal{O};\mathbf{175}}$ under the exchange of $j_1 \leftrightarrow j_2$, which is incompatible with the symmetries of $M(j_1, j_2)$, as can be seen in (5.17).

Thirdly, Table 1 lists the contributions to $\mathcal{F}_{\mathcal{O}\mathcal{O}}(z)$ in two regimes, at weak coupling (one loop) and at strong coupling.[22] We observe the presence of divergences, at one loop in the singlet channel, and at strong coupling in all non-vanishing channels but the **105**. The appearance of divergences at weak coupling is not surprising and is related to the cross-talk between scalar detectors, as explained in Section 2.2.3. We recall that the cross-talk can be eliminated by imposing the additional condition on the detector matrices, $[S, S'] = 0$, Eq. (2.38). As explained in Section 5.2 (see also Eq. (D.5)), this condition has the effect of suppressing half of the y-structures in (5.4) and (5.5), see (5.8) and (5.9). Equivalently, half of the irreps on the right-hand side of (6.3) also drop out, namely **1**, **15** and **20′**. So, we can reinterpret $[S, S'] = 0$ as a condition for

[21] Notice that t_i are conjugate variables to j_i in the sense $[t_i, j_k] = \delta_{ik}t_i$. In practice, they act as shifts of the arguments of the kernel.

[22] The correlation function and its Mellin amplitude at strong coupling were computed in [38–40]. More details about the event shapes at strong coupling will be presented elsewhere.

Table 2
Charge-scalar correlations. The channel $\mathbf{20'}$ vanishes identically for symmetry reasons. The channel **15** is removed by the condition (D.6).

$\langle \mathcal{Q}\mathcal{O}\rangle$	$P_R^{\mathcal{Q}\mathcal{O}}(t_1,t_2)$	$\mathcal{F}^{(1)}_{\mathcal{Q}\mathcal{O};R}$	$\mathcal{F}^{(\infty)}_{\mathcal{Q}\mathcal{O};R}$
15	$\frac{1}{2}(t_1+t_2-\frac{1}{4})$	$\frac{\ln(1-z)}{8(1-z)}$	∞
$\mathbf{20'}$	$\frac{1}{2}(t_1-t_2)$	0	0
175	1	$-z\frac{\ln(1-z)}{1-z}$	$2z^2$

removing some of the divergences in the Mellin integrals. In the absence of this condition the channel $\mathbf{20'}$ remains finite at one loop, but diverges at strong coupling.[23] The two remaining channels **84** and **105** give finite contributions at one loop, but the former diverges at strong coupling. We can avoid this divergence if we impose a stronger condition, $Y_2 = Y_3$ (see (D.6)). Its effect is to suppress all channels but the **105**, which turns out to be finite both at one loop and at strong coupling.

Our next choice of detectors is $\mathcal{A} = \mathcal{Q}$ and $\mathcal{B} = \mathcal{O}$. In this case, the sum in (6.1) runs over the overlap of irreducible representations in the tensor product

$$\mathbf{15}\times\mathbf{20'} = \mathbf{15}+\mathbf{20'}+\mathbf{45}+\overline{\mathbf{45}}+\mathbf{175}, \tag{6.7}$$

with those in (6.3), i.e. $R = \mathbf{15}, \mathbf{20'}, \mathbf{175}$. We can represent the results in a manner similar to the scalar case discussed above, introducing

$$K_{\mathcal{Q}\mathcal{O},R}(j_1,j_2;z) = P_R^{\mathcal{Q}\mathcal{O}}(t_1,t_2)K(j_1,j_2;z), \tag{6.8}$$

where the kernel K and t_1, t_2, are defined in Eqs. (5.25) and below (6.4), respectively. The results are summarized in Table 2. The channel $\mathbf{20'}$ is antisymmetric under the exchange of (j_1, j_2) which results in an identically vanishing contribution. The channel **15**, while finite at one loop, diverges at strong coupling and only the **175** yields a finite contribution in this regime. The strong-coupling correlations can be rendered finite again by imposing the stronger condition (D.6), which eliminates all channels apart from the **175**.

With the choice $\mathcal{A} = \mathcal{B} = \mathcal{Q}$ we are dealing with the overlap of (6.3) and

$$\mathbf{15}\times\mathbf{15} = \mathbf{1}+\mathbf{15}_s+\mathbf{15}_a+\mathbf{20'}+\mathbf{45}+\overline{\mathbf{45}}+\mathbf{84}, \tag{6.9}$$

which consists of the irreps $\mathbf{1}+\mathbf{15}_a+\mathbf{15}_s+\mathbf{20'}+\mathbf{84}$ (notice the degeneracy of the **15**, appearing in a symmetric and an antisymmetric versions). Once again, the kernels of all channels can be written in the form

$$K_{\mathcal{Q}\mathcal{Q},R}(j_1,j_2;z) = P_R^{\mathcal{Q}\mathcal{Q}}(t_1,t_2,z)K(j_1,j_2;z), \tag{6.10}$$

and we have tabulated the polynomials $P_R^{\mathcal{Q}\mathcal{Q}}$ in Table 3. An interesting new feature is that $P_{\mathbf{1}}^{\mathcal{Q}\mathcal{Q}}$ and $P_{\mathbf{20'}}^{\mathcal{Q}\mathcal{Q}}$ explicitly depend on z. At one loop we need no condition since all five channels are finite (the two channels $\mathbf{15_s}$ and $\mathbf{15_a}$ give identically vanishing contributions for symmetry reasons). However, at strong coupling we again observe a divergence in the singlet channel. The difference with the previous case is that now the singlet can only be removed by imposing a stronger condition $Y_2 = Y_3$. Its effect is to suppress all channels but the **84**, which is finite both at one loop and at strong coupling.

[23] A mechanism to tame them is discussed at length in Refs. [13,14].

Table 3
Charge–charge correlations. Notice that the polynomial in this case explicitly depends on the variable z. The channel $\mathbf{15_s}$ vanishes identically for symmetry reasons. The channels $\mathbf{1}$ and $\mathbf{20'}$ are removed by the condition $Y_2 = Y_3$.

$\langle \mathcal{Q}\mathcal{Q}\rangle$	$P_R^{\mathcal{Q}\mathcal{Q}}(t_1, t_2, z)$	$\mathcal{F}^{(1)}_{\mathcal{Q}\mathcal{Q};R}$	$\mathcal{F}^{(\infty)}_{\mathcal{Q}\mathcal{Q};R}$
$\mathbf{1}$	$\frac{2}{3}(1 + 15(t_1 + t_2) + 25\frac{1-z}{z})$	$-\frac{2(25-24z)\ln(1-z)}{3(1-z)}$	∞
$\mathbf{15_a}$	$t_1 - t_2$	0	0
$\mathbf{15_s}$	0	0	0
$\mathbf{20'}$	$\frac{5}{3}(3 - \frac{4}{z})$	$-5\frac{(3z-4)\ln(1-z)}{3(1-z)}$	$\frac{10(3z-4)z^2}{3}$
$\mathbf{84}$	1	$-\frac{z\ln(1-z)}{(1-z)}$	$2z^3$

Summarizing the various tables above, we remark the following interesting property, generalizing (6.2) and (6.6). For all choices of the two detectors, the kernels corresponding to the R-symmetry channel with the highest value of the quadratic Casimir of $SU(4)$, are identical:

$$K_{\mathcal{E}\mathcal{E};\mathbf{1}} = K_{\mathcal{E}\mathcal{Q};\mathbf{15}} = K_{\mathcal{E}\mathcal{O};\mathbf{20'}} = K_{\mathcal{Q}\mathcal{Q};\mathbf{84}} = K_{\mathcal{Q}\mathcal{O};\mathbf{175}} = K_{\mathcal{O}\mathcal{O};\mathbf{105}}. \tag{6.11}$$

This is a non-obvious corollary of $\mathcal{N} = 4$ superconformal symmetry, which will be investigated in our future work [43].

Finally, putting together the one-loop results for the event shape functions (6.1) from the different tables, we exactly reproduce the one-loop results of the amplitude calculations (without rearrangement into irreducible R-symmetry representations) listed in (4.18) and (4.19). For instance,

$$\mathcal{F}_{\mathcal{Q}\mathcal{Q}}(z) = \sum_{R=\mathbf{1},\mathbf{15}_s,\mathbf{15}_a,\mathbf{20'},\mathbf{84}} \omega_R^{\mathcal{Q}\mathcal{Q}} \mathcal{F}_{\mathcal{Q}\mathcal{Q};R}(z), \tag{6.12}$$

with $\omega_R^{\mathcal{Q}\mathcal{Q}}$ given by (D.12).

7. Conclusions

In this paper we studied the weighted cross sections describing the angular distribution of various global charges (energy, R-charge) in the final states of $\mathcal{N} = 4$ SYM created from the vacuum by a source. We applied the approach developed in the companion paper [14] and computed them starting from Euclidean correlation functions both at weak and strong coupling.

The starting point of our analysis was a relation between the weighted cross sections and Wightman correlation functions involving various flow operators. We defined three different types of the flow operators based on certain components of the $\mathcal{N} = 4$ stress-tensor multiplet: the half-BPS scalar operators, the R-symmetry currents and the energy–momentum tensor. In addition, we used the half-BPS scalar operator as a source that creates the physical state out of the vacuum. Then, the weighted cross section is determined by the Wightman correlation function involving different components of the $\mathcal{N} = 4$ stress-energy multiplet in a particular detector limit which includes sending some of the operators to the null infinity and subsequently integrating over their light-cone coordinates.

The Euclidean version of such correlation functions have a number of remarkable properties in $\mathcal{N} = 4$ SYM. In particular, three- and four-point correlators of operators belonging to the $\mathcal{N} = 4$ stress-energy multiplet are uniquely determined by analogous correlation functions of half-BPS scalar operators. The corresponding relations do not depend on the coupling constant and will be explained in more detail in an upcoming publication. The next step consisted in the analytical continuation of the Euclidean correlation functions to their Wightman counterparts following the Lüscher–Mack procedure [36]. We demonstrated that the most efficient and convenient way to do this is via the Mellin representation for the correlation functions.

In this way, we derived a master formula which yields an all-loop expression for the weighted cross sections as a convolution of the Mellin amplitude, defined by the Euclidean correlation function, with a coupling-independent 'detector kernel' determined by the choice of the flow operators. We performed thorough checks for single- and double-detector correlations to leading order at weak coupling and found perfect agreement with the conventional amplitude calculations of the corresponding observables in $\mathcal{N} = 4$ SYM. We would like to emphasize that our approach is applicable to all orders in the weak coupling expansion as well as at strong coupling. In the latter case, we made use of the prediction for the four-point correlation functions of half-BPS operators, obtained via the AdS/CFT correspondence, to compute the double correlations at strong coupling.

There are several directions in which the construction presented in this paper can be extended even further. Notice that the Mellin amplitude for the four-point correlation function of half-BPS operators is known to two loops and it should be possible to extend it beyond using the recent progress in computing the correlation function up to six loops [44]. This opens up a possibility to compute the flow correlations at higher orders of perturbative expansion and confront them with techniques based on Keldysh–Schwinger diagram technique [45]. We will address this question in a forthcoming publication.

Another important issue that has to be developed further concerns remarkable relations between the detector kernels corresponding to different flow operators and in different R-symmetry channels, Eqs. (6.2), (6.6) and (6.11). They lead to analogous relations between the weighted cross sections. We expect that there should exist a supersymmetric Ward identity that directly relates various weighted cross section studied in this paper. Finally, infrared finiteness of the charge flow correlations at weak coupling, the origin of the divergences at strong coupling in some R-symmetry channels require a more detailed study. These and other issues will be addressed elsewhere.

Acknowledgements

We would like to thank Vladimir Braun, Simon Caron-Huot, Lance Dixon, James Drummond, Gerhard Mack, Juan Maldacena, Gavin Salam, Raymond Stora and Ivan Todorov for useful discussions. The work of A.B. was supported by the US National Science Foundation under the grant No. PHY-1068286 and CNRS. G.K. and E.S. acknowledge partial support by the French National Agency for Research (ANR) under contract StrongInt (BLANC-SIMI-4-2011). A.Z. was supported in part by the US National Science Foundation under Grant No. PHY-0756966. A.B., S.H. and A.Z. are grateful to the Institut de Physique Théorique (Saclay) for the hospitality extended to them at various stages of the project. S.H., G.K. and E.S. would like to thank the Simons Center for Geometry and Physics (Stony Brook) for hospitality during completion of this paper.

Appendix A. Cross-talk between scalar detectors

By construction, the flow operators should commute with each other. As was mentioned in Section 2.2, this property is not obvious from their operator definition, Eqs. (2.14), (2.19) and

(2.28), due to the possibility for the same particle to go subsequently through various detectors. For two detectors oriented along two different spatial directions $\vec{n}$ and $\vec{n}'$, the momentum of such a particle should vanish. This means that the commutator of the flow operators, say $[\mathcal{O}(\vec{n}; S), \mathcal{O}(\vec{n}'; S')]$, can receive a contribution from particles with zero momenta only. To investigate this, we use the representation of the scalar flow operator (2.33) in terms of annihilation/creation operators of scalars combined with the identity[24]

$$\int_0^\infty d\tau\, \tau^\ell \delta^{(4)}(k - n\tau) = 2k_0^{\ell-1} \delta_+\big(k^2\big)\delta^{(2)}(\Omega_{\vec{k}} - \Omega_{\vec{n}}) \tag{A.1}$$

with $n^\mu = (1, \vec{n})$ being a light-like vector, $n^2 = 0$. Thus, we obtain an equivalent representation for the flow operator (for $\ell = 0$),

$$\mathcal{O}(\vec{n}; S) = \frac{1}{2(2\pi)^3} \sum_{i=1}^{6} S_i \int_0^\infty d\tau\, \big(\phi^i a^\dagger(n\tau)\big)\big(\phi^i a(n\tau)\big), \tag{A.2}$$

where $(\phi^i a(n\tau)) \equiv \sum_{I=1}^6 \phi^i_I a^I(n\tau)$. Notice that each additional factor of k_0 on the right-hand side of (A.1) is translated into a factor of τ in the integral on the left-hand side. This implies that the charge and energy flow operators, $\mathcal{Q}(\vec{n}; Q)$ and $\mathcal{E}(\vec{n})$, respectively, admit a representation similar to (A.2) with the important difference that the τ-integral involves additional factors of τ and τ^2, respectively (see Eq. (4.6)).

Making use of the commutation relation

$$\big[a^I(k), a^{\dagger J}(p)\big] = (2\pi)^3 2k_0 \delta^{(3)}(\vec{k} - \vec{p})\delta^{IJ}, \tag{A.3}$$

we find from (A.2)

$$\begin{aligned}\big[\mathcal{O}(\vec{n}; S), \mathcal{O}\big(\vec{n}'; S'\big)\big] = {} & \frac{1}{2(2\pi)^3} \sum_{i,j=1}^{6} S_i S'_j \big(\phi^i \phi'^j\big) \int_0^\infty d\tau_1 d\tau_2\, \tau_2 \delta^{(3)}\big(\tau_1 \vec{n} - \tau_2 \vec{n}'\big) \\ & \times \big[\big(\phi^i a^\dagger(n\tau_1)\big)\big(\phi'^j a\big(n'\tau_2\big)\big) - \big(\phi'^j a^\dagger\big(n'\tau_2\big)\big)\big(\phi^i a(n\tau_1)\big)\big],\end{aligned} \tag{A.4}$$

where ϕ^i, ϕ'^j and S, S' define the detector matrices (2.32) and $(\phi^i \phi'^j) = \sum_1^6 \phi^i_I \phi'^j_I$. The delta function localizes the τ-integral at $\tau_1 = \tau_2 = 0$ but leads to an ambiguous expression of the form $0 \times \delta(0)$. To carefully evaluate it we approximate the delta function and examine the following test integral involving an arbitrary test function $f(\tau_1, \tau_2)$

$$\begin{aligned}&\int_0^\infty d\tau_1 d\tau_2\, \tau_2 \delta^{(3)}\big(\tau_1 \vec{n} - \tau_2 \vec{n}'\big) f(\tau_1, \tau_2) \\ &\quad = \lim_{\epsilon \to 0} (\pi\epsilon)^{-3/2} \int_0^\infty d\tau_1 d\tau_2\, \tau_2 \mathrm{e}^{-(\tau_1\vec{n} - \tau_2\vec{n}')^2/\epsilon} f(\tau_1, \tau_2) \\ &\quad = \pi^{-3/2} \int_0^\infty d\tau_1 d\tau_2\, \tau_2 \mathrm{e}^{-(\tau_1\vec{n} - \tau_2\vec{n}')^2} \lim_{\epsilon \to 0} f\big(\epsilon^{1/2}\tau_1, \epsilon^{1/2}\tau_2\big) = \frac{1}{4\pi} \frac{f(0,0)}{1 - (\vec{n}\vec{n}')},\end{aligned} \tag{A.5}$$

24 To verify this identity it suffices to integrate both sides with a test function.

where in the second relation we rescaled the integration variables as $\tau_i \to \epsilon^{1/2}\tau_i$. Applying this identity to an appropriately chosen function $f(\tau_1, \tau_2)$ we find from (A.4)

$$\begin{aligned}&\big[\mathcal{O}(\vec{n}; S), \mathcal{O}\big(\vec{n}'; S'\big)\big]\\&= \frac{1}{4(2\pi)^4}\sum_{i,j=1}^{6}\frac{S_i S'_j(\phi^i\phi'^j)}{1-(\vec{n}\vec{n}')}\big[\big(\phi^i a^\dagger(0)\big)\big(\phi'^j a(0)\big) - \big(\phi'^j a^\dagger(0)\big)\big(\phi^i a(0)\big)\big]\\&= \frac{1}{4(2\pi)^4}\frac{a^{\dagger I}(0)(SS'-S'S)_{IJ}a^J(0)}{1-(\vec{n}\vec{n}')},\end{aligned} \tag{A.6}$$

where in the second relation we applied (2.32).

We conclude from (A.6) that, for general detector matrices S and S', the scalar flow operators do not commute. Moreover, in agreement with our expectations, the commutator receives a contribution from particles with zero momentum only. We recall that for the charge and energy flow operator, the integral representation analogous to (A.2) contains additional factors of τ. Calculating $[\mathcal{O}(\vec{n}; S), \mathcal{Q}(\vec{n}'; Q)]$ and $[\mathcal{O}(\vec{n}; S), \mathcal{E}(\vec{n}')]$ as in (A.6), we find that the additional factor of τ makes both commutators vanish. The same applies to all remaining commutators involving charge and energy flow operators.

Appendix B. *SU*(4) versus *SO*(6)

To simplify the R-symmetry structure of the correlation functions, throughout the paper we use two different but equivalent sets of isotopic (or harmonic) variables, Y^I and $(y_{AB}, \tilde{y}^{AB})$. The former defines a complex $SO(6)$ null vector $\sum_{I=1}^6 Y^I Y^I = 0$, whereas the latter carries a pair of $SU(4)$ indices $A, B = 1, \ldots, 4$ and satisfies the relations

$$y_{BA} = -y_{AB}, \qquad \tilde{y}^{AB} = \frac{1}{2}\epsilon^{ABCD} y_{CD}. \tag{B.1}$$

The variables Y and y are related to each other as follows:

$$Y_I = \frac{1}{\sqrt{2}}(\Sigma_I)^{AB} y_{AB}, \quad y_{AB} = \frac{1}{\sqrt{2}}\epsilon_{ABCD}(\Sigma_I)^{CD} Y_I, \tag{B.2}$$

where $(\Sigma_I)^{AB}$ are the (chiral) Dirac matrices for $SO(6)$. They satisfy the relations

$$\sum_{I=1}^{6}(\Sigma_I)^{AB}(\Sigma_I)^{CD} = \frac{1}{2}\epsilon^{ABCD}, \qquad \frac{1}{2}\epsilon_{ABCD}(\Sigma_I)^{AB}(\Sigma_J)^{CD} = \delta_{IJ} \tag{B.3}$$

and can be expressed in terms of the 't Hooft symbols $\Sigma_I^{AB} = (\eta_I^{AB}, i\bar{\eta}_I^{AB})$ [46]. Combining $(\Sigma_I)^{AB}$ with their complex conjugates $(\bar{\Sigma}_I)_{AB} = \overline{(\Sigma_I)^{AB}}$, we obtain the generators of the fundamental representation of $SU(4)$:

$$(\Gamma_{IJ})^A_C = -(\Gamma_{JI})^A_C = \frac{1}{2}(\Sigma_I)^{AB}(\bar{\Sigma}_J)_{BC} - (I \leftrightarrow J), \quad (\Gamma_{IJ})^A_A = 0. \tag{B.4}$$

We then use (B.2) and (B.3) to get the following identity

$$\begin{aligned}(Y_1Y_2) \equiv \sum_I Y_1^I Y_2^I &= \frac{1}{4}\epsilon^{ABCD}(y_1)_{AB}(y_2)_{CD} = \frac{1}{2}(y_1)_{AB}(\tilde{y}_2)^{AB}\\&= \frac{1}{2}(y_2)_{AB}(\tilde{y}_1)^{AB}.\end{aligned} \tag{B.5}$$

In the special case $Y_1^I = Y_2^I$, or equivalently $(y_1)_{AB} = (y_2)_{AB}$, it follows from $(Y_1 Y_1) = 0$ that

$$\frac{1}{2}\epsilon^{ABCD}(y_1)_{AB}(y_1)_{CD} = (y_1)_{AB}(\tilde{y}_1)^{AB} = 0. \tag{B.6}$$

Making use of (B.1) and (B.2) we can obtain two equivalent representations for various operators in terms of $SO(6)$ and/or $SU(4)$ harmonic variables.

In particular, the projected scalar field admits two representations,

$$(Y\Phi) = \sum_I Y^I \Phi^I = y_{AB}\phi^{AB} = \tilde{y}^{AB}\tilde{\phi}_{AB}, \tag{B.7}$$

where Φ^I and ϕ^{AB} are related to each other as

$$\phi^{AB} = \frac{1}{\sqrt{2}}(\Sigma_I)^{AB}\Phi^I, \qquad \tilde{\phi}_{AB} = \frac{1}{2}\epsilon_{ABCD}\phi^{CD} \tag{B.8}$$

and the scalar field satisfies the additional reality condition $\tilde{\phi}_{AB} = (\phi^{AB})^*$. Notice that we do not impose a similar condition on y_{AB} and treat $(y_{AB})^*$ as independent variables

$$\bar{y}^{AB} = (y_{AB})^* \neq \tilde{y}^{AB}. \tag{B.9}$$

Then, the half-BPS operator $O(x, Y) = \mathrm{tr}[(Y\Phi)^2]$ and its Hermitian conjugate $[O(x, Y)]^\dagger = \mathrm{tr}[(\overline{Y}\Phi)^2] = O(x, \overline{Y})$ take the form

$$O(x, Y) = \mathrm{tr}\big[\big(y_{AB}\phi^{AB}\big)^2\big], \qquad O(x, \overline{Y}) = \mathrm{tr}\big[\big(\bar{y}^{AB}\tilde{\phi}_{AB}\big)^2\big], \tag{B.10}$$

where $\phi^{AB} = \phi^{AB,a}T^a$, $\tilde{\phi}_{AB} = \tilde{\phi}^a_{AB}T^a$ and the $SU(N_c)$ generators are normalized as $\mathrm{tr}[T^aT^b] = \frac{1}{2}\delta^{ab}$ (with $a, b = 1, \dots, N_c^2 - 1$). The total transition probability involves the two-point correlation function of such operators,

$$\begin{aligned} \big\langle O(x_1, \overline{Y})O(x_2, Y)\big\rangle &= \frac{N_c^2 - 1}{2}\left[\frac{1}{2}y_{A_1B_1}\bar{y}^{A_1B_1}D(x_1 - x_2)\right]^2 \\ &= \frac{N_c^2 - 1}{2}\big[(Y\overline{Y})D(x_1 - x_2)\big]^2, \end{aligned} \tag{B.11}$$

where $(Y\overline{Y}) = \frac{1}{2}y_{A_1B_1}\bar{y}^{A_1B_1}$ and $D(x)$ denotes the propagator of a free scalar field,

$$\begin{aligned} &\big\langle \Phi^{I,a}(x_1)\Phi^{J,b}(x_2)\big\rangle = \delta^{ab}\delta^{IJ}D(x_1 - x_2), \\ &\big\langle \phi^{A_1B_1,a_1}(x_1)\tilde{\phi}^{a_2}_{A_2B_2}(x_2)\big\rangle = \frac{1}{4}\delta^{a_1a_2}\big(\delta^{A_1}_{A_2}\delta^{B_1}_{B_2} - \delta^{A_1}_{B_2}\delta^{B_1}_{A_2}\big)D(x_1 - x_2). \end{aligned} \tag{B.12}$$

The explicit expression for $D(x)$ contains a prescription,

$$D_F(x) = -\frac{1}{4\pi^2}\frac{1}{x^2 - i\epsilon}, \qquad D_W(x) = -\frac{1}{4\pi^2}\frac{1}{x^2 - i\epsilon x_0}, \tag{B.13}$$

for Feynman (time-ordered) and Wightman correlation functions, respectively.

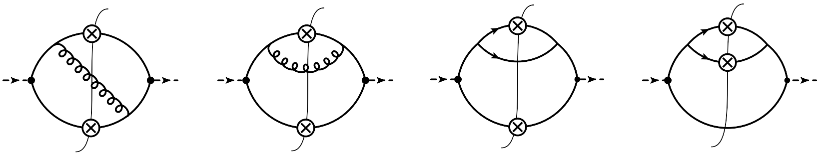

Fig. 6. One-loop correction to scalar–scalar and charge–charge correlations. Crosses denote detectors and the thin line stands for the unitarity cut.

Appendix C. Scalar, charge and energy correlations at one loop

In this appendix, we compute scalar–scalar, charge–charge and energy–energy correlations to lowest order in the coupling, using amplitude techniques.

To one-loop order, the scalar–scalar correlation $\langle\mathcal{O}(\vec{n})\mathcal{O}(\vec{n}')\rangle$ receives contributions only from the final state $|\mathrm{ssg}\rangle$ involving a pair of scalars and a gluon. The relevant Feynman diagrams are shown in Figs. 6(a) and (b). For the charge–charge correlation $\langle\mathcal{Q}(\vec{n})\mathcal{Q}(\vec{n}')\rangle$ there is an additional contribution from the state $|\mathrm{s}\lambda\lambda\rangle$ and it comes from the diagrams shown in Figs. 6(c) and (d). To compute their contribution, we have to combine the transition amplitudes given by (3.2) with the corresponding $SU(4)$ weight factors and perform the integration over the phase space of the particles in the final state.

Let us start with the scalar–scalar correlation. It is simpler to do the calculation using the $SO(6)$ notation. To compute the R-symmetry factor corresponding to the diagrams in Figs. 6(a) and (b) it suffices to perform a Wick contraction between the scalar fields in the source $O(0,Y)=\mathrm{tr}[(Y\Phi)^2]$ and the sink $O(x,\bar{Y})=\mathrm{tr}[(\bar{Y}\Phi)^2]$ and the creation/annihilation operators in the expression for the scalar flow operator (2.31), $\mathcal{O}(\vec{n},S)\sim S_{IJ}a^{\dagger I}a^J$:

$$2\big\langle(\bar{Y}\Phi)\mathcal{O}(\vec{n},S)(Y\Phi)\big\rangle\big\langle(\bar{Y}\Phi)\mathcal{O}\big(\vec{n}',S'\big)(Y\Phi)\big\rangle\sim 2\big(Y^I S_{IJ}\bar{Y}^J\big)\big(Y^{I'}S'_{I'J'}\bar{Y}^{J'}\big)$$
$$=2(Y\bar{Y})^2\langle S\rangle\big\langle S'\big\rangle, \tag{C.1}$$

where the notation was introduced for $\langle S\rangle=(Y^I S_{IJ}\bar{Y}^J)/(Y\bar{Y})$ and $(Y\bar{Y})=Y^I\bar{Y}^I$. Here the overall factor of 2 takes into account the symmetry of the diagrams under the exchange of the detectors. The two diagrams in Figs. 6(a) and (b) have the same R-factor and, therefore, the one-loop correction to the scalar–scalar correlation has the factorized form

$$\big\langle\mathcal{O}(\vec{n})\mathcal{O}\big(\vec{n}'\big)\big\rangle=\sigma_{\mathrm{tot}}^{-1}\int \mathrm{dPS}_3\big(k_1^0k_2^0\big)^{-1}(YS\bar{Y})\big(YS'\bar{Y}\big)|\mathcal{M}_{O_{\mathbf{20'}}\to\mathrm{s}(k_1)\mathrm{s}(k_2)\mathrm{g}(k_3)}|^2$$
$$\times\big[\delta^{(2)}(\Omega_{\vec{k}_1}-\Omega_{\vec{n}})\delta^{(2)}(\Omega_{\vec{k}_2}-\Omega_{\vec{n}'})+\delta^{(2)}(\Omega_{\vec{k}_1}-\Omega_{\vec{n}'})\delta^{(2)}(\Omega_{\vec{k}_2}-\Omega_{\vec{n}})\big], \tag{C.2}$$

where the matrix element is given by (3.2) and the phase space integral is defined in (3.4).

To perform the integration over the phase space of the three particles in (C.2) it is convenient to introduce the two-particle invariant masses $s_{ij}=(k_i+k_j)^2$ with $k_1+k_2+k_3=q$. In the rest frame of the source $q^\mu=(q_0,\vec{0})$ we have

$$s_{12}=q_0^2(1-\tau_3),\qquad s_{23}=q_0^2(1-\tau_1),\qquad s_{13}=q_0^2(1-\tau_2), \tag{C.3}$$

where the variables $\tau_i=2k_{i,0}/q_0$ are related to the energy of the particles and satisfy the conditions $0\le\tau_i\le1$ and $\tau_1+\tau_2+\tau_3=2$. Then,

$$\int \mathrm{dPS}_3\, \delta^{(2)}(\Omega_{\vec{k}_1} - \Omega_{\vec{n}})\delta^{(2)}(\Omega_{\vec{k}_2} - \Omega_{\vec{n}'})$$

$$= \frac{q_0^2}{64(2\pi)^5} \int_0^1 d\tau_1 d\tau_2\, \tau_1\tau_2\, \delta(1 - \tau_1 - \tau_2 + \tau_1\tau_2 z), \tag{C.4}$$

where $z = (1 - \cos\theta)/2$. In this way, we obtain from (C.2)

$$\langle \mathcal{O}(\vec{n})\mathcal{O}(\vec{n}')\rangle = \frac{g^2}{32\pi^4} \frac{(YS\bar{Y})(YS'\bar{Y})}{q_0^2(Y\bar{Y})^2}$$

$$\times \int_0^1 d\tau_1 d\tau_2 \frac{\tau_1 + \tau_2 - 1}{(1 - \tau_1)(1 - \tau_2)} \delta(1 - \tau_1 - \tau_2 + \tau_1\tau_2 z) \tag{C.5}$$

and arrive at (3.21).

The analysis of the charge–charge correlations goes along the same lines. To one-loop order, $\langle \mathcal{Q}(\vec{n})\mathcal{Q}(\vec{n}')\rangle$ receives contributions from the diagrams shown in Figs. 6(a)–(d). In this case, for computing the R-symmetry factor, it is convenient to use the $SU(4)$ representation for the source and sink operators, Eq. (B.10). For the diagrams in Figs. 6(a) and (b) we use the scalar part of the charge flow operator $\mathcal{Q}(\vec{n}) \sim Q^A_B a^\dagger_{AC} a^{CB}$, Eqs. (2.20) and (2.22), and perform the Wick contractions

$$Q^{A_3}_{B_3}\langle y_{A_1B_1}\phi^{A_1B_1} a^\dagger_{A_3C_3}\rangle\langle a^{C_3B_3}\bar{y}^{A_2B_2}\bar{\phi}_{A_2B_2}\rangle (Q')^{A_4}_{B_4}\langle y_{A'_1B'_1}\phi^{A'_1B'_1} a^\dagger_{A_4C_4}\rangle\langle a^{C_4B_4}\bar{y}^{A'_2B'_2}\bar{\phi}_{A'_2B'_2}\rangle$$

$$\sim Q^{A_3}_{B_3}(Q')^{A_4}_{B_4} y_{A_1B_1}\bar{y}^{A_2B_2} y_{1,A'_1B'_1}\bar{y}^{A'_2B'_2}\delta^{A_1}_{A_3}\delta^{B_1}_{C_3}\delta^{C_3}_{A_2}\delta^{B_3}_{B_2}\delta^{A'_1}_{A_4}\delta^{B'_1}_{C_4}\delta^{C_4}_{A'_2}\delta^{B_4}_{B'_2}$$

$$\sim Q^{A_3}_{B_3} y_{A_3B_1}\bar{y}^{B_1B_3}(Q')^{A_4}_{B_4} y_{A_4B'_1}\bar{y}^{B'_1B_4} \equiv \mathrm{tr}(\bar{y}Qy)\,\mathrm{tr}(\bar{y}Q'y). \tag{C.6}$$

For the diagrams in Figs. 6(c) and (d) we have to use the gluino part of the charge flow operator, $\mathcal{Q}(\vec{n}) \sim Q^A_B a^\dagger_{A,1/2} a^B_{-1/2}$. Going through the calculation of the $SU(4)$ factors, we find that for the diagram in Fig. 6(c) it is given by (C.6) whereas for the diagram in Fig. 6(d) we have

$$Q^{A_3}_{B_3}(Q')^{A_4}_{B_4} y_{A_3A_4}\bar{y}^{B_3B_4} \equiv \mathrm{tr}(\bar{y}QyQ')\,\mathrm{tr}(\bar{y}y) = \mathrm{tr}(\bar{y}Q'yQ)\,\mathrm{tr}(\bar{y}y)$$

$$= \mathrm{tr}(yQ\bar{y}Q')\,\mathrm{tr}(\bar{y}y), \tag{C.7}$$

where the second relation follows from antisymmetry of y and $\bar{y}$ under exchange of the $SU(4)$ indices. There is one more diagram of the type 6(d) in which the fermion lines have opposite orientation. Its $SU(4)$ factor can be obtained by the substitution $y_{AB} \to \tilde{\bar{y}}_{AB} \equiv \frac{1}{2}\epsilon_{ABCD}\bar{y}^{CD}$ and $\bar{y}^{AB} \to \tilde{y}^{AB} \equiv \frac{1}{2}\epsilon^{ABCD} y_{CD}$, and reads $\mathrm{tr}(\tilde{\bar{y}}Q\tilde{y}Q')\,\mathrm{tr}(\bar{y}y)$. Then, the one-loop correction to $\langle \mathcal{Q}(\vec{n})\mathcal{Q}(\vec{n}')\rangle$ takes the following form

$$\langle \mathcal{Q}(\vec{n})\mathcal{Q}(\vec{n}')\rangle = 4\frac{\mathrm{tr}(yQ\bar{y})}{\mathrm{tr}(y\bar{y})}\frac{\mathrm{tr}(yQ'\bar{y})}{\mathrm{tr}(y\bar{y})}(I_{a+b} + I_c) + \frac{\mathrm{tr}[yQ'\bar{y}Q + \tilde{\bar{y}}Q'\tilde{y}Q]}{2\,\mathrm{tr}(y\bar{y})} I_d, \tag{C.8}$$

where I_{a+b} denotes the contribution of the diagrams shown in Figs. 6(a) and (b)

$$I_{a+b} = \frac{2[\mathrm{tr}(\bar{y}y)]^2}{\sigma_{\mathrm{tot}}} \int \mathrm{dPS}_3\, \delta^{(2)}(\Omega_{\vec{k}_1} - \Omega_{\vec{n}})\delta^{(2)}(\Omega_{\vec{k}_2} - \Omega_{\vec{n}'})|\mathcal{M}_{O_{\mathbf{20'}}\to s(k_1)s(k_2)g(k_3)}|^2, \tag{C.9}$$

and similarly for I_c and I_d,

$$I_c = \frac{2[\mathrm{tr}(\bar{y}y)]^2}{\sigma_{\rm tot}} \int \mathrm{dPS}_3\, \delta^{(2)}(\Omega_{\vec{k}_1} - \Omega_{\vec{n}})\delta^{(2)}(\Omega_{\vec{k}_2} - \Omega_{\vec{n}'})|\mathcal{M}_{O_{\mathbf{20}'}\to s(k_1)\lambda(k_2)\lambda(k_3)}|^2,$$
$$I_d = \frac{2[\mathrm{tr}(\bar{y}y)]^2}{\sigma_{\rm tot}} \int \mathrm{dPS}_3\, \delta^{(2)}(\Omega_{\vec{k}_2} - \Omega_{\vec{n}})\delta^{(2)}(\Omega_{\vec{k}_3} - \Omega_{\vec{n}'})|\mathcal{M}_{O_{\mathbf{20}'}\to s(k_1)\lambda(k_2)\lambda(k_3)}|^2. \quad \text{(C.10)}$$

The evaluation of these integrals goes along the same lines as before: we go to the new variables (C.3), replace the matrix elements by their explicit expressions (3.2) and integrate over the phase space using the relation (C.4). In this way, we obtain

$$I_{a+b} = \frac{a}{8\pi^2}\frac{(z-2)\ln(1-z) - 2z}{z^2(1-z)},$$
$$I_c = \frac{a}{4\pi^2}\frac{(1-z)\ln(1-z) + z}{z^2(1-z)},$$
$$I_d = -\frac{a}{4\pi^2}\frac{\ln(1-z)}{z^2}. \quad \text{(C.11)}$$

The substitution of these relations into (C.8) yields (3.23).

Finally, the one-loop correction to the energy–energy correlation $\langle \mathcal{E}(n)\mathcal{E}(n')\rangle$ is given by (3.15). We replace the transition amplitudes in (3.15) by their explicit expressions (3.2) and take into account the symmetry of the integration measure under the exchange of any pair of particles to obtain

$$\big\langle \mathcal{E}(n)\mathcal{E}\big(n'\big)\big\rangle = 16\pi g^2 \int \mathrm{dPS}_3\, k_1^0 k_2^0 \delta^{(2)}(\Omega_{\vec{k}_1} - \Omega_{\vec{n}})\delta^{(2)}(\Omega_{\vec{k}_2} - \Omega_{\vec{n}'})\frac{4(q^2)^2}{s_{12}s_{13}s_{23}}, \quad \text{(C.12)}$$

where the last factor has the same origin as the one in (3.5). Using (C.3) and (C.4), we find

$$\big\langle \mathcal{E}(n)\mathcal{E}\big(n'\big)\big\rangle = \frac{g^2 q_0^2}{8(2\pi)^4}\int_0^1 \frac{d\tau_1 d\tau_2\,(\tau_1\tau_2)^2}{(1-\tau_1)(1-\tau_2)(\tau_1+\tau_2-1)}\delta(1-\tau_1-\tau_2+\tau_1\tau_2 z)$$
$$= \frac{g^2 q_0^2}{8(2\pi)^4}\frac{1}{z(1-z)}\int_0^1 \frac{d\tau_1}{1-z\tau_1}. \quad \text{(C.13)}$$

Replacing $z = (1-\cos\theta)/2$ we arrive at (3.16).

Appendix D. R-symmetry invariant structures

In this appendix, we discuss explicit expressions for the R-symmetry factors ω_R in (6.1). We will use the same notation as in the amplitude computations, but in addition we also introduce

$$\langle S\rangle = \frac{(YS\bar{Y})}{(Y\bar{Y})}, \qquad [S] = \frac{(YSY)}{(Y\bar{Y})}, \qquad \overline{[S]} = \frac{(\bar{Y}S\bar{Y})}{(Y\bar{Y})},$$
$$\big\langle SS'\big\rangle = \frac{(YSS'\bar{Y})}{(Y\bar{Y})}, \qquad \overline{\big\langle SS'\big\rangle} = \frac{(YS'S\bar{Y})}{(Y\bar{Y})}, \qquad \big(SS'\big) = \mathrm{tr}\big(SS'\big). \quad \text{(D.1)}$$

With this notation, we find the following explicit expressions for $\omega_R^{\mathcal{O}\mathcal{O}}$:

$$\begin{aligned}
\omega_{\mathbf{1}}^{\mathcal{O}\mathcal{O}} &= \frac{1}{6}(SS'),\\
\omega_{\mathbf{15}}^{\mathcal{O}\mathcal{O}} &= \frac{1}{6}\{\langle SS'\rangle - \overline{\langle SS'\rangle}\},\\
\omega_{\mathbf{20'}}^{\mathcal{O}\mathcal{O}} &= \frac{1}{6}\left\{\langle SS'\rangle + \overline{\langle SS'\rangle} - \frac{1}{3}(SS')\right\},\\
\omega_{\mathbf{84}}^{\mathcal{O}\mathcal{O}} &= \frac{1}{6}\left\{[S]\overline{[S']} + \overline{[S]}[S'] - 2\langle S\rangle\langle S'\rangle - \frac{1}{2}\left(\langle SS'\rangle + \overline{\langle SS'\rangle}\right) + \frac{1}{10}(SS')\right\},\\
\omega_{\mathbf{175}}^{\mathcal{O}\mathcal{O}} &= \frac{1}{6}\left\{[S]\overline{[S']} - \overline{[S]}[S'] - \frac{1}{2}\left(\langle SS'\rangle - \overline{\langle SS'\rangle}\right)\right\},\\
\omega_{\mathbf{105}}^{\mathcal{O}\mathcal{O}} &= \frac{1}{6}\left\{[S]\overline{[S']} + \overline{[S]}[S'] + 4\langle S\rangle\langle S'\rangle - \frac{4}{5}\left(\langle SS'\rangle + \overline{\langle SS'\rangle}\right) + \frac{1}{10}(SS')\right\}.
\end{aligned} \tag{D.2}$$

We recall that in order to rewrite the basis structures Y_R in the correlation function notation of Section 5.2, one has to make the replacements $S^{IJ} \to Y_2^I Y_2^J$, $(S')^{IJ} \to Y_3^I Y_3^J$, $Y \to Y_4$, $\overline{Y} \to Y_1$. Converting the structures (D.2) into correlation function ones, we get

$$\omega_R^{\mathcal{O}\mathcal{O}} \to (Y_2Y_3)^2\mathcal{Y}_R(t_1, t_2), \tag{D.3}$$

with $t_1 = (Y_1Y_2)(Y_3Y_4)/((Y_1Y_4)(Y_2Y_3))$, $t_2 = (Y_1Y_3)(Y_2Y_4)/((Y_1Y_4)(Y_2Y_3))$ and

$$\begin{aligned}
\mathcal{Y}_{\mathbf{1}} &= 1\\
\mathcal{Y}_{\mathbf{15}} &= t_1 - t_2\\
\mathcal{Y}_{\mathbf{20'}} &= t_1 + t_2 - \frac{1}{3}\\
\mathcal{Y}_{\mathbf{84}} &= (t_1 - t_2)^2 - \frac{1}{2}(t_1 + t_2) + \frac{1}{10}\\
\mathcal{Y}_{\mathbf{175}} &= t_1^2 - t_2^2 - \frac{1}{2}(t_1 - t_2)\\
\mathcal{Y}_{\mathbf{105}} &= t_1^2 + t_2^2 + 4t_1t_2 - \frac{4}{5}(t_1 + t_2) + \frac{1}{10}.
\end{aligned} \tag{D.4}$$

The polynomials $\mathcal{Y}_R$ coincide with the eigenfunctions $Y_{nm}(t_1, t_2)$ of the quadratic Casimir operator of $SU(4)$ for the irreps with Dynkin labels $[n-m, 2m, n-m]$, as listed in Appendix B in [47].

Further, the condition (2.38) for absence of cross-talk between the two scalar detectors, $[S, S'] = 0$, is translated into $(Y_2Y_3)(Y_2^I Y_3^J - Y_2^J Y_3^I) = 0$. This condition has two solutions, the weaker constraint $(Y_2Y_3) = 0$ or the stronger $Y_2 = Y_3$.[25] Inserting these constraints back into (D.2), we find that the weaker one implies

$$(Y_2Y_3) = 0 \to (SS') = \langle SS'\rangle = \langle S'S\rangle = 0 \to \omega_{\mathbf{1}}^{\mathcal{O}\mathcal{O}} = \omega_{\mathbf{15}}^{\mathcal{O}\mathcal{O}} = \omega_{\mathbf{20'}}^{\mathcal{O}\mathcal{O}} = 0, \tag{D.5}$$

while the stronger constraint yields, in addition to (D.5),

$$Y_2 = Y_3 \to [S]\overline{[S']} = \overline{[S]}[S'] = \langle S\rangle\langle S'\rangle \to \omega_{\mathbf{84}}^{\mathcal{O}\mathcal{O}} = \omega_{\mathbf{175}}^{\mathcal{O}\mathcal{O}} = 0. \tag{D.6}$$

[25] The variables Y_i are projective, so without loss of generality we can set $Y_2 = Y_3$ instead of $Y_2 \propto Y_3$.

Thus, the strong version (D.6) of the condition for absence of cross-talk results in only one surviving R-symmetry structure, $\omega_{\mathbf{105}}^{\mathcal{O}\mathcal{O}} \neq 0$.

Inversely, we can ask the question which conditions on the projection variables Y and on the detector matrices S and S' eliminate all R-symmetry structures but $\omega_{\mathbf{105}}^{\mathcal{O}\mathcal{O}}$. Assuming that the detector matrices satisfy the stronger form of the no-cross-talk condition, $SS' = 0$ (instead of $[S, S'] = 0$), from (D.2) we derive the additional conditions

$$[S]\overline{[S']} = \overline{[S]}[S'] = \langle S\rangle\langle S'\rangle. \tag{D.7}$$

These can be solved by, e.g., the following choice of the auxiliary variables (used in Ref. [14]):

$$Y = (1, 0, 1, 0, i, i), \qquad S = \operatorname{diag}(1, -1, 0, 0, 0, 0), \qquad S' = \operatorname{diag}(0, 0, 1, -1, 0, 0). \tag{D.8}$$

In a similar fashion, we can deal with basis structures in the case of charge–scalar correlations. Indeed, we can write (up to normalization)

$$\begin{aligned}
\omega_{\mathbf{15}}^{\mathcal{Q}\mathcal{O}} &= 4\big[\langle QS\rangle + \overline{\langle QS\rangle}\big],\\
\omega_{\mathbf{20'}}^{\mathcal{Q}\mathcal{O}} &= 4\big[\langle QS\rangle - \overline{\langle QS\rangle}\big],\\
\omega_{\mathbf{175}}^{\mathcal{Q}\mathcal{O}} &= 4\left[\langle S\rangle\langle Q\rangle - \frac{1}{8}\big\{\langle QS\rangle + \overline{\langle QS\rangle}\big\}\right].
\end{aligned} \tag{D.9}$$

Here $\langle QS\rangle = Y^I Q^{IJ} S^{KL} \overline{Y}^L$, and we have rewritten the detector matrix $Q^{IJ} = -Q^{JI} = (\Gamma^{IJ})_A^{\ B} Q_B^{\ A}$ in $SO(6)$ notation, with the help of the $SO(6)$ gamma matrices defined in (B.4).

In the case of the charge–charge correlations, the relevant R-invariant building blocks can be written in the form

$$\begin{aligned}
&\mathcal{Z}_1 = \operatorname{tr}\big(QQ'\big), \qquad \mathcal{Z}_2 = \frac{\operatorname{tr}(yQ\bar{y})\operatorname{tr}(yQ'\bar{y})}{[\operatorname{tr}(y\bar{y})]^2},\\
&\mathcal{Z}_3 = \frac{\operatorname{tr}(yQQ'\bar{y})}{\operatorname{tr}(y\bar{y})}, \qquad \mathcal{Z}_4 = \frac{\operatorname{tr}(yQ'Q\bar{y})}{\operatorname{tr}(y\bar{y})}, \qquad \mathcal{Z}_5 = \frac{\operatorname{tr}(yQ\bar{y}Q')}{\operatorname{tr}(y\bar{y})}.
\end{aligned} \tag{D.10}$$

The additional structure appearing in the second term in (3.24) is not independent:

$$\begin{aligned}
&\frac{\operatorname{tr}(\tilde{\bar{y}}Q\tilde{y}Q')}{\operatorname{tr}(y\bar{y})} = \mathcal{Z}_5 - \frac{1}{2}\mathcal{Z}_1 - (\mathcal{Z}_3 + \mathcal{Z}_4)\\
&\quad\rightarrow \quad \big\langle Q, Q'\big\rangle = 2\mathcal{Z}_5 - \frac{1}{2}\mathcal{Z}_1 - (\mathcal{Z}_3 + \mathcal{Z}_4).
\end{aligned} \tag{D.11}$$

The R-symmetry factors ω_R are constructed from them as follows (up to normalization):

$$\begin{aligned}
\omega_{\mathbf{1}}^{\mathcal{Q}\mathcal{Q}} &= -\frac{1}{5}\mathcal{Z}_1,\\
\omega_{\mathbf{15_a}}^{\mathcal{Q}\mathcal{Q}} &= -\frac{1}{5}[\mathcal{Z}_3 - \mathcal{Z}_4],\\
\omega_{\mathbf{15_s}}^{\mathcal{Q}\mathcal{Q}} &= -\frac{1}{5}\big[\mathcal{Z}_1 - 4(\mathcal{Z}_3 + \mathcal{Z}_4)\big],\\
\omega_{\mathbf{20'}}^{\mathcal{Q}\mathcal{Q}} &= -\frac{1}{5}\big[\mathcal{Z}_1 - 3(\mathcal{Z}_3 + \mathcal{Z}_4) + 6\mathcal{Z}_5\big],\\
\omega_{\mathbf{84}}^{\mathcal{Q}\mathcal{Q}} &= -\frac{1}{5}\big[\mathcal{Z}_1 - 40\mathcal{Z}_2 - 5(\mathcal{Z}_3 + \mathcal{Z}_4) + 10\mathcal{Z}_5\big].
\end{aligned} \tag{D.12}$$

Finally, the two correlations involving energy detectors have particularly simple R-symmetry factors:

$$\omega_{\mathbf{1}}^{\mathcal{E}\mathcal{E}} = 1, \qquad \omega_{\mathbf{15}}^{\mathcal{E}\mathcal{Q}} = 8\langle Q\rangle, \qquad \omega_{\mathbf{20'}}^{\mathcal{E}\mathcal{O}} = 2\langle S\rangle. \tag{D.13}$$

Appendix E. Scalar detector in Mellin space

In this appendix we compute the function $K(j_1, j_2; z)$ defined in (5.24). Replacing the function $f(j_1, j_2; x_1, x_{2-}, x_{3-})$ in (5.24) with its explicit expression (5.20) we find

$$K(j_1, j_2; z) = \frac{1}{16\pi^5} q^2\big((nn')/2\big)^{-j_1-j_2+1} \int \frac{d^4x_1 e^{iqx_1}}{(-x_1^2 + i\epsilon x_1^0)^{j_1+j_2}} \\ \times \int_{-\infty}^{\infty} dx_{2-}\big((x_1 n) - x_{2-} - i\epsilon\big)^{j_1-1}(-x_{2-} + i\epsilon)^{j_2-1} \\ \times \int_{-\infty}^{\infty} dx_{3-}\big((x_1 n') - x_{3-} - i\epsilon\big)^{j_2-1}(-x_{3-} + i\epsilon)^{j_1-1}. \tag{E.1}$$

The evaluation of the x_--integrals is straightforward, making use of the Schwinger representation for the factors involved

$$\int_{-\infty}^{\infty} dx_{2-}\big((x_1 n) - x_{2-} - i0\big)^{j_1-1}(-x_{2-} + i0)^{j_2-1} \\ = \frac{2\pi i^{j_2-j_1}}{\Gamma(1-j_1)\Gamma(1-j_2)} \int_0^{\infty} d\omega_1 \omega_1^{-j_1-j_2} e^{-i\omega_1(x_1 n)}. \tag{E.2}$$

Here we left the final integration intact, which helps in evaluating the x_1-integral in (E.1),

$$K(j_1, j_2; z) = \frac{q^2((nn')/2)^{-j_1-j_2+1}}{4\pi^3[\Gamma(1-j_1)\Gamma(1-j_2)]^2} \\ \times \int_0^{\infty} d\omega_1 d\omega_2 (\omega_1\omega_2)^{-j_1-j_2} D_{j_1+j_2}\big(q - \omega_1 n - \omega_2 n'\big) \tag{E.3}$$

where the notation was introduced for

$$D_j(q) = \int \frac{d^4x_1 e^{iqx_1}}{(-x_1^2 + i\epsilon x_1^0)^j} = 2\pi^3 \frac{(q^2/4)^{j-2}\theta(q^0)\theta(q^2)}{\Gamma(j)\Gamma(j-1)}. \tag{E.4}$$

Computing the ω-integrals in (E.3) we find

$$K(j_1, j_2; z) = \left(\frac{z}{1-z}\right)^{1-j_1-j_2} \frac{2\pi}{\sin(\pi(j_1+j_2))[\Gamma(j_1+j_2)\Gamma(1-j_1)\Gamma(1-j_2)]^2}. \tag{E.5}$$

References

[1] G.F. Sterman, S. Weinberg, Jets from quantum chromodynamics, Phys. Rev. Lett. 39 (1977) 1436.

[2] Z. Kunszt, P. Nason, G. Marchesini, B.R. Webber, QCD at LEP, in: Proceedings, Z Physics at LEP 1, vol. 1, Geneva, 1989, pp. 373–453.

[3] O. Biebel, Experimental tests of the strong interaction and its energy dependence in electron positron annihilation, Phys. Rep. 340 (2001) 165.

[4] C.L. Basham, L.S. Brown, S.D. Ellis, S.T. Love, Energy correlations in electron–positron annihilation: testing QCD, Phys. Rev. Lett. 41 (1978) 1585;
C.L. Basham, L.S. Brown, S.D. Ellis, S.T. Love, Electron–positron annihilation energy pattern in Quantum Chromodynamics: asymptotically free perturbation theory, Phys. Rev. D 17 (1978) 2298;
C.L. Basham, L.S. Brown, S.D. Ellis, S.T. Love, Energy correlations in electron–positron annihilation in Quantum Chromodynamics: asymptotically free perturbation theory, Phys. Rev. D 19 (1979) 2018.

[5] M. Dasgupta, G.P. Salam, Event shapes in e^+e^- annihilation and deep inelastic scattering, J. Phys. G 30 (2004) R143, arXiv:hep-ph/0312283.

[6] T. Kinoshita, Mass singularities of Feynman amplitudes, J. Math. Phys. 3 (1962) 650.

[7] T.D. Lee, M. Nauenberg, Degenerate systems and mass singularities, Phys. Rev. 133 (1964) B1549.

[8] W.L. van Neerven, Infrared behavior of on-shell form-factors in $N = 4$ supersymmetric Yang–Mills field theory, Z. Phys. C 30 (1986) 595.

[9] N.A. Sveshnikov, F.V. Tkachov, Jets and quantum field theory, Phys. Lett. B 382 (1996) 403, arXiv:hep-ph/9512370.

[10] G.P. Korchemsky, G. Oderda, G.F. Sterman, Power corrections and nonlocal operators, arXiv:hep-ph/9708346.

[11] G.P. Korchemsky, G.F. Sterman, Power corrections to event shapes and factorization, Nucl. Phys. B 555 (1999) 335, arXiv:hep-ph/9902341.

[12] A.V. Belitsky, G.P. Korchemsky, G. Sterman, Energy flow in QCD and event shape functions, Phys. Lett. B 515 (2001) 297, arXiv:hep-ph/0106308.

[13] D.M. Hofman, J. Maldacena, Conformal collider physics: energy and charge correlations, J. High Energy Phys. 0805 (2008) 012, arXiv:0803.1467 [hep-th].

[14] A.V. Belitsky, S. Hohenegger, G.P. Korchemsky, E. Sokatchev, A. Zhiboedov, From correlation functions to event shapes, arXiv:1309.0769 [hep-th].

[15] P.S. Howe, P.C. West, Nonperturbative Green's functions in theories with extended superconformal symmetry, Int. J. Mod. Phys. A 14 (1999) 2659, arXiv:hep-th/9509140;
P.S. Howe, P.C. West, Operator product expansions in four-dimensional superconformal field theories, Phys. Lett. B 389 (1996) 273, arXiv:hep-th/9607060.

[16] E. D'Hoker, D.Z. Freedman, W. Skiba, Field theory tests for correlators in the AdS/CFT correspondence, Phys. Rev. D 59 (1999) 045008, arXiv:hep-th/9807098.

[17] P.S. Howe, E. Sokatchev, P.C. West, Three point functions in $N = 4$ Yang–Mills, Phys. Lett. B 444 (1998) 341, arXiv:hep-th/9808162.

[18] S. Lee, S. Minwalla, M. Rangamani, N. Seiberg, Three point functions of chiral operators in $D = 4$, $N = 4$ SYM at large N, Adv. Theor. Math. Phys. 2 (1998) 697, arXiv:hep-th/9806074.

[19] S. Penati, A. Santambrogio, D. Zanon, Two point functions of chiral operators in $N = 4$ SYM at order g^4, J. High Energy Phys. 9912 (1999) 006, arXiv:hep-th/9910197;
S. Penati, A. Santambrogio, D. Zanon, More on correlators and contact terms in $N = 4$ SYM at order g^4, Nucl. Phys. B 593 (2001) 651, arXiv:hep-th/0005223.

[20] J.C. Collins, Sudakov form-factors, Adv. Ser. Dir. High Energy Phys. 5 (1989) 573, arXiv:hep-ph/0312336.

[21] Z. Kunszt, D.E. Soper, Calculation of jet cross sections in hadron collisions at order α_s^3, Phys. Rev. D 46 (1992) 192.

[22] A. Galperin, E. Ivanov, S. Kalitsyn, V. Ogievetsky, E. Sokatchev, Unconstrained $N = 2$ matter, Yang–Mills and supergravity theories in harmonic superspace, Class. Quantum Gravity 1 (1984) 469.

[23] P.S. Howe, G.G. Hartwell, A superspace survey, Class. Quantum Gravity 12 (1995) 1823.

[24] A. Banfi, G.P. Salam, G. Zanderighi, Infrared safe definition of jet flavor, Eur. Phys. J. C 47 (2006) 113, arXiv:hep-ph/0601139.

[25] J.C. Collins, D.E. Soper, Back-to-back jets in QCD, Nucl. Phys. B 193 (1981) 381;
J.C. Collins, D.E. Soper, Nucl. Phys. B 213 (1983) 545 (Erratum);
J.C. Collins, D.E. Soper, Back-to-back jets: Fourier transform from B to K-transverse, Nucl. Phys. B 197 (1982) 446.

[26] O.T. Engelund, R. Roiban, Correlation functions of local composite operators from generalized unitarity, J. High Energy Phys. 1303 (2013) 172, arXiv:1209.0227 [hep-th].
[27] B. Eden, P.S. Howe, P.C. West, Nilpotent invariants in $N = 4$ SYM, Phys. Lett. B 463 (1999) 19, arXiv:hep-th/9905085.
[28] B. Eden, P.S. Howe, C. Schubert, E. Sokatchev, P.C. West, Extremal correlators in four-dimensional SCFT, Phys. Lett. B 472 (2000) 323, arXiv:hep-th/9910150.
[29] F. Gonzalez-Rey, I.Y. Park, K. Schalm, A note on four point functions of conformal operators in $N = 4$ superYang–Mills, Phys. Lett. B 448 (1999) 37, arXiv:hep-th/9811155.
[30] B. Eden, P.S. Howe, C. Schubert, E. Sokatchev, P.C. West, Four point functions in $N = 4$ supersymmetric Yang–Mills theory at two loops, Nucl. Phys. B 557 (1999) 355, arXiv:hep-th/9811172.
[31] B. Eden, P.S. Howe, C. Schubert, E. Sokatchev, P.C. West, Simplifications of four point functions in $N = 4$ supersymmetric Yang–Mills theory at two loops, Phys. Lett. B 466 (1999) 20, arXiv:hep-th/9906051.
[32] B. Eden, A.C. Petkou, C. Schubert, E. Sokatchev, Partial nonrenormalization of the stress tensor four point function in $N = 4$ SYM and AdS/CFT, Nucl. Phys. B 607 (2001) 191, arXiv:hep-th/0009106.
[33] B. Eden, C. Schubert, E. Sokatchev, Three loop four point correlator in $N = 4$ SYM, Phys. Lett. B 482 (2000) 309, arXiv:hep-th/0003096.
[34] M. Bianchi, S. Kovacs, G. Rossi, Y.S. Stanev, Anomalous dimensions in $N = 4$ SYM theory at order g^4, Nucl. Phys. B 584 (2000) 216, arXiv:hep-th/0003203.
[35] N.I. Usyukina, A.I. Davydychev, Exact results for three and four point ladder diagrams with an arbitrary number of rungs, Phys. Lett. B 305 (1993) 136;
N.I. Usyukina, A.I. Davydychev, Some exact results for two loop diagrams with three and four external lines, Phys. At. Nucl. 56 (1993) 1553, arXiv:hep-ph/9307327, Yad. Fiz. 56 (11) (1993) 172.
[36] M. Luscher, G. Mack, Global conformal invariance in Quantum Field Theory, Commun. Math. Phys. 41 (1975) 203.
[37] G. Mack, D-independent representation of Conformal Field Theories in D dimensions via transformation to auxiliary Dual Resonance Models. Scalar amplitudes, arXiv:0907.2407 [hep-th].
[38] G. Arutyunov, S. Frolov, Scalar quartic couplings in type IIB supergravity on AdS(5) $\times$ S^5, Nucl. Phys. B 579 (2000) 117, arXiv:hep-th/9912210.
[39] G. Arutyunov, S. Frolov, Four point functions of lowest weight CPOs in $N = 4$ SYM(4) in supergravity approximation, Phys. Rev. D 62 (2000) 064016, arXiv:hep-th/0002170.
[40] G. Arutyunov, S. Frolov, A.C. Petkou, Operator product expansion of the lowest weight CPOs in $N = 4$ SYM(4) at strong coupling, Nucl. Phys. B 586 (2000) 547, arXiv:hep-th/0005182;
G. Arutyunov, S. Frolov, A.C. Petkou, Nucl. Phys. B 609 (2001) 539 (Erratum).
[41] J.M. Martin-Garcia, xAct: efficient tensor computer algebra, http://www.xact.es.
[42] A.G.-P. Gomez-Lobo, J.M. Martin-Garcia, Spinors: a Mathematica package for doing spinor calculus in General Relativity, Comput. Phys. Commun. 183 (2012) 2214, arXiv:1110.2662 [gr-qc].
[43] A.V. Belitsky, S. Hohenegger, G.P. Korchemsky, E. Sokatchev, A. Zhiboedov, in preparation.
[44] B. Eden, P. Heslop, G.P. Korchemsky, E. Sokatchev, Hidden symmetry of four-point correlation functions and amplitudes in $N = 4$ SYM, Nucl. Phys. B 862 (2012) 193, arXiv:1108.3557 [hep-th].
[45] L.V. Keldysh, Diagram technique for nonequilibrium processes, Zh. Eksp. Teor. Fiz. 47 (1964) 1515, Sov. Phys. JETP 20 (1965) 1018.
[46] A.V. Belitsky, S.E. Derkachov, G.P. Korchemsky, A.N. Manashov, Superconformal operators in $N = 4$ superYang–Mills theory, Phys. Rev. D 70 (2004) 045021, arXiv:hep-th/0311104.
[47] M. Nirschl, H. Osborn, Superconformal Ward identities and their solution, Nucl. Phys. B 711 (2005) 409, arXiv:hep-th/0407060.